STUDY OF BIOGAS PRODUCTION FROM DISTILLERY WASTE WATER OVER IMMOBILISED BIOMASS

BY

CHIRCHIR ABRAHAM

A THESIS SUBMITTED IN PARTIAL FULFILMENT OF THE REQUIREMENTS FOR THE AWARD OF THE DEGREE OF MASTER OF SCIENCE IN CHEMICAL AND PROCESS ENGINEERING, SCHOOL OF ENGINEERING

MOI UNIVERSITY
ELDORET

2018

DECLARATION

DECLARATION BY THE STUDENT

…….. ……..

Chirchir, Abraham **Date**

TEC/PGCP/07/08

DECLARATION BY THE SUPERVISORS

This thesis has been submitted for examination with our approval as Moi University supervisors.

Prof. Kirimi Kiriamiti,

Department of Chemical & Process Eng., Moi University

Signature…….. Date.....……

Prof. Ochieng' Aoyi,

Department of Chemical and Process Eng., Moi University

Signature…….. Date.....……

DEDICATION

To

God, my late father Hosea Kogo and mother,

for

the support, love and encouragement they gave me in life.

ABSTRACT

In a molasses distillery, a lot of waste water is generated as the bottoms product. These waters contain a lot of organics, are dark brown in colour and have low pH. Their free disposal is harmful to the environment. Anaerobic digestion has been the most preferred treatment technique of this water. Besides stabilizing the effluents, anaerobic treatment enable the recovery of energy in the form of biogas. However, there are problems associated with this method. Low pH, high salinity, recalcitrant compounds, inhibitory substances and oxygen permeation are the major problems that lower the degree of effluent stabilisation. New developments are being explored to suppress these effects. Currently, the focus is on cell biological immobilisation. This study investigated the immobilisation of methanogenic consortia using conditioned natural zeolite and calcium alginate polymers and benchmarked them with an unsupported system. The main focus was to enable the utilisation of high strength substrate besides increasing biogas yield and suppressing process instabilities due to oxygen permeation. The specific objectives considered included the determination of the sorption carrying capacity of the consortia, determination of the most suitable organic loading, biogas yield and degree of waste water stabilization. Also, the identification of applicable microbial growth models and evaluation of the rate controlling step of the process formed part of the specific objectives. The experimental process involved preparation and characterization of the support media and the waste water followed by immobilization of the consortia unto the support material. The most suitable operational parameters of pH and system temperature were then determined. Batch studies of biogas generation then followed where the kinetics of the processes were evaluated. Further studies were done on calcium alginate supported system on its operational behaviour with regards to mass transfer. The rate limiting step in the process was then identified. From the results obtained, it was determined that the sorption capacity of the consortia at 25 ° C was 13.2 mg/g amino acid per zeolite support mass. The most suitable initial organic loading was obtained to be 25 g/l COD_i , in all the systems although the highest initial strength of 75 g/l COD_i was considered as the focus of making the comparisons. Activated natural zeolite supported system registered the highest effluent stabilization of 44% on organic loading of 75 g/l COD_i . The system supported by calcium alginate registered the highest biogas yield of $84.5\,cm^3/g\,COD_i$ on organic loading of 75 g/l COD_i . All the systems conformed to Modified Gompertz's kinetics as opposed to Monod's and Andrew's kinetics. As regards the kinetic system performance, the reaction rate constants for the unsupported, activated natural zeolite and calcium alginate supported systems were obtained to be 0.1055, 1.2348 and 0.6750 day^{-1} respectively. The substrate kinetic behaviour of calcium alginate supported system, registered a Damkolhler number of 0.0643 with respect to substrate diffusive transfer and biochemical substrate degradation rates. It was therefore concluded that substrate degradation rate was the rate limiting step. The results obtained on the two support materials can be used to design a system that is able to utilize high strength waste water without dilution. This consequently reduces the hydraulic loading on the system. It was recommended that antagonistic agents like phosphates and sodium salts should be eliminated first before the experiment commences as they caused the dissolution of calcium alginate beads. Finally, identification of the specific inhibitors causing longer adaptation periods should be done so that preliminary treatment strategies could be formulated to avoid the longer fermentation periods shown by the natural zeolite supported system.

TABLE OF CONTENTS

LIST OF TABL

LIST OF FIGURES

ACKNOWLEDGEMENTS

I would like to acknowledge individuals, groups of people and organizations that greatly assisted me in the course of doing my experiments. Their invaluable encouragement, advice and material support went great lengths to making this work a success. Some of these people and institutions include the following: my supervisors, Professor Ochieng Aoyi and Professor Kirimi Kiriamiti, Mr Sarmat Chemjor, Professor Anil Kumar, Professor Namango Sitati, Professor Ambrose Kiprop, Professor Joel Kibiiy, Dr. Milton Arimi, National Science Council, My Master of Science Classmates, My family members, the Kogo's and most importantly, the unseen Hand of God.

LIST OF SYMBOLS AND ACRONYMS

BOD	Biological Oxygen Demand
Cc1	concentration of amino acid in g/l for the system having initial COD of 0 g/l
Cc2	concentration of amino acid in g/l for the system having initial COD of 25 g/l
Cc3	concentration of amino acid in g/l for the system having initial COD of 50 g/l
Cc4	concentration of amino acid in g/l for the system having initial COD of 75 g/l
CCp1	Cumulative biogas produced by the system having initial COD of 0 g/l over the entire digestion period
CCp2	Cumulative biogas produced by the system having initial COD of 25 g/l over the entire digestion period
CCp3	Cumulative biogas produced by the system having initial COD of 50 g/l over the entire digestion period
CCp4	Cumulative biogas produced by the system having initial COD of 75 g/l over the entire digestion period
COD	Chemical Oxygen Demand
COD_i	Initial Chemical Oxygen Demand
Cp1	Volume of biogas produced by the system having initial COD of 0 g/l
Cp2	Volume of biogas produced by the system having initial COD of 25 g/l
Cp3	Volume of biogas produced by the system having initial COD of 50 g/l
Cp4	Volume of biogas produced by the system having initial COD of 75 g/l
Cs1	Substrate concentration for the system having initial COD of 0 g/l
Cs2	Substrate concentration for the system having initial COD of 25 g/l

Cs3	Substrate concentration for the system having initial COD of 50 g/l
Cs4	Substrate concentration for the system having initial COD of 75 g/l
FA	Fatty Acids
HRT	Hydraulic Retention Times
Ks	Monod constant
NF	Nano Filtration
RO	Reverse Osmosis
SEM	Scanning Electron Microscope
SRB	Sulfate Reducing Bacteria
SRT	Solids Retention Time
TAN	Total Ammonia Nitrogen
TDS	Total Dissolved Solids
TFC	Thin Film Composite Membranes
TN	Total Nitrogen
TOC	Total Organic Carbon
TP	Total Phosphates
TSS	Total Suspended Solids
UASB	Upflow Anaerobic Sludge Blanket
UV-VIS	Ultra Violet-Visible Light Spectrophotometer
VFA	Volatile Fatty Acids

DEFINITION OF TECHNICAL TERMS

Acclimatization	automatic adjustment of microorganisms to the surrounding environment
Aerobic respiration	Harvesting chemical energy in the form of Adenosine Tri-Phosphate from food molecules, with oxygen as an electron receptor
Amino acid	An organic molecule having both carboxylic and amino groups and they form monomers of proteins
Anaerobic respiration	Respiration that occur in a few groups of bacteria leaving in an environment that is stuffed of oxygen They have sulphates and nitrates as electron acceptors
Biomass	The dry weight organic matter comprising a group of organisms in a particular habitat
DNA polymerase	An enzyme that catalyses the elongation of new DNA during replication
DNA probe	A chemically synthesized, radioactively labeled segment of nucleic acid used to find a gene of interest
DNA	Deoxyribonucleic acid, is a double stranded compound and can replicate in the transmission of characters
Enzymes	A class of proteins serving as catalysts
Essential nutrient	A chemical element required by animals and plants and cannot be synthesized within itself
Eutrophication	Excessive richness of nutrients in a water body which may cause dense growth of plant life and death of animal life from lack of oxygen
Fatty acid	A long chain carboxylic acid
Fermentation	A catabolic process that makes a limited amount of ATP from glucose without an electron transport chain and produces ethyl alcohol or lactic acid
Gene	DNA fragment
Hydraulic retention times	refers to the residence time spent by a substrate in a bioreactor

Hydrolysis	A process that splits the molecules by the addition of water
Immobilisation	this is the process of attaching microbes to a support material so as to restrict them to specific areas under specific environments
Recalcitrant	Substances which are difficult to degrade biochemically
Vinasse	Molasses distillery waste water

CHAPTER ONE

INTRODUCTION

1.1 Background of the Study

Sugar cane molasses are by-products of the sugar-extraction processes and are often used as raw materials in alcohol distilleries. The production of vinasses in a traditional alcohol factory is in the range of 8–15 litres of molasses wastewaters per litre of ethanol obtained [CITATION Moh05 \l 1033]. These wastes are strongly acidic (pH 4–5), have a high-organic content, chemical oxygen demand (COD in the range of 80–100 g/l) and biochemical oxygen demand (BOD) (40–50 g/l), strong odor and dark brown color [CITATION Sat07 \l 1033]. Their free disposal presents a serious challenge to the natural ecosystem and can cause considerable environmental problems [CITATION Moh05 \l 1033]. Alcohol distilleries are rated as one of the 17 most polluting industries[CITATION Sat07 \l 2057]. Apart from high organic content, distillery wastewater also contain nutrients in the form of nitrogen (1660–4200 mg/l), phosphorus (225–3038 mg/l) and potassium (9600–17,475 mg/l) that can lead to eutrophication of water bodies. Further, its dark color hinders photosynthesis by blocking sunlight and is therefore deleterious to aquatic life [CITATION Sat07 \l 1033]. In the treatment of these wastes, anaerobic digestion is the most preferred because, it has a number of advantages. It uses low energy, has a high transformation of the organic matter by anaerobic bacteria into biogas, minimal sludge formation and low nutrient demands. The production of biogas enables the process to generate energy in addition to the reduced energy uptake [CITATION Che07 \l 1033 \m van97]. The net energy realized can reduce operational costs by a large margin compared to the high-energy uptake aerobic processes.

However, the dark color remains a problem after anaerobic treatment, which therefore requires a post-treatment before its safe disposal into the environment [CITATION Jag00 \l 1033]. Although anaerobic digestion of most types of distillery wastewaters is feasible and quite attractive from an energy perspective, the presence of inhibitory substances such as phenolic compounds severely hinders the anaerobic process. They slow down the kinetics, increases acclimatization periods and reduces mean rates of methane production, and yield coefficients [CITATION Che07 \l 1033]. These limitations then dictate the utilization of high hydraulic retention times (HRT). Many phenolic compounds are known to be toxic and interfere with the activity of methanogenic bacteria. In addition, the high salinity of this waste (average conductivity of 40 mS/cm) also causes osmotic pressure problem to the micro-organisms responsible for the anaerobic process [CITATION Che07 \l 1033]. Studies of technologies such as incineration, physico-chemical treatment, composting, and biological treatment show that they require high reagent dosages and generate large amounts of sludge [CITATION Sat07 \l 1033]. Besides the problem of color, inhibition and high COD levels, there is a problem of using highly diluted substrates as undiluted ones are deleterious to the microbes. The dilution process results into high hydraulic loads.

1.2 Statement of the Problem

Currently there is no conventionally agreed design of a commercial process that is able to work on high strength waste water and effectively reduce both BOD and COD. sThese conventional cases have their high strength waste waters diluted to allow degradation to be possible. These processes increase the hydraulic load of the system and consequently bring problems of dewatering. It is also associated with increased pumping costs. Besides, the unsupported process has low conversion percentages of

organics leading to discharge of effluents that are high in COD. Their free disposals create habitats for pathogens and are associated with foul odors.

The dwindling fossil fuel reserves have called for the exploitation of other alternative energy sources. The renewable energy from biomass is particularly the attractive option.

This project therefore examined the possibilities of improving biogas production and efficient effluent stabilization from molasses waste water via immobilized methanogens on zeolite and calcium alginate gel supports. This approach was designed to improve on the methane production volumes, facilitate high effluent stabilization, enhance the use of high strength influents, suppress salinity problems and impart high process tolerances to external disturbances like oxygen seepage into the process.

1.3 General Objective

The general objective was to improve the yield of biogas from the organic matter and simultaneously stabilize the effluents by a higher degree.

1.4 Specific Objectives

(a) To determine the adsorption capacity of adsorbent supports on microbial systems.
(b) To determine the most suitable organic loading in batch fermentors at mesophillic conditions.
(c) To determine the biogas yield from molasses distillery wastewater in both the supported and non-supported systems
(d) To determine the degree of distillery waste water stabilization at the end of anaerobic digestion on differently supported systems.
(e) To identify the microbial growth models which the biodegradation process follow.

(f) To compare the stability margins of the supported systems with the unsupported one when exposed to sterile air.
(g) To evaluate the rate controlling step between diffusive mass transport and biochemical degradation in calcium alginate supported system.

1.5 Scope

This research was limited to the following areas:

- Preparation of the support materials.
- Testing the physico-chemical characteristics of the support material.
- The generation of biogas in batch fermentors at mesophillic conditions.
- Measurement of the methane yield.
- Analysis of the parameters that promote the optimal generation of biogas over a support material.
- Measurement of the degree of stability of the system upon oxygen exposure.
- Determination of the rate controlling step between diffusive substrate flux and biochemical degradation of the substrate.

1.6 Justification

The world today needs more and more energy because of the ever increasing population and industrialisation. The dwindling fossil fuel reserves, which constitutes the highest energy source, is raising the world concern. The exploration of renewable energy source appears to be the definitive solution. Renewable energy produces non-deleterious emissions to the environment, is sustainable and has the capability of being generated from organic wastes which are abundant in nature. Molasses waste water is a secondary waste from alcohol distilleries. It contains high COD and BOD

levels and therefore is a useful carbon source for bioenergy production as a non-main stream product of sugar-cane manufacture.

This project was aimed at generating biogas from this organic waste in a more effective manner. The findings of this project could assist in promoting environmental integrity by keeping the pollutants in the distillery effluent at acceptable levels.

In summary therefore, the project explored the recovery of a valuable product from a sugar manufacturing waste in the most effective manner.

CHAPTER TWO
LITERATURE REVIEW

2.1 Wastewater Generation and Characteristics

Distillery waste water is generated from different processes. The most abundant streams include spent wash, cleaning effluent, and cooling water effluent. Their respective characteristics are listed in table 2.1 for a typical alcohol manufacturing process.

Table 2.1: Table of sample quantities and characteristics of wastewater streams [CITATION Yeo97 \l 1033]

Parameter	Specific waste water generation (m^3/m^3 alcohol)	Color	pH	Suspended solids (mg/l)	BOD (mg /l)
Spent wash	14.4	Dark brown	4.6	615	36500
Fermentercleaning	0.6	Yellow	3.5	3000	4000
Fermenter cooling	0.4	Colorless	6.3	220	105
Condenser cooling	2.9	Colorless	9.2	400	45
Floor wash	0.8	Colorless	7.3	175	100
Bottling plant	14.0	Hazy	7.6	150	10
Other	0.8	Pale yellow	8.1	100	30

The main source of wastewater generation is the distillation step wherein large volumes of dark brown effluent is generated in the temperature range of 71–81 ºC [CITATION Yeo97 \m Pat03 \m Nan02 \l 1033].

The characteristics of the spentwash depend on the raw material used. It is estimated that 88% of the molasses constituents end up as waste [CITATION Jai02 \l 1033]. Molasses spentwash have very high levels of BOD, COD, COD/BOD ratio as well as

high potassium, phosphorus and sulfate content. The typical characteristic of this spent wash is summarized in Table 2.2.

Table 2.2: Table showing characteristics of spent wash by[CITATION Wil00 \m Pat99 \l 2057]

Characteristics	Feedstock	
	Cane molasses [CITATION Pat99 \l 1033]	Beet molasses [CITATION Wil00 \l 1033]
COD (mg/l)	65,000-130,000	91,100
BOD (mg/l)	30,000-70,000	44,900
Mean COD/BOD ratio	2.49	1.95
Total Solids (mg/l)	30,000-100,000	-
Total suspended solids (mg/l)	350	-
Total dissolved solids (mg/l)	80,000	-
Total nitrogen (mg/l)	1000-2000	3569
Total phosphorous (mg/l)	800-1200	163
Potassium (mg/l)	8,000-12,000	10,030
Sulphur as SO_4 (mg/l)	2,000-6,000	3716
pH	3.0-5.4	5.35

In addition, cane molasses spentwash contains low molecular weight compounds such as lactic acid, glycerol, ethanol and acetic acid [CITATION Wil00 \l 1033]. Cane molasses also contains around 2% of a dark brown pigment, the melanoidins that impart color to the spentwash [CITATION Kal01 \l 1033]. Melanoidins are low and high molecular weight polymers formed as one of the final products of Maillard reaction, which is a non-enzymatic browning reaction resulting from the reaction of reducing sugars and amino compounds [CITATION Mar04 \l 1033]. This reaction proceeds effectively at temperatures above 50 ^{o}C and pH 4–7. Only 6–7% degradation

of the melanoidins is achieved in the conventional anaerobic–aerobic effluent treatment process [CITATION Gon00 \l 1033]. Due to their antioxidant properties, melanoidins are toxic to many microorganisms involved in wastewater treatment [CITATION Sir04 \l 1033]. Apart from melanoidins, spentwash contains other colorants such as phenolics, caramel and melanin. Phenolics are more pronounced in cane molasses wastewater whereas melanin is significant in beet molasses [CITATION God99 \l 1033].

The waste water generated from the distilleries can be treated using various conventional processes. These processes can be categorized into two major groups: biological and physico-chemical processes. The physico-chemical methods of waste water treatment have a number of disadvantages: they utilize large amounts of reagent doses and generate large volumes of sludge. Section 2.2 outlines in detail the various principles and challenges of physico-chemical means of treatment.

2.2 Physico-Chemical Treatment

Even though biological treatment results in significant COD removal, the effluent has been known to still retain the dark color [CITATION Ina99 \l 1033]. The color imparting melanoidins are barely affected by conventional biological treatment such as methane fermentation and the activated sludge process [CITATION Mig93 \l 1033]. Various physico-chemical treatment options have been explored including:

2.2.1 Adsorption

The adsorption capacity of an adsorbent depends not only on its surface area, but also on its internal pore structure, surface characteristics and the presence of functional groups on pore surface. All these characteristics depend on both the precursor used and the method of preparation [CITATION Ism05 \l 1033]. The overall adsorption

process may be controlled either by one or more steps like film or external diffusion, pore diffusion, surface diffusion and adsorption on the pore surface or a combination of more than one step. In batch adsorption, the diffusive mass transfer can be related by an apparent diffusion coefficient, which will fit the experimental sorption data [CITATION Sri06 \l 1033]. In order to determine the potential rate controlling steps, kinetic models should be established. Equilibrium isotherms such as the Langmuir, Freundlich, two-site Langmuir, Langmuir-Freundlich, Redlich-Peterson, Tóth, and Dubinin-Radushkevitch can be used to model the experimental data for the removal of organics [CITATION Ony04 \l 1033]. Activated carbon is a widely used adsorbent for the removal of organic pollutants from wastewater but the relatively high cost restricts its usage. Chemically modified bagasse using 2-diethylaminoethyl chloride hydrochloride and 3-chloro-2 hydroxypropyltrimethylammonium chloride is capable of decolorizing diluted spentwash [CITATION Man06 \l 1033]. Adsorption by commercially available powdered activated carbons results in only 18% color removal. However, combined treatment using coagulation–flocculation with polyelectrolyte followed by adsorption results in almost complete decolorization [CITATION Sek98 \l 1033]. Low cost adsorbents such as pyorchar (activated carbon both in granular and powder form, manufactured from paper mill sludge) and bagasse fly ash have been studied for this application. Ramteke et al (1989) reported color removal up to 98% with pyorchar. However, to achieve the same level of color removal, larger doses of the indigenously prepared powdered and granular pyorchar are required in comparison with commercial activated carbon. Mall and Kumar (1997) compared the color removal using commercial activated carbon and bagasse flyash. 58% color removal was reported with 30 g/l of bagasse flyash and 80.7% with 20 g/l of commercial activated carbon. Since the bagasse fly ash has high carbon content and

the adsorbed organic material further increases its heating value, the spent adsorbent can be used for making fire briquettes.

2.2.2 Coagulation and Flocculation

Alum and iron salts have been reported not to be effective coagulants in color removal when used alone without combining with adsorption [CITATION Ina99 \l 1033]. Lime and ozone treatment with anaerobically digested effluent has also been explored by Inanc et al (1999). The optimum dosage of lime was found to be 10 g/l resulting in 82.5% COD removal and 67.6% reduction in color in a 30 min period. $FeCl_3$ and $AlCl_3$ were also tested for decolorization of biodigested effluent and showed similar removal efficiencies. About 93% reduction in color and 76% reduction in TOC were achieved when either $FeCl_3$ or $AlCl_3$ was used alone. The process was independent of chloride and sulfate ion concentration but was adversely affected by high fluoride concentration. However in the presence of high flocculent concentration (40 g/l), addition of 30 g/l CaO enhanced the decolorization process resulting in 93% color removal. This was attributed to the ability of calcium ions to destabilize the negatively charged melanoidins. Further, the formation of calcium fluoride (CaF_2) also precipitates the fluoride ions. Almost complete color removal (98%) of biologically treated distillery effluent has been reported with conventional coagulants such as ferrous sulfate, ferric sulfate and alum under alkaline conditions [CITATION Pan03 \l 1033]. The best results were obtained using Percol 47, a commercial organic anionic polyelectrolyte, in combination with ferrous sulfate and lime. The combination resulted in 99% reduction in color and 87 and 92% reduction in COD and BOD, respectively.

2.2.3 Oxidation Process

Oxidation by ozone could achieve 80% decolorization for biologically treated spentwash with simultaneous 15–25% COD reduction [CITATION Alf00 \l 2057 \m Pen03]. It also improves biodegradability of the effluent. However, ozone only transforms the chromophore groups but does not degrade the dark colored polymeric compounds in the effluent [CITATION Alf00 \m Pen03 \l 1033]. The oxidation of effluent with chlorine results in 97% color removal but the color reappears after a few days [CITATION Man03 \l 1033]. Ozone in combination with Ultra Violet radiation enhances spentwash degradation in terms of COD.

2.2.4 Membrane Treatment

Pre-treatment of spentwash with ceramic membranes prior to anaerobic digestion is reported to halve the COD from 36,000 to 18,000 mg/l [CITATION Cha94 \l 1033]. In addition to COD reduction, the pre-treatment also improved the efficiency of the anaerobic process possibly due to the removal of inhibiting substances. Reverse osmosis (RO) has also been employed for distillery wastewater treatment.

In a recent study, Nataraj et al (2006) reported pilot trials on distillery spentwash using a hybrid nanofiltration (NF) and RO process. Both the NF and RO stages employed thin film composite (TFC) membranes. NF was primarily effective in removing the color and colloidal particles accompanied by 80%, 95% and 45% reduction in total dissolved solids (TDS), conductivity and chloride concentration, respectively at an optimum feed pressure of 30–50 bar. The subsequent RO operation at a feed pressure of 50 bar resulted in 99% reduction each in COD, potassium and residual TDS.

2.2.5 Evaporation/Combustion

Molasses spentwash containing 4% solids can be concentrated to a maximum of 40% solids in a quintuple-effect evaporation system with thermal vapor recompression [CITATION Bha04 \l 1033 \m Gul04]. The condensate with a COD of 280 mg/l can be used in fermenters. The concentrated mother liquor is spray dried using hot air at 180 ^{o}C to obtain a desiccated powder with a calorific value of around 3200 kcal/kg. The powder is typically mixed with 20% agricultural waste and burnt in a boiler. However, this method consumes a lot of energy and is therefore less economical on a commercial scale.

2.3 Biological Treatment

2.3.1 Anaerobic Process

Studies of anaerobic treatment of distillery waste water have been extensively made. It has been documented that anaerobic treatment provides a good and cheap method of reducing pollution from agricultural and industrial operations while at the same time reducing the operations' usage of fossil fuels[CITATION Che07 \l 2057]. It is widely used for the treatment of municipal sludge and also applied in the treatment of organic industrial wastes including fruit and vegetable processing and agricultural wastes. In the studies by Chen et al (2007) numerous significant advantages were identified such as low sludge production, low energy requirement and possible energy recovery. Compared to mesophilic digestion, thermophilic anaerobic digestion has additional benefits including a high degree of waste stabilization, more thorough destruction of viral and bacterial pathogens, and improved post-treatment sludge dewatering [CITATION Loe85 \l 1033]. The high organic content of molasses spentwash makes anaerobic treatment attractive in comparison to direct aerobic treatment. Therefore, biomethanation is the primary treatment step and is often

followed by two-stage aerobic treatment before discharge into a water body or on land for irrigation [CITATION Nan02 \l 1033]. Aerobic treatment alone is not feasible due to the high energy consumption for aeration, cooling, and other needs. Also, 50% of the COD is converted to sludge after aerobic treatment [CITATION Sen05 \l 1033]. In contrast, anaerobic treatment converts over half of the effluent COD into biogas [CITATION Wil00 \l 1033]. Anaerobic treatment can be successfully operated at high organic loading rates.

The performance and treatment efficiency of anaerobic process can be influenced both by inoculum source and feed pre-treatment. In particular, thermal treatment of wastewaters can result in rapid degradation of organic matter leading to lower hydraulic residence time (HRT), higher loading rate and BOD reduction. Further, addition of micronutrients (iron, boron and molybdenum) was also identified to eliminate long adaptation periods.

Anaerobic lagoons are the simplest option for the anaerobic treatment of distillery spentwash. However, large area requirement, odor problem and chances of ground water pollution restrict its usage [CITATION Pat99 \l 1033]. It also offers the advantage of separating the hydraulic retention time (HRT) from solids retention time (SRT) so that slow growing anaerobic microorganisms can remain in the reactor independent of wastewater flow.

Therefore, in comparison with the other methods, anaerobic digestion of distillery waste water portents the greatest advantages from an economic stand-point. The associated biogas production is in itself one of the most advantageous benefits derived from the process. However, its production is a complex biochemical process that

involves several micro-organisms of different genera acting concurrently in symbiotic relationship.

2.3.2 Aerobic Treatment

The post-anaerobic treatment effluent typically has high organic loading and is dark brown in color and therefore, a secondary aerobic treatment is at times necessary. Solar drying of biomethanated spentwash is one option commonly used. However, the large land area requirement limits this practice. Besides, solar drying beds become non-functional during the rainy season. The other aerobic treatment options include: aquaculture, constructed wetlands, and biocomposting.

2.3.3 Mechanism of Biogas Production

The sub-processes in which biogas generation takes place have been studied and documented. It has been noted that the process of biomethanation is complex and that consists of a series of biochemical reactions catalyzed by enzymes from a consortium of different bacteria[CITATION Jag11 \l 2057]. The same work outlined that organic matter is degraded from its polymeric form to methane and carbon dioxide with traces of other associated substances like hydrogen sulphide and hydrogen. Biomethanation is undertaken through a series of several reactions mediated by a number of enzymes from different classes of microorganisms. The process involves four major steps: hydrolysis, acidogenesis, acetogenesis and methanogenesis as shown in Figure 2.1

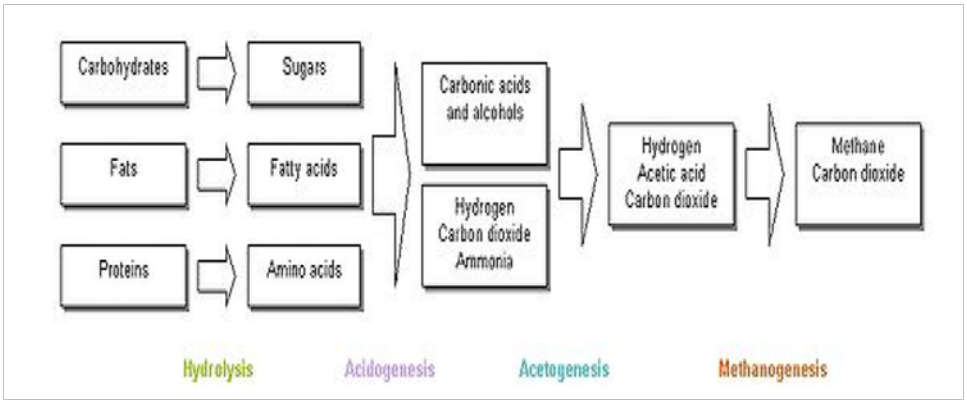

Figure 2.: Different stages of biomethanation (Jagadish et al, 2011)

The first step, hydrolysis, involves enzyme-mediated transformation of insoluble organic material and higher molecular mass compounds such as lipids, polysaccharides, proteins, fats, nucleic acids, etc. into soluble organic materials such as monosaccharides and amino acids. The microbial type aiding in this process are strict anaerobes that include bactericides, clostridia and facultative bacteria such as streptococci. The efficiency of this step, according to Gavanji and Javad (2013), influences the extent of biomethanation as it dictates the level of carbon source that shall be available for the process.

The second step is acidogenesis and involves further breakdown of the remaining components by acidogenic bacteria. They utilise products of hydrolysis. They are facultatively anaerobes and can grow under acid conditions. They need oxygen and carbon source to produce acetic acid. This oxygen is derived from the one dissolved in solution and that which is chemically bound to substances undergoing metabolism. Therefore, the acid-producing bacteria create an anaerobic condition which is essential for the methane producing microorganisms [CITATION MJa13 \l 2057]. Acetogenesis is the third stage. Here, the products of acidogenesis are further digested by acetogens to produce acetic acid, carbon dioxide and hydrogen. The last step is methanogenesis. It involves the conversion of acetic acid, hydrogen and carbon

dioxide into a mixture of methane and carbon dioxide by a consortium of methanogenic bacteria. The consortium is of the following species: methanosarcina spp. that utilize acetates, methanothrix spp that utilize acetates too, methanobacterium which utilizes hydrogen and methanococcus that utilizes formates. They are obligate anaerobes and very sensitive to environmental changes [CITATION MJa13 \l 2057]. The entire process of biomethanation proceeds with the mediating microbes relating to each other symbiotically. Acid producing bacteria create an atmosphere that is deficient of oxygen and supplies the target substrate a condition that is ideal for methane-producing bacteria. Conversely, methane-producing microorganisms use the intermediates of the acid-producing bacteria thereby avoiding the build-up of toxic wastes to suppress the activity of the acid producing microbes [CITATION MJa13 \l 2057]. According to Ponitz (1999), the metabolic activity involved in microbiological methanation is dependent on the following factors: medium temperature, availability of nutrients, biomethanation operational configuration, pH and inhibitory substances amongst other factors.

Temperature plays an important role in the rates of microbial metabolism. In principle, anaerobic fermentation is possible between temperatures of 3°C and 70°C. The rate of bacteriological methane production increases with temperature and the associated free ammonia. Ammonia may inhibit the propagation of biomethanation process as temperature of the medium is increased. Temperatures of below 15°C are not economically feasible as the kinetics tend to be very slow [CITATION MJa13 \l 2057]. According to Gavanji and Javad (2013), for bacteria to grow, they need more than just a supply of organic substances as a source of carbon and energy. Certain mineral nutrients are required in addition to carbon, oxygen and hydrogen, e.g. nitrogen, sulfur, phosphorous, potassium, calcium, magnesium and a number of trace

elements that include iron and manganese. Ordinary agricultural residues or municipal sewage usually contain adequate amounts of these elements. Higher concentration of any individual substance usually has also been known to portent an inhibitory effect.

The retention time is also a factor in that affects the microbial activity. This can be dictated by the reactor configurations. The true retention time can be obtained in a batch reactor. Selection of a suitable retention time thus depends not only on the process temperature, but also on the type of substrate used as some substrates take longer than others to degrade [CITATION MJa13 \l 2057].

pH values of the medium affect the growth of microbes greatly. Methane-producing bacteria live best under neutral to slightly alkaline conditions. Once the process of fermentation has stabilized under anaerobic conditions, the pH will normally take on a value of between 7 and 8.5. Due to the buffer effect of carbon dioxide-bicarbonate (CO_2 - HCO_3^-) and ammonia-ammonium (NH_3 - NH_4^+), the pH level is rarely taken as a measure of substrate acids and/or potential biogas yield. A digester containing a high volatile-acid concentration requires a somewhat higher-than-normal pH value. If the pH value drops below 6.2, the medium will have a toxic effect on the methanogenic bacteria [CITATION Mah13 \l 2057]

Nitrogen inhibition and C/N ratio is also known to cause inhibitory effect if the levels are above or lower than the ones required. Gavanji and Javad (2013) noted that a relatively low nitrogen concentration may inhibit the process of fermentation. He identified that inhibition occurs at a nitrogen concentration of roughly 1700 mg ammonium-nitrogen (NH_4-N) per liter substrate. However, given enough time, the methanogens are capable of adapting to NH_4-N concentrations in the range of 5000-7000 mg/l substrate, so long as free ammonia level does not exceed 200-300 mg NH_3-

N per liter substrate. It is also noteworthy that the rate of ammonia dissociation in water depends on the process temperature and the pH value of the substrate. Microorganisms need both nitrogen and carbon for assimilation into their cell structures. From consideration the experiments of various authors, Gavanji and Javad (2013) concluded that the metabolic activity of methanogenic bacteria can be optimized at a C/N ratio of approximately 8-20, whereby the optimum point varies from case to case, depending on the nature of the substrate [CITATION Pon99 \l 2057].

2.3.4 Inhibition of Microbial Degradation of Waste Water

Besides nitrogen inhibition, other inhibitory substances are often found also to be leading cause of anaerobic reactor upset and failure since they are present in substantial concentrations in molasses wastewaters and sludge. A wide variety of substances have been reported to be inhibitory to the anaerobic digestion processes. An inhibitory material causes adverse shifts in the microbial population and may inhibit bacterial growth. It is usually indicated by a decrease of the steady-state rate of methane gas production and accumulation of organic acids [CITATION Kro79 \l 2057]. There are many substances known to inhibit microbial growth, and subsequently causing instability of the anaerobic digestion. Mere presence of a substance may not exhibit inhibition but its percentage in the substrate is the important aspect. Anaerobic digestion shows considerable variation in the inhibition/toxicity levels as per every toxicant. The major reason for these variations is the complexity of the anaerobic digestion process where mechanisms such as antagonism, synergism, acclimation, and complexing significantly affect the phenomenon of inhibition. The commonly known inhibitors include the following:

a) Ammonia

Ammonia is produced by the biological degradation of the nitrogenous matter, mostly in the form of proteins and urea. The quantity of ammonia that will be generated from an anaerobic biodegradation of organic substrate is estimated using the following stoichiometric relationship [CITATION Tch93 \l 2057].

$$C_aH_bO_cN_d+\left(\frac{4a-b-2c+3d}{4}\right).H_2O \underset{\rightarrow}{yields}\left(\frac{4a+b-2c-3d}{8}\right)CH_4+\left(\frac{4a-b+2c+3d}{8}\right)CO_2+dN H_3$$

Several mechanisms for ammonia inhibition have been proposed, such as a change in the intracellular pH, increase of maintenance energy requirement, and inhibition of a specific enzymatic reaction [CITATION Whi95 \l 2057]. Ammonium ion (NH_4^+) and free ammonia, (NH_3) are the two principal forms of inorganic ammonia in aqueous solution. Free ammonia has been suggested to be the main cause of inhibition since it is freely membrane-permeable [CITATION Kro79 \l 2057]. The hydrophobic ammonia molecule may diffuse passively into the cell, causing proton imbalance, and/or potassium deficiency [CITATION Gal98 \l 2057]. Among the four types of anaerobic microorganisms, the methanogens are the least tolerant and the most likely to cease growth due to ammonia [CITATION Kay94 \l 2057]. As ammonia concentrations were increased in the range of 4051–5734 mg NH_3-N. L^{-1}, acidogenic populations in the granular sludge was hardly affected while the methanogenic population lost 56.5% of its activity [CITATION Kos88 \l 2057]. There is conflicting information in the literature about the sensitivity of aceticlastic and hydrogenotrophic methanogens. Some research based on the comparison of methane production and growth rate indicated that the inhibitory effect was in general stronger for the aceticlastic than for the hydrogenotrophic methanogens [CITATION Kos84 \m Zee85 \l 2057] while others observed the relatively high resistance of acetate

consuming methanogens to high total ammonia nitrogen levels as compared to hydrogen utilizing methanogens [CITATION Zee85 \m Wie86 \l 2057]. Among the methanogenic strains commonly isolated from sludge digesters such as, Methanospirillum hungatei, Methanosarcina barkeri, Methanobacterium thermoautotrophicum, and Methanobacterium formicicum. Methanospirillum hungatei was the most sensitive, being inhibited at 4.2 g/l; the other three strains tested were resistant to ammonia levels higher than 10 g/l [CITATION Jar87 \l 2057].

b) Factors controlling Ammonia inhibition

There are a number of factors that promote ammonia inhibition. They include the following: Concentration, pH, temperature, presence of other ions and acclimation.

The level of ammonia concentration has a resounding effect on microbial inhibition. It is thought that ammonia concentrations below 200 mg/l are beneficial to anaerobic process. This is because their nitrogen is required by micro-organisms for proper growth [CITATION Liu02 \l 2057]. Ammonia concentrations of 1.7 to 14 g/l, measured as total ammonium nitrogen, have been reported to cause a 50% reduction in methane production [CITATION Kro79 \l 2057]. The varying inhibition by ammonia concentrations is attributed to differences in substrates and inocula, environmental conditions and acclimatization [CITATION Ang94 \m Has86 \l 2057].

pH values have also been known to affect the degree of severity of ammonia toxicity. It is known to greatly hinder treatment of wastes containing high total ammonium nitrogen [CITATION Has86 \m Kro79 \m Han99 \l 2057]. Several authors concur that the actual toxic form of ammonia is the free ammonia. Therefore, an increase in

the pH value favours its existence in the solution thereby suppressing the kinetics of microbial growth [CITATION Bor96 \l 2057]. The instabilities caused by ammonia toxicity results into the accumulation of volatile fatty acids which subsequently leads to a decrease in pH and thereby declining concentration of free ammonia. The interaction between free ammonia, volatile fatty acids and pH may lead to an inhibited steady state. This is a phenomenon whereby the system is running but with reduced product yields [CITATION Ang93 \l 2057 \m Ang931]. It is also reported that if the pH is controlled to within the growth optimum of microbes then ammonia toxicity may be reduced [CITATION Bha89 \l 2057]. It has been established that adjusting pH to 7.4 resulted into the consumption of volatile fatty acids upto a concentration of 20mg/l. At this pH, ammonia induced inhibition prevelant at low pH values was reduced leading to better yields [CITATION Bra81 \l 2057]. Though ammonia could be at its safe level, the reactor performance may be lowered because both the methanogenic and acidogenic microorganisms have a unique optimal pH which may not correspond to that promoting safe level of ammonia [CITATION Kro79 \l 2057].

Temperature affects both microbial growth and concentration of free ammonia. High temperature increases the rate of metabolism of substrates and concurrently raising the levels of free fatty acids in the medium. Anaerobic fermentation of substrates containing high amounts of free ammonia at thermophilic temperatures are inhibited more profoundly than at mesophilic temperatures [CITATION Bra81 \l 2057]. Experiments were carried out at thermophilic digestion of 50 ^{o}C with total ammonium nitrogen of above 3 g/L and biodegradation was found to be very difficult [CITATION Has83 \l 2057]. It is also reported that decreasing temperatures from 60 ^{o}C to 37 ^{o}C in anaerobic systems containing high ammonia concentration showed suppressed inhibition from free ammonia [CITATION Ang94 \l 2057 \m Han99].

The presence of ions like those of Na^{+}, Ca^{2+}, and Mg^{2+} have also been reported to demonstrate antagonism to ammonia inhibition. This is a phenomenon in which the toxicity of one ion is decreased by the presence of other ion(s) [CITATION Bra81 \l 2057] From other experiments, it was noted that 0.15 M ammonia in a culture medium reduced the methane production from acetic acid by 20%. Subsequent, addition of 0.002–0.05 M Na^{+} produced 5% more methane compared to that from the control (a sample without addition of inhibitor) [CITATION Kug64 \l 2057]. Therefore, the presence of the other ions showed synergistic effect on anaerobic degradation.

Microbial acclimatization to the culture medium has been reported to have an effect on ammonia toxicity. Increasing free ammonia concentration slowly has been reported to suppress their toxicity due to conditioned tolerance. This adaptation may be the result of internal changes in the predominant species of methanogens, or because of a shift in the methanogenic population [CITATION Zee85 \l 2057]. Once adapted, the microorganisms can retain viability at concentrations far exceeding the initial inhibitory concentrations.

c) Sulfide

The process of biogas production is associated with reduction of sulphates by the sulphate reduction bacteria. The primary inhibition is attributed to the competition of the same substrate by the sulphate reducing bacteria and the methanogenic consortia. Secondary inhibition results from the toxicity of sulfide to various bacteria groups. The most responsible form of toxic sulphide is Hydrogen sulphide because of its capability to diffuse through the cell membrane of microbes [CITATION And82 \l 2057 \m Col98]

d) Light metals ions (Na, K, Mg, Ca, and Al)

The presence of light metal salts affects the osmotic balance of the microbial population. They cause dehydration of cells thereby hindering the biochemical kinetics. It is also reported that, cations have greater effect to inhibition than anions do [CITATION deB84 \l 2057 \m Yer97].

e) Heavy metals

Heavy metals have been known to cause digester upsets when they accumulate to toxic levels. They are not most commonly assimilated into the structural materials like the other metal ions. They build up in reactors to levels which hinder the normal digestion process. They cause inhibition by binding with the protein molecules in enzymes or by replacing naturally occurring metals in enzyme prosthetic groups thereby disrupting the normal functioning of the enzymes. Heavy metals of particular concern are: copper, chromium, iron, cobalt, zinc, cadmium and nickel [CITATION Jin98 \l 2057 \m Swa69]

f) Organics

It is reported by Chen et al, (2007) that a wide range of organic compounds inhibit anaerobic processes. Organic chemicals which are poorly soluble in water or adsorbed to the surfaces of sludge solids may accumulate to high levels in anaerobic digesters. In the same work, it is outlined that the accumulation of polar pollutants in bacterial membranes cause the membranes to swell and leak, disrupting ion gradients and eventually causing cell lysis [CITATION Hei94 \m Sik94 \l 2057]. Organic compounds which have been reported to be toxic to the anaerobic processes include alkyl benzenes [CITATION Yan86 \l 2057], halogenated benzenes, nitrobenzenes, phenol and alkyl phenols, halogenated phenols, nitrophenols, alkanes, halogenated

aliphatics, alcohols, halogenated alcohols, aldehydes, ethers, ketones, acrylates, carboxylic acids, amines, nitriles, amides, and pyridine and its derivatives [CITATION Liu98 \l 2057].

Immobilisation of cells has been known to suppress the effects of inhibitors [CITATION Sye09 \l 2057]. Various immobilization techniques have been studied based on the interaction mechanism between the supports and microbial system. Singh and Prerna (2009) studied the effect of retaining microbes inside the reactor and the effect this had on degradation of organics. They noted that there was an enhanced stability and performance in anaerobic reactors. The retention of microbes in the reactor could be achieved through two techniques: that of using a dense bacterial granula like in the case of UASB reactors using inert or active carriers in packed bed reactors. The packing medium in the packed-bed reactor and the granular sludge in the UASB reactor serve as a filter preventing bacterial washout and also providing a larger surface area for faster biofilm development and improved methanogenesis. Yang et al, (2004) noted that, specific surface area, porosity, surface roughness, pore size, and orientation of the packing material played an important role in anaerobic reactor performance. It was also outlined that biofilm or fixed-film reactors depended on the natural tendency of mixed microbial populations to adsorb onto surfaces and to form a biofilm. According to [CITATION Yan04 \l 2057] many carrier materials have been investigated regarding their suitability as supports for biofilm, including cheap, readily available materials like sand, clay, glass, quartz and a number of plastics. In nature, microorganisms are found inhabiting virtually every environment. They can even be found in the most remote areas. They have been known to occupy the outer and inner surfaces of stone, gravel or sand according to [CITATION Yan04 \l 2057]. The formed biofilm plays an important role in the water self-

cleaning ability. It also forms the media with which further growth of microorganism is achieved. This enhances biological water treatment further like for instance denitrification and the intensification of aerobic and anaerobic wastewater treatment. The development of biofilm on supports has been known to improve the conversion rates by reducing its sensitivity toward concentration variations and inhibiting substance. Picanco et al (2001) reported that the type and characteristics of the support material related directly to the efficiency of removal of organic matter in fixed-bed reactors. Researchers concur with the findings that organic support material has a higher affinity than inorganic material. Reticular polyurethane foam has a high specific surface area which can reach 2400 m^2/m^3, and a porosity of 97%. It was therefore recognised to be an excellent colonization matrix for an anaerobic filter reactor [CITATION Huy83 \l 2057]. From different findings, there is an agreement that pore size is one of the most important parameter for microbiological and engineering requirements in high-efficiency beds [CITATION Bre90 \l 2057]. According to investigation by Caine et al (1991) the comparison of the conventional units and fixed film bioreactors demonstrated that fixed film reactors performed efficiently at higher organic loading rates (OLR) than the latter. This could be due to the more effective biomass retention in the reaction zone achieved. This consequently results into higher cellular retention times. Immobilized biomass anaerobic reactors also show better responses to organic shock loads and toxic inputs. In many cases, immobilized biomass reactors completely recover their performance after such deleterious occurrences [CITATION Cai91 \l 2057]. Novel immobilisation techniques that offer greater elasticities on operation are currently being explored. They are mostly in the category of active supports. This has been explored in detail the section 2.3.5

2.3.5 Cell Immobilization

Cell immobilization fall into two categories: the active and passive types [CITATION Sye09 \l 2057]. Active immobilization offers new frontiers of cell localization. This is due to the enhanced benefits as opposed to the free cell system. Entrapment and binding are the two most common strategies of active cell immobilization. Physical entrapment on a porous matrix is the mostly preferred technique because of the ease and versatility associated with it. Some of the most commonly used porous matrices include agar, chitosan, polyacrylamide, metal screens, silica gel, polyurethanes, etc. Immobilization by binding involves chemical interaction of various matrix layers [CITATION Sye09 \l 2057]. In the case of alginates, they form their networks by ion-exchange gelation mostly between sodium and calcium cations.

On the other hand, passive immobilization of cells involves the growth of biological films. The films are multi-layered and they grow on solid supports. These supports may-be biologically inert or active. The interactions between the cells and the support material are normally intricate and complex. For most mixed cultures, biofilms are produced due to the presence of some polymer producing organisms that enhance and stabilize their formation [CITATION Sye09 \l 2057].

However, the transport of the substrate across the entrapment networks depends on several factors and can limit the rate of biochemical process. The major focus of this work is on active immobilization through the chemical binding and cell entrapment techniques.

Immobilisation by physico-chemical binding of the microbial system has been studied by several authors. Lalov et al, (2001) used a co-polymer of polyacrylonitryle and polyacrylamide as the support material for the consortium. It was suggested that,

micro-organisms attach unto the adsorbent beds via hydroxymethyl groups originating from the supports and amino groups from the methanogenic cells. Since the cell walls of methanogens are made up of proteins and other organic compounds with amino groups, they take part in that reaction that results into covalent bonding. The support-cell interaction forms a conjugated system of active biomass that are immobile [CITATION Lal01 \l 2057].

Since methanogenic consortia are versatile unicellular prokaryotes of the family archibacta, they have small sizes ranging from 0.5-3.0 µm diameters a cell [CITATION Sye09 \l 2057]. A typical adsoption media has larger pores than the prokaryotic cells. Considering sodium chloride activated natural zeolite for instance, it is a porous adsorbent with net negative surface charges having pore sizes ranging from 30-150 µm. Its pore sizes and pores structure can be seen from the SEM micrograph scan in Error: Reference source not found [CITATION Kit14 \l 1033]. Since the methanogenic consortia are far much smaller than these adsorbent pores, the type of cell-adsorbent interaction that usually occur is intra-particle adsorption in the mesopores of the matrix.

The methanogenic consortia are covered by cell walls with the outer surfaces of the cell walls surrounded by slimy, gummy substance, the slime layer [CITATION Sye09 \l 1033]. These layers are active areas in microbes as they can interact with various surfaces of certain polarities including zeolite supports. From BET analysis, Kitinya et al, (2014) reported a surface area of 33.455 m^2/g and pore volume of 9.584 cm^3/g on activated natural zeolite. These results together with the SEM micrograph in Error: Reference source not found[CITATION Kit14 \l 2057] emphasizes the porous adsorption process as opposed to a monolith surface adsorption.

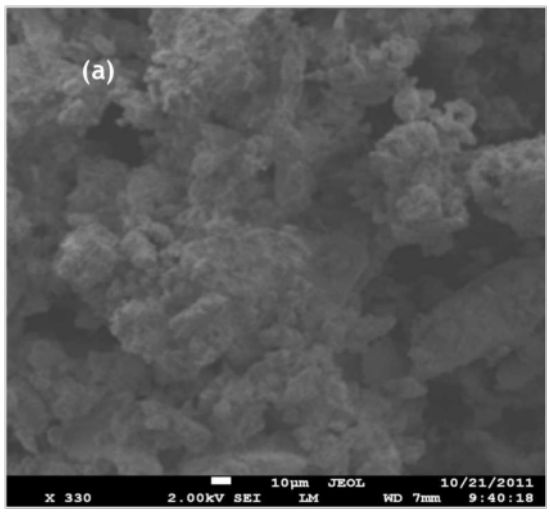

Figure 2. SEM image of natural zeolite (Kittaya et al, 2014)

Cell entrapment using calcium alginate on the other hand occurs through the cross-linking of the guluronic and mannuronic acids which form cross-links. Alginate is a linear polymer based on two monomeric units, β -D-mannuronic acid and α -L-guluronic acid. The classical Haworth formulas for these monomers are shown in Figure 2.3, while Figure 2.4 illustrates the chair formulas, which is a clearer picture of the three-dimensional arrangement of the molecules [CITATION Pen72 \l 2057].

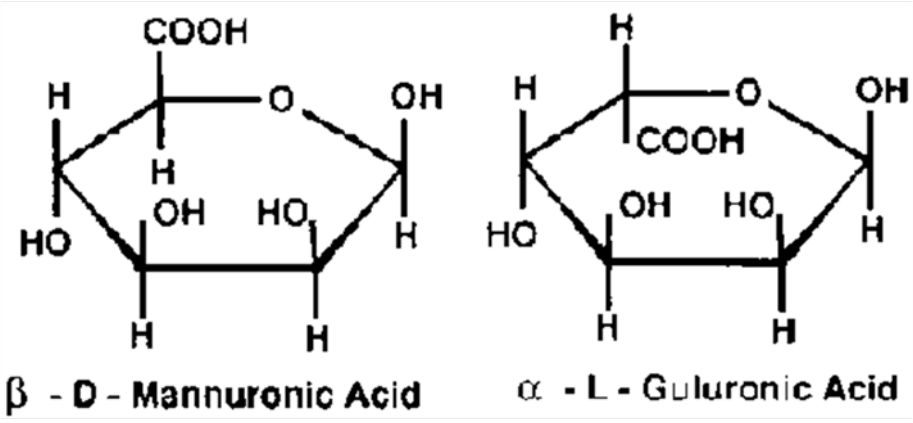

Figure 2.3: Formulas of the two monomeric units of alginic acid

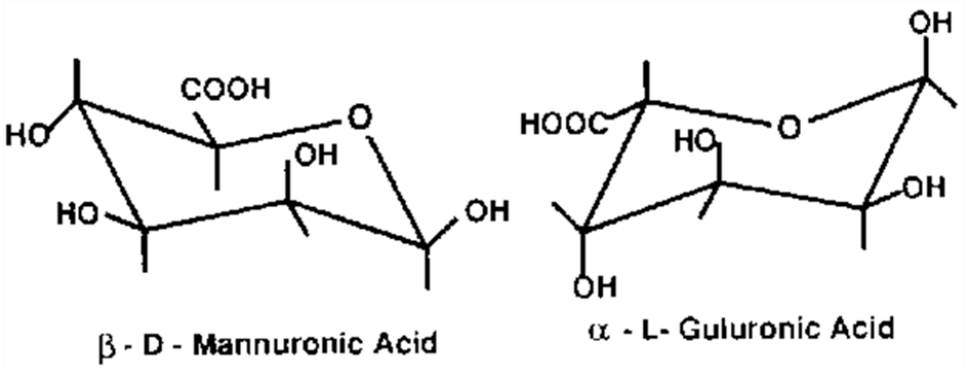

Figure 2.4 Formulas of guluronic and mannuronic acids expressed as chair forms

Alginic acid can either be water soluble or insoluble depending on the type of the associated salt. The salts of sodium, other alkali metals, and ammonia are soluble, whereas the salts of polyvalent cations, e.g., calcium, are water insoluble, with the exception of magnesium. The alginate polymer itself is anionic (i.e., negatively charged) overall. Polyvalent cations bind to the polymer whenever there are two neighboring guluronic acid residues. Essentially, the polyvalent cations are responsible for the cross-linking of both different polymer molecules and different parts of the same polymer chain [CITATION Ste \l 1033]. Addition of calcium chloride to sodium alginic acid leads to cross-linking of the two uronic acids and the subsequent displacement of the sodium ion [CITATION Ste \l 2057]. This leads to the hardening of the gel. The amount of calcium chloride added dictates the degree of hardening of the gel. The gel formed in this manner is porous and thus allows for smaller molecules to permeate through and not others. Various structures of gels can be obtained based on how the cross-linking moulding process is performed. Most commonly, round beads with hard cases encapsulating either cells or enzymes are the forms normally prepared. This technique of immobilization is mostly used in enzymes. However, there is little information available on the use of the same in the immobilization of cells more so on mixed cultures.

2.3.6 Mass Transport on an Immobilized System

In supported anaerobic processes, biomass can either aggregate to form a film around the support or adhere to each other to form a dense mass. These biological systems dictate the dynamics with which the substrates and products are transported across them. The material transfer may be described by mass transfer coefficients or by effective diffusivities both encompassing all solute, solvent and local geometry interactions. Molecular diffusion has been considered the major transport mechanism and diffusivities are lower than the correspondent value in water [CITATION AGB99 \l 2057]. There is evidence however of mass transport via convective flow of bulk liquid within a porous structure in aerobic system as outlined by de Beer et al (1994). In their work, they identified internal flows using a confocal laser microscope technique. The work by de Beer et al (1994) lays emphasis on the need to do more research on transport phenomena on anaerobic biofilms. Mass transfer limitations in methanogenic processes and the effects of external flows have been referred to as active agents of internal mass transport processes in anaerobic systems [CITATION Kit92 \l 2057 \m Bri97]. According to Brito and Melo (1997), this hypothesis hasn't been verified and quantified experimentally. This is also in agreement with work published by Alphenaar et al (1993) and Kato et al (1994). The most commonly used mass transport regimes for systems immobilized on porous membranes is the local two film theory. Brito and Melo (1999) studied the effect of biofilm on substrate transport using the two film theory. He used a flow cell made of semi-circular acrylic glass of radius 0.025 m connected to a porous membrane of 0.22 μ m pore sizes. The membrane was prepared to measure 0.030 m width by 0.107 m length. He then observed the surface of the film offline using a video monitor connected to a microscope video-camera equipped with a lens of magnification X200. The

measurement of the film thickness was done using a digital micrometer, Mitutoyo. He then analysed the biofilm samples using scanning electron microscope for their thickness and surface morphology. The kinetics of mass transfer were monitored using the lithium ion obtained from Lithium Chloride. The measurement of the time change concentration of the ion was done using both flame photometry and conductivity measurements. The mass transfer kinetics were analysed based on the following material conservation laws:

$$V\frac{dC_2}{dt'} = Aj \quad \ldots\ldots\ldots\ldots\ldots\ldots\ldots\ldots\ldots\ldots\ldots 2.2$$

Or

$$V\frac{dC_2}{dt'} = Ak\left(C_1 - C_2\right) \quad \ldots\ldots\ldots\ldots\ldots\ldots\ldots 2.3$$

where V refers to the volume of the diffusion side, compartment II (m^3), C_1 and C_2 are the lithium concentrations in the two sides of the membrane, compartment I and II (mg/l), A is the area of mass transfer of the membrane (m^2), j is the mass transfer flux (mg/m^2h), k (m/h) is the overall mass transfer coefficient and t ' is the time when the sample of lithium was taken for mass transfer measurement. Considering C_1 constant, separating variables and integrating with the boundary conditions (C_2 =0, t = 0), the following equation is obtained:

$$\ln\frac{\left(C_1 - C_{2(t')}\right)}{C_1 - C_{2(t'=0)}} = t$$

Mass transfer coefficients across the different media, i.e. liquid film, biofilm and membrane are combined in an overall mass transfer coefficient, k_t. Brito and Melo

(1999) outlined that, if k_b is the internal (biofilm) mass transfer coefficient, its reciprocal is the difference between the overall mass transfer resistances evaluated with and without biofilm, respectively, neglecting partition effects:

$$\frac{1}{k_b}=\frac{1}{k_t}-\frac{1}{k_{ml}} \quad \text{.....2.5}$$

Where $k_{(t=t)} = k_t$ is the overall mass transfer coefficient and $k_{(t=0)} = k_{ml}$ is the external mass transfer coefficient plus the membrane mass transfer coefficient (without the biofilm on the membrane). Brito and Melo (1999) opted that instead of making assumptions about biofilm kinetics or inactivating the biomass, lithium chloride was used as a non-reactive tracer that was able to diffuse through the biofilm. He kept Lithium ion concentration lower than 500 mg/l to avoid possible inhibition effects. Concentration in the diffusion side was typically maintained between 1-10 mg/l of Lithium ion. In summary, Brito and Melo (1999) observed that, during biofilm formation under liquid velocities of 1.5 and 13.2 m/h, a range which most anaerobic bioreactors operate under, internal mass transfer coefficients were routinely measured. Mass transfer coefficients attained pseudo steady-state values between $2-4\times10^{-3} m/h$ and there was no dependence observed between bulk flow and internal mass transport rates. In studying the transport phenomena of substrates across the support, it will be possible to explain the various variations that normally occur in the formulated mathematical models. Inamdar (2009) outlined that in packed systems, the rate controlling step in the course of substrate degradation shall dictate the final kinetics. The rate controlling step is always taken to be the slowest step. The two dorminant processes that directly affect the rate of biomethanation include: the rate of mass transfer of the substrate into the core site of biological metabolism and the rate of biochemical reaction of the substrate at the site of metabolism. To identify the rate

controlling step amongst the two processes, Inamdar (2009) suggested a test parameter can be used to decipher this, the Damkohler's number (N_{Da}). Damkohler's number, is a dimensionless quantity and is given by:

$$N_{Da} = \frac{\mu_{max}}{K_L[S_b]} \quad \ldots\ldots\ldots\ldots\ldots\ldots\ldots\ldots\ldots\ldots 2.6$$

where $[S_b]$ is arithmetic mean concentration of substrate in the bulk liquid in g/l , K_L is the liquid phase mass transfer coefficient in m/min and μ_{max} is the maximum reaction rate per unit of external surface area ($g/l.min$)

The analysis of the rate controlling step using the Damkohler's number is suitable for supported system whereby the microbial consortia is immobilised within a solid boundary like in the case of a membrane type. This is because in this case it is easier to evaluate K_L using two film theory of mass transfer as in the case used by Brito and Melo (1999). However, evaluation of K_L is difficult with the two film theory in the case of a system supported on an adsorbent bed. Weber and Morris (1963) proposed a model based on the intra-particle diffusion for sorption data of adsorbates from solution:

$$q_t = k_{id}\sqrt{t} + A \quad \ldots\ldots\ldots\ldots\ldots\ldots\ldots\ldots\ldots\ldots 2.7$$

Where q_t is the adsorption quantity (mg/g) at time t (min), k_{id} is the diffusion rate constant ($mg/gmin^{1/2}$) and A (mg/g) is a constant that provides information on the thickness of the boundary layer [CITATION web63 \l 2057]. In a system that is rapidly stirred, the value of A diminishes to about zero. At this state of rapid stirring, the rate of mass transfer is enhanced and therefore the system would probably be controlled by the rate of biochemical degradation especially so if the adsorbent packing is freely suspended. If the mixing is moderate, then most likely intra-

particular mass transfer controls the rate of biomethanation. If this mechanism is true, then a plot of q_t against $\sqrt{t}$ shall exhibit a straight line. The gradient of this line shall be the diffusion rate constant. If the data of q_t vs $\sqrt{t}$ exhibits a multi-linear plot, then it implies that other processes or sorption mechanisms control the rate of biomethanation[CITATION web63 \l 2057].

2.3.7 Kinetics of Biomethanation and their Mathematical Models

Fermentation process involves the utilization of nutrients by micro-organisms from a medium and a subsequent conversion into biological compounds. Part of the nutrients go into the supply of energy, some go into the biosynthesis of associated products while others are assimilated into the cellular materials of micro-organisms as in the case of biomass growth. The growth of biomass is in terms of size and numbers. The features of this growth vary as per the genome of the microbe and the essential nutrient requirements. The presence or absence of these factors of growth greatly hinders the kinetics of biomass growth [CITATION Sye09 \l 2057]. The study of these growth factors and how they affect the product formation has been an elaborate area of study. Models have also been formulated to represent the observed phenomena of growth as the factors are varied. Biomethanation process on distillery waste water depends on a number of factors. The most notable one is the concentration of substrate. Higher concentrations of substrates inhibit the biomethanation process. The actual life case is structured and segregated in that it contains discrete, heterogeneous cells with multi-component substances [CITATION Sye09 \l 2057]. However, if cell to cell heterogeneity doesn’t substantially influence kinetic process, then balanced growth approximation can be assumed. In this case, the idealized case of unsegragated and unstructured model is assumed [CITATION Sye09 \l 2057]. The kinetic information of biomethanation can be obtained based on the reactor configuration. A

simplified case for the study of the fermentation behavior is to assume spatial uniformity and even mixing in the reactor set-up. Since batch reactors in anaerobic systems are the easiest to control, they are the most commonly used. Therefore, a detailed consideration of the batch reactor kinetics is important. In an ideal batch reactor, growth proceeds in a manner that nothing is added or removed until the process is completed. The concentration of cells, substrates and products vary with time [CITATION Sye09 \l 2057].

The behavior of the system is analyzed using material balances in the culture:

$$\frac{d}{dt}\left(V_R \times C_i\right) = V_R . r_{fi} \ldots\ldots\ldots\ldots\ldots\ldots\ldots\ldots\ldots\ldots 2.8$$

where, V_R is the culture volume, C_i refers to the moles of i per unit culture volume and r_{fi} is the rate of formation of i per unit culture volume per unit time. Since no liquid is added or removed, then V_R is constant and thus:

$$\frac{d}{dt}\left(C_i\right) = r_{fi} \ldots\ldots\ldots\ldots\ldots\ldots\ldots\ldots\ldots\ldots\ldots\ldots 2.9$$

r_{fi} depend on growth medium parameters and the state of cell population which include factors like morphology, composition and age distribution of cells. In a balanced growth, the average cellular sysnthesis are not affected by the growing cells. The net rate of cell mass growth, r_x is given by:

$$r_x = \mu X \ldots\ldots\ldots\ldots\ldots\ldots\ldots\ldots\ldots\ldots\ldots\ldots\ldots\ldots 2.10$$

Where, μ is net specific growth rate of cells per time [CITATION Sye09 \l 2057].

μ takes different forms and considers various aspects of the microbial system. Each form of μ constitute a model that takes into consideration various factors that affect the system. The most basic form is the Monod model proposed in 1942. It takes into consideration the saturation isotherm to relate to the growth rate of biomass in the prevailing feed concentration. It is expressed in the form:

$$\mu = \frac{\mu_{max} S}{K_s + S} \ldots\ldots\ldots\ldots\ldots\ldots\ldots\ldots\ldots\ldots\ldots\ldots\ldots\ldots 2.11$$

where μ is the specific growth rate (day^{-1}), S is the substrate concentration (g/l), μ_{max} is the maximum specific growth rate and K_s is the Monod's constant. Since microbes require many substrates in their growth, Monod model assumes that all but one limiting substrate are present in excess of the requirement and that substrate relates to S. Other type of models relate to cellular processes that are inherent to the system in question. They include terms that account for aspects like, presence of an inhibitor, limitations due to the carrying capacity, competition for the culture medium etc [CITATION Jan08 \l 2057]. Other examples of growth models include:

The Tessier model $\mu = \mu_{max}\left[1 - e^{\left(\frac{-S}{K_s}\right)}\right] \ldots\ldots\ldots\ldots\ldots\ldots 2.12$

The Moser Model $\mu = \mu_{max}\left[1 - K_s S^{(-\lambda)}\right]^{-1} \ldots\ldots\ldots\ldots\ldots\ldots 2.13$

The Contois model $\mu = \mu_{max}\left[\frac{S}{BX + S}\right]$ where BX is $K_{sx} \ldots\ldots 2.14$

The Andrews Model $\mu = \frac{\mu_{max} S}{K_m + S + \frac{S^2}{K_I}} \ldots\ldots\ldots\ldots\ldots\ldots\ldots\ldots\ldots\ldots 2.15$

(Considers systems having inhibiting substances)

Writing the material balance equation for batch fermentation with S being the limiting substrate:

$$V_R \frac{d}{dt}(S) = V_R . r_s \ldots\ldots\ldots\ldots\ldots\ldots\ldots\ldots\ldots\ldots\ldots\ldots\ldots\ldots\ldots 2.16$$

where r_s is the rate of conversion of substrate per unit volume of the reactor. There is a yield coefficient constant defined as: $Y_{\frac{X}{S}} = \frac{\Delta X}{\Delta S}$, which can be re-written as,

$$Y_{\frac{X}{S}} \frac{dS}{dt} = \frac{-dX}{dt} \quad \text{.....2.17}$$

Also,

$$Y_{\frac{X}{S}} \times r_s = -\mu . X \quad \text{.....2.18}$$

Thus,

$$Y_{\frac{X}{S}} \frac{dS}{dt} = -\mu . X \quad \text{.....2.19}$$

Also,

$$\frac{dS}{dt} = -\mu . X \frac{1}{Y_{\frac{X}{S}}} \quad \text{.....2.20}$$

It can also be written that:

$$Y_{\frac{X}{S}} = Y = \frac{\Delta X}{\Delta S} = \frac{X - X_O}{S_O - S} \quad \text{.....2.21}$$

Upon re-arranging becomes:

$$S = S_O - \frac{X - X_O}{Y_{\frac{X}{S}}} \quad \text{.....2.22}$$

If the Monod Model of growth is assumed, then

$$\left(\frac{\mu_{max} S}{K_s + S} \right) V_R . X = V_R . \frac{dX}{dt} \quad \text{.....2.23}$$

Thus,

$$\frac{dX}{dt} = \left(\frac{\mu_{max} S}{K_s + S} \right) X \quad \text{.....2.24}$$

Integrating with the boundary conditions as t = 0, $X = X_o$ and t = t, X = X the following equation is obtained:

$$t = \frac{(K_S . Y + S_O Y + X_O)}{\mu_{max}(YS_O + X_O)} . \ln\left(1 + \frac{Y(S_O - S)}{X_O}\right) - \frac{K_S . Y}{\mu_{max}(YS_O + X_O)} . \ln\left(\frac{S}{S_O}\right) \ldots..2.25$$

The above equation can be used to estimate the time needed in the growth of micro-organisms [CITATION Sye09 \l 2057]. Besides the models taking into account the cellular processes, there are other kinetic models that take into account the environmental factors that dictate the carrying capacity of the nutrient medium and the reactor configuration. These models are sigmoidal in nature. They are unstructured models and depict microbial density versus time in their profile. From the works of Zwietering et al, (1990) it is outlined that predictive modelling in future is quite promising and can be applied in predicting the shelf life of products, detecting of critical parts of production and in the optimization of production of products. In order to build these models, growth had to be measured and modelled. Bacterial growth often show a phase in which the specific growth rate start at a value of zero and then accelerates to a maximal value (μ_{max}) in a certain period of time, resulting in a lag time, λ. In addition, growth curves contain a final phase in which the rate decreases and finally reaches zero, so that an asymptote, A is reached. When the growth curve is defined as the logarithm of the number of organisms plotted against time, these growth rate changes result in a sigmoidal curve.

The growth models of this nature are found in a number of literature and most of them are semi-empirical. They include Gompertz, Richards, Stannard, Schnute, the logistic model etc. They describe only the number of organisms and do not include the consumption of substrate as the other models based on the Monod equation would do.

The model doesn't put emphasis on the substrate as it assumes there is enough substrate to allow the process to proceed to intolerable levels of biomass. Since sigmoidal growth curves are for general application, the parameters in them have no meaning in microbiology. Re-parameterization therefore is necessary so as to generate their modified forms which can be applicable to microbial growth systems.

To do this, derivation of equations with biological parameters as functions of a basic equation is done and then evaluation of these parameters is expedited. The obtained biological parameters are then substituted in sigmoidal formula. Amongst these models, Modified Gompertz equation has been the most widely used. Therefore, its detailed consideration is important. Gompertz equation is of the form:

$$y = a.\exp\left[-\exp(b-ct)\right] \quad \text{.....2.26}$$

The inflection point of the curve is obtained by the second derivative of the function with respect to t:

$$\frac{dy}{dt} = ac.\exp\left[-\exp(b-ct)\right].\exp(b-ct) \quad \text{.....2.27}$$

$$\frac{d^2y}{dt^2} = ac^2.\exp\left[-\exp(b-ct)\right].\exp(b-ct).\left[\exp(b-ct)-1\right] \quad \text{.....2.28}$$

At the inflection point, where t = t_i, the second derivative is equal to zero:

$$\frac{d^2y}{dt^2} = 0\ tends¿\ t_i = \frac{b}{c} \quad \text{.....2.29}$$

The expression for the maximum specific growth rate is then derived by calculating the first derivative at the inflection point as:

$$\mu_{max} = \left(\frac{dy}{dt}\right)_{t_i} = \frac{ac}{e} \quad \text{.....2.30}$$

The parameter c in the Gompertz equation can be substituted for by $c=\mu_{max}e/a$. The description of the tangent line through the inflection point is:

$$y=\mu_{max}.t+\frac{a}{e}-\mu_{max}t_i \quad \text{.....2.31}$$

The intercept on the t-axis of the tangent line through the point of inflection has the meaning of the lag time of the system.

$$0=\mu_{max}.t+\frac{a}{e}-\mu_{max}t_i \quad \text{.....2.32}$$

Using equations 2.29, 2.30 and 2.32, it is obtained that:

$$\lambda=\frac{(b-1)}{c} \quad \text{.....2.33}$$

The parameter b is replaced by:

$$b=\frac{\mu_{max}e}{a}\lambda+1 \quad \text{.....2.34}$$

When t approaches infinity, the asymptotic value is attained.

$$t\to\infty; y\to a \wedge A=a$$

If the parameter a is replaced by A in the Gompertz equation, then the Modified Gompertz equation is obtained as:

$$y=A.\exp\left\{-\exp\left[\frac{\mu_{max}.e}{A}(\lambda-t)+1\right]\right\} \quad \text{.....2.35}$$

[CITATION Zwi90 \l 2057]

2.4 Trends in Biomethanation over Supported Biomass

A number of publications are abundantly available on the treatment of the distillery waste water using anaerobic digesters. From the general study of these publications, they have dealt with diluted distillery waste waters and the conventional passive immobilisation of consortium in both continuous and batch systems. Some authors have carried out studies on active immobilisation of cells for instance Lalov et al

(2001). However, most of them have carried out experiments based on diluted distillery waste waters. Information on the use of high strength distillery waste water is scanty and limitations prevail on the use of the available data in the design of a pilot unit that utilises active immobilisation techniques especially in the case of using cross-linked co-polymer gels.

As of the case of the calcium alginate gel immobilisation, there is scanty information on the behaviour of the gel membranes in terms of mass transport as compared to the rate of biochemical activity of the immobilised cells. Information pertaining to the rate controlling step in the high strength heterogeneous substrate degradation of distillery waste water is very scarce and almost impossible to come by. Therefore, with this very limited data, it may not be possible to design a sound engineering system based on immobilised cells using calcium alginate gels.

Also, there is very little available data relating to the behaviour of bound cells through active adsorption on conditioned natural zeolite. This makes it necessary to carry-out more studies on the behaviour of biomethanation systems when the consortium is bound to activated natural zeolite support.

The core objective of this investigation therefore, was to study the missing gap that exists in supported biomass systems. The identified and studied were on the effect which different immobilisation media impart on the kinetics of biomethanation, oxygen tolerance levels, response to high strength substrate charge, rate controlling step between intra-particular material flux and biochemical reaction rate and level of tolerance to electrolyte loading. The system kinetics was studied and the biochemical digestion parameters were determined. Mathematical models that represented the system behaviour were also generated. The behaviour of systems towards oxygen

charges were also established besides the determination of the rate controlling step in the biochemical degradation process.

CHAPTER THREE
RESEARCH DESIGN AND METHODOLOGY

3.1 Materials and Methods

Waste water used for the project was obtained from temperature stabilization lagoons after the distillation stage in a molasses distillery in accordance to the consulted literature. Unique support media that had unrelated immobilization structure were used since the experiment focused on studying how different immobilization techniques affected various output dependant variables of physical concern. A choice of activated natural zeolite (sodium chloride activated clinoptilolite) and calcium alginate polymer were prepared. Calcium alginate gel had a starting precursor as sodium alginate gel. Their immobilization behaviors were then compared with that of the unsupported system. Because of the unique characteristics demonstrated by the calcium alginate immobilized system, further studies were done on its operational phenomenon. The consequential behavior of diffusive mass flux and biochemical degradation of the substrate was the subject considered, and the limiting case was evaluated.

3.2 Materials

The materials and preliminary preparation stages that were carried out prior the real study were of five categories, namely: the wastewater preparation and characterization, the immobilization media preparation and characterization, the cultivation and immobilization of the inoculums, determination of the most suitable cultivation temperature and finally, determination of the most suitable initial reactor pH.

3.2.1 Collection and Characterization of the Cultivation Substrate

The cultivation substrate used was collected from temperature stabilization lagoons after the distillation unit in Agro-Chemicals Ltd., Muhoroni, Kenya. The sampling of the waste water at the collection point was done in accordance to the standard procedures of sample waste water collection. The samples were immediately refrigerated and maintained at a temperature of about 4 °C. The waste water was then transported to Moi University, under this condition. It was then characterized for the following parameters: pH, Dissolved oxygen (DO), Chemical oxygen demand (COD), Biological oxygen demand (BOD), Total solids (TS), Total suspended solids (TSS) and Total nitrogen (TN).

The determination of the pH was done using the glass electrode technique. The glass electrode has hydrogen ion responsive electrode as the sensing element. Three samples of the same substrate were measured to volumes of 50 ml and placed in 100 ml beaker. A pH meter was then inserted into each beaker then left for 2 minutes under a gentle and continuous stirring at 250 rpm. The pH reading was then made from the liquid crystal display screen and the average pH value determined. The meter type used was Hanna, H1 2211 pH/ORP.

The COD was determined using closed reflux chrome colorimetric technique. Here, the digestion vials and their caps were washed with 20% sulphuric acid solution to prevent contamination. 1 ml of the sample was then put into the vials and mixed with 2.5 ml of a digestion solution (potassium dicromate solution). It was then followed by 3.5 ml conc. sulphuric acid reagent solution. The tubes were then tightly capped and each was inverted several times to mix completely. The sealed vials containing the mixture were then digested in a block digestor at 150^{o}C under total reflux for 2 h. The

mixtures were then cooled, then the tubes were wiped and the absorbance of the solution was taken at 600 nm in a Shimadzu UV-VIS spectrophotometer.

In the BOD measurements, the DO was determined instrumentally using, Hanna HI 9142 dissolved oxygen meter. The water of formulation was redistilled in the presence of alkaline permanganate and aerated overnight at 20 ^{o}C with clean compressed air from an air filtering pump. 1 ml each of 0.25M $CaCl_2$, 0.23M $MgSO_4$, 0.00154M $FeCl_3$ and phosphate buffer solutions (Prepared by dissolving 8.5 g of KH_2PO_4, 21.75 g of K_2HPO_4, 33.4 g of Na_2HPO_4 and 1.7 g of NH_4Cl in 1 litre double distilled water) was then mixed with 1 litre of the aerated double distilled water. 1.5 ml effluent of the Moi University aerobic biological lagoon was then used for seeding. The waste water was then diluted to 10 % its initial strength using the standard dilution solution and carefully siphoned into BOD bottles while avoiding air entrainment. One set of the solutions in the BOD bottles was used in the determination of the oxygen level using the DO meter while rest were incubated at 20 ^{o}C for five days. After the five days, the BOD content of all the incubated samples of the set were determined and following relation was used in the calculation:

$$BOD \in mg\ per\ litre\left(5\ days\ 20^{0}C\right)=\frac{\left(DO_0-DO_5-B\right)X\ 100}{of\ the\ sample\ used}$$

where DO_0 was the initial DO content in mg/l, DO_5 was the DO content after incubation for five days and B was the blank correction determined by the difference in the DO contents of the blank at start of incubation and after the five day incubation period.

In the total solids determination, three sets of the wastewater each containing 100 ml volumes were dried in an oven at 105 °C until there were no more changes in their

weights. The differences in their weights were then determined and an average percentage of their total solids was then calculated.

In the measurement of suspended solids, three samples of the wastewater each containing 25 ml were measured. The samples were then filtered using a filter paper and the filtration was aided by a vacuum pump. The filter cake was then dried at a temperature of 105 °C until constant weights were obtained. The average suspended solid matter was then calculated.

Total nitrogen was determined using potassium persulfate digestion under alkaline conditions. The persulfate oxidation technique for total nitrogen in waste water was performed under heated alkaline conditions in an autoclave at 120 ºC where all the organic and inorganic forms of nitrogen were oxidized to nitrates. As the reaction proceeded NaOH was consumed and the pH of the solution dropped to <2.2 which was a good demonstration that proper oxidation had taken place. The digested sample was then analysed for nitrate using Shimadzu UV-VIS spectrophotometer. The obtained absorbance was then compared against the standard curve of a known nitrogen containing substance initially analysed.

3.2.2 Preparation and Characterization of the Immobilization Media

The sodium alginate gel was purchased from Sigma Aldrich Co. Ltd as powder and no prior preparation was required as it was relatively in its pure form. Clinoptilolite was purchased from Jax Industries, South Africa in its raw form. It was double washed, air dried, milled and sieved to particle size ranges of 150-300 µm.

The activation of cleaned clinoptilolite was done using 2 M NaCl solution. 100g of the cleaned and air-dried natural zeolite was measured and added to 2 M NaCl solution then stirred continuously at 250 rpm for 72 hours. The solution was then

vacuum filtered. The now conditioned natural zeolite was double washed with distilled water to remove the residual NaCl. Finally, it was vacuum filtered and air-dried for 24 hours. For any adsorbent to be fully characterized, the following parameters need to be analysed: adsorption capacity, adsorption surface area, internal pore structure, pore sizes, pore volume, surface morphology, optimal adsorption temperature and the functional groups responsible for adsorption. Adsorption surface area, pore size, pore volume, surface morphology and activation temperature were specified from other people's work in various documentations. However, adsorption capacity was determined in this study through experiments.

In the determination of the adsorption capacity, batch experiments were carried out using 100 ml stoppered conical flasks containing 50 ml of the inoculum having a concentration of 10 g/L biomass peptides measured as amino acids in solution. To this solution, 5 g of the conditioned natural zeolite was added and stirred at 250 rpm for 24 hours. The solution was then vacuum filtered and the cake re-suspended in 100 ml of distilled water. The suspension was once again vacuum filtered and the filtrates from the two stages were mixed and biomass amino acid concentration was again determined. The final mass of biomass peptide in the filtrate was then calculated and the carrying capacity of the activated clinoptilolite determined. In order to correct for any adsorption of biomass due to containers, control experiments were carried out without the addition of the adsorbent and finally the correction was done.

3.2.3 Cultivation and Immobilization of the Mixed Methanogenic Consortia Innoculum

The mixed methanogenic culture used in the experiment was obtained from anaerobic digester sludge collected from Agro-chemical ltd. The culture medium was a standard

consortium that had its constituent species and their respective abundance earlier determined by the company. They were used in respective proportion as the mother culture was in Agro-Chemical Ltd. The consortia was enriched and maintained in a fresh anaerobic growth medium containing the constituents shown in Table 3.1

Table 3.3: The microbial growth medium

Component	Amount	Function of component
Vinasse (carbon source, g)	50	C and energy source
K_2HPO_4 (g)	25	pH buffer; P and K source
KH_2PO_4(g)	20	pH buffer; P and K source
$CaCl_2$(g)	1.0	Ca^{2+} source
$MgSO_4$ $7H_2O$(g)	5.0	S and Mg^{2+} source
$FeSO_4$ $7H_2O$(g)	0.1	Fe^{2+} source
$MnSO_4$ $7H_2O$(g)	0.05	Mn^{2+} Source
$CaCl_2$ $6H_2O$(g)	0.1	Ca^{2+} source
$AlK(SO_4)_2 12H_2O$(g)	0.01	Al^{3+} and K^+ source
NH_4Cl(g)	1.0	N source
Water(g)	Top up to 1 litre	Dissolving solution
pH	7.0	

Enrichment involved the collection of the cells by centrifugation at 5000 g for 20 minutes under anaerobic conditions. The enriched methanogenic culture was then adapted to the substrate in a batch reactor under strict anaerobic conditions at 40°C.

The concentration and viability of the cells was monitored by both tracking the biogas produced and performing the biomass amino acid content test [CITATION Lee92 \l 1033] using Lowry procedure. The Lowry procedure involved the reaction of the peptide nitrogen with the copper (II) ions under alkaline conditions and the subsequent reduction of the Folin-Ciocalteayphosphomolybdicphosphotungstic acid to heteropolymolybdenum blue by the copper-catalyzed oxidation of aromatic acids. This reaction was accompanied by colour change which corresponds to the amount of amino acids initially present. The absorbance of the reduced solution was then

measured using Shimadzu Double Beam, UV-VIS spectrophotometer at a wavelength of 600 nm. Since the value of absorbance corresponds to the concentration of the amino acids present, the obtained absorbance was related to the initially pre-determined concentration from the tryophthan polypeptides of the standard bovine serum albumin used to generate the standard curve. The bovine serum albumin was purchased from Sigma Aldrich co., USA. Since the Lowry method is known to be sensitive to pH changes, the pH of the assay solution was maintained at 10 - 10.5 using NaOH and $NaCO_3$ solution and very small volumes of sample were also used (0.25 ml) as these would have little or no effect on pH of the reaction mixture. Also since the method is sensitive to low concentrations of polypeptides, concentrations ranging from 0.10 - 2 mg of polypetides per mL were therefore maintained. After the experiment, the pH of the final solution was then checked to confirm if it was still within the 10-10.5 range. If any solution had its pH falling below 10.0, then more dilutions were done to make it fall within the range. A variety of compounds are known to interfere with the Lowry procedure. They include some amino acid derivatives, certain buffers, drugs, lipids, sugars, salts, nucleic acids and sulphydryl reagents, ammonium ions, zwitterionic buffers, nonionic buffers and thiol compounds among others. Some of these substances are present in the distillery waste water. Therefore, to suppress their effect some were eliminated by enrichment through centrifugation, rinsing and subsequent dilution of the culture. The final enriched methanogenic consortium was adjusted to a polypeptide concentration of 10 g/L and stored in a deep freezer at temperatures of below 4 ^oC. Enrichment through centrifugation, rinsing in fresh media and re-suspension in a fresh solution is able to eliminate the effects of the interfering substances [CITATION Lal01 \l 2057].

In the immobilization of the mixed methanogenic consortium onto an activated

natural zeolite support, the experiment was carried out in a batch mode. The pH of the wastewater was adjusted using sodium hydroxide and hydrochloric acid. The biomass from enriched methanogenic population adapted to molasses distillery waste water at concentration of 10 g/L polypeptides was used for immobilization. The biomass cells were suspended and washed in an oxygen-free phosphate buffer, and then adjusted using the same buffer to attain a biomass concentration of 10 mg protein per ml. The obtained suspension was then added to the pre-activated natural zeolite support and stirred anaerobically using a magnetic stirrer for 24 hours at 25^{o}C. The support together with the immobilized biomass was then repeatedly washed with a sterilized nutrient solution until no free biomass in the washing waters was observed. Concentration of biomass before and after adsorption was monitored by carrying out polypeptide measurement with the Lowry procedure. 10 g of the now immobilized biomass obtained by centrifugation was then used to inoculate each of the batch reactors in the biomethanation stage.

The immobilization of the enriched and adapted methanogenic consortium into calcium alginate beads involved the cross-linkage formations of micro-porous micelles to form alginate capsules. This process was carried out by dissolving 9 g of sodium alginate powder in 300 ml of the enriched methanogenic consortium prepared to have a concentration of 10 mg/L of polypeptide biomass. The solution was then stirred in an inert environment, of only nitrogen gas, at 250 rpm until all sodium alginate was completely dissolved. The final solution contained 3% alginate by weight. The entrained bubbles were then degassed, by gently tapping on the walls of the container. In an inert environment, the cell-sodium alginate mixture was dripped from a height of 20 cm at a rate of 10 drops per minute, into 1000 ml cross-linking solution. The mixture was then stirred for 1 hour with the aid of a magnetic stirrer.

Gel formation was achieved as soon as the sodium alginate drops come into direct contact with the calcium chloride solution but it took about 1 hour for the formed beads to case-harden. The beads formed were about 2 mm in diameter. The beads were then washed with fresh calcium crosslinking solution. 10 g of calcium alginate immobilized consortium were then measured and inoculated into the batch reactors in the biomethanation stage.

3.2.4 Determination of the most suitable Fermentation Temperature

In this study, four experimental set-ups operating in batch mode were conducted each having the same initial organic loading of COD 50 g/l according to Lalov et al, (2001) and adjusted to have an initial pH of 7.0. Each set-up was subjected to different temperatures. The respective temperature ranges set were: 30, 35, 40 and 45 ^{o}C. The agitation rate was moderate shaking for 10 minutes over intervals of 8 hours. The dependant output variable considered was the cumulative amount of biogas generated which was later analysed as a property that depended on the fermentation temperature.

3.2.5 Determination of the most suitable initial pH of Fermentation

In this study, four experimental set-ups operating in batch mode were conducted each having the same COD loading of 50 g/l and adjusted to have a fermentation temperature 40 ^{o}C obtained as the optimal value in section 3.2.4. Each batch reactor was set to have different initial pH levels. The respective initial pH ranges were: 5.0, 6.0, 7.0 and 8.0. The reagents were then subjected to a moderate agitation for 10 minutes over intervals of 8 hours. The dependant output variable considered was the cumulative amount of biogas generated which was later analysed as a parameter that depended on the initial pH of the reactor.

3.3 Batch Studies of Biogas Generation

Three experimental sets of batch processes were conducted in the biomethanation of distillery waste water, where in each set, there were four individual experiments. The first set contained the culture medium and the inoculum without the support material whereas the second and third sets contained activated natural zeolite and the calcium alginate material as supports respectively. The parameters studied included the initial organic loading, the biomethanation time change and sterile air exposure intervals required to cause irreversible change in the biochemical activities. The first set acted as a control experiment and was used as datum of comparison of the inherent effects imparted by the support material on the output variables. The output variables of importance considered were the levels of residual COD at equilibrium and the ultimate cumulative amount of biogas generated. The value of these parameters at every time interval informed the optimal settings of the manipulatable variables and factors of the experiment. From these variables, the analysis of the study was drawn.

3.3.1 Choice of Suitable Organic Loading

To each set of experiment, variations of the organic loading measured in terms of COD were done over four intervals of 0, 25, 50 and 75 g/L at a mesophilic temperature range of 40 ^{o}C. Organic loading values were chosen as to mimic the conventional distillery waste water fermentation dilutions. The contact time was allowed to be at the maximum level where equilibrium of the slowest reaction was attained. The optimal pH of the mixture was also set at the initially pre-determined value of 7.0. The agitation rate was moderate shaking for 10 minutes over intervals of 8 hours. The most suitable initial organic loading was then calculated in terms two output variables: the highest yield realized and the highest percentage of waste water stabilization.

3.3.2 Oxygen Tolerance Levels

A second set of experiments having the pre-determined optimal organic loading was set up so as to test the system resilience to accidental or deliberate oxygen exposures. Each system was set at a pH of 7.0 over mesophilic temperature of 40 ^{o}C. Eight experimental set ups were done in each factor chosen and the oxygen tolerance levels was evaluated in each. When the system attained the pseudo-steady state at the exponential phase of microbial growth, sterile air-bubbling was carried out on each set-up at different exposure intervals. The intervals of exposure for eight experiments of the three sets were for: 15, 30, 45, 60, 75, 90, 105 and 120 minutes.

3.3.3 Distinguishing the rate controlling step in the Calcium Alginate supported System

A third set of experiment was conducted so as to study the effect of mass transfer resistance on calcium alginate membrane. The calcium alginate capsules were prepared in the same manner outlined in section 3.2.3. The beads encapsulating distilled water were immersed into 100 ml solution of 50 g/l COD glucose. The rate of movement of the substrate from the solution bulk into the capsule core was then studied. The rate of diffusion of the substrate was measured and then compared with the rate of biochemical degradation of the same. The rate controlling step was then analysed using Damkohler's number, N_{Da} [CITATION Sye09 \l 2057]. Damkohler's number, is a dimensionless quantity and is given by:

$$N_{Da}=\frac{\mu_{max}}{K_L\left[S_b\right]}$$

where $\left[S_b\right]$ is arithmetic mean concentration of substrate in the bulk liquid in g/l , K_L is the liquid phase mass transfer coefficient in m/min and μ_{max} is the

maximum reaction rate per unit of external surface area ($g/l.min$). The kinetic study of degradation of the substrate having initial concentration of 50 g/l COD was performed in the same manner as that of distillery waste water outlined in section 3.3.1. In the experiment, eight set-ups each having 100 ml of 50 g/l COD glucose were prepared in conical flasks and to each flask, 20 beads of the immobilized distilled water were then immersed. The set-ups were subjected to moderate agitation using a magnetic stirrer at 250 rpm for varying time periods. The agitations and diffusion process were allowed to last for 0, 10, 20, 30,40,50,60 and 70 minutes from the first to the eight flasks respectively. The core contents of the beads were finally with-drawn and analysed for the COD of the substrate.

3.3.4 Kinetic Batch Study

For batch kinetic studies, a predetermined optimal organic loading rate of COD 50 g/l was set and the batch reactor subjected to moderate agitation for 10 minutes at 8 hour intervals. The digestion temperature was set at 40 ^{o}C and the initial pH of the system was 7.0. At pre-determined time intervals, the cumulative volume of biogas produced was measured and a small portion of solution (1 ml) was withdrawn and analysed for residual COD and amino acid content. The time-variation of the dependant output parameters were then computed.

3.3.5 Experimental Design

The experimental design used was a classical approach where the variables and/factors were considered one at a time and their corresponding optimal values determined. The subsequent input variable values were determined on the basis of the obtained optimal quantity values of the preceding parameters. The initial organic loading, biochemical reaction time and the time interval of oxygen exposures were

chosen as the independent variables. The residual COD, amino acid content, cumulative biogas volume and biological activity response were regarded as the dependant output response variables of the experiment. The latter output variable involved qualitative measurement whereas the former were determined quantitatively. The table showing the design of experiments is shown in appendix E.

3.3.6 Instruments and Quantitative Chemical Analysis

The initial and residual COD levels were digested in a Hanna block digester and the resultant digestate was measured using UV-VIS Double Beam Spectrophotometer at a wavelength of 600 nm. The inferential relationship between organic load concentration and absorbance was predetermined by calibration performance using potassium hydrogen phthalate standard solution. The COD calibration curve was then generated from the results of the standard. The polypeptide content was measured using Lowry procedure whereby the incubated solution was tested for absorbance using a UV-VIS Double Beam Spectrophotometer at a wavelength of 600 nm. The inferential relationship between polypeptide concentration and absorbance was predetermined by calibration performance using bovine serum albumin standard at an alkaline environment.

CHAPTER FOUR
RESULTS AND DISCUSSION

The degradation process of distillery waste water was studied and an attempt was made to link them to their attributes upon characterization. Their recalcitrant nature particularly showed much more dominant relationship with their low pH values and electrolyte levels present. Though the presence of inhibitors was not studied, distillery waste water is known to contain active anti-oxidants, the melanoidins, which are formed in the Maillard amino-carbonyl reaction [CITATION Jag00 \l 1033] . This was observed from the result in which the use of these substrates without prior pre-treatment exhibited lower levels of performance. From the kinetic results of the experiment, development of models that closely represented the real phenomena was done. Through these models, kinetic parameters that represented the measures of system response and performance were evaluated and discussed in section 4.7.1, 4.7.3, 4.7.3, 4.8 and 4.9. Additionally, from the models, the inherent biochemical and mass transfer kinetics in calcium alginate supported system were also demonstrated. From the forms adopted by these models, their effects and interactions to each other and unto the system were demonstrated.

4.1 Characterization of the Waste Water

Waste water characteristics are more or less similar in most alcohol distilleries. However, there can be a few variations depending on the upstream processes and the upstream microbial system genera used in the primary alcohol fermentation. From the preliminary waste water characterization, vinasse showed the ability to be biologically degraded because its biodegradability index was obtained to be below the value of 3 (Table 4.1 on the COD/BOD ratio). High total suspended solids of 12,450 mg/l also present suggested that problems of sludge bulking in most reaction vessels could

occur [CITATION Jim03 \l 1033]. The significant differences between the values of total suspended solids obtained in this experiment and those from various documentations could have been occasioned by the differences in the sampling points of the waste water from the temperature stabilization lagoons. The determination of potassium, phosphorous and sulphur as sulphate analysis was not conducted because of the limited equipment in the chemical engineering laboratory.

Table 4.4: Comparison of waste water characteristics from Agro-Chemicals Co. Ltd and those by Pathade (1999)

Characteristics	Feedstock	
	Cane vinasse (Obtained results)	Cane vinasse [CITATION Pat99 \l 2057]
COD (mg/l)	75,000	65,000-130,000
BOD (mg/l)	28,000	30,000-70,000
Mean COD/BOD ratio	2.68	2.49
Total Solids (mg/l)	58,058	30,000-100,000
Total suspended solids (mg/l)	12,450	350
Total dissolved solids (mg/l)	-	80,000
Total nitrogen (mg/l)	1400	1000-2000
Total phosphorous (mg/l)	-	800-1200
Potassium (mg/l)	-	8,000-12,000
Sulphur as SO_4 (mg/l)	-	2,000-6,000
pH	4.11	3.0-5.4

4.2 Characterization of the Immobilization Media

For more information on the behavior of the adsorption medium in a biomethanation process, some characteristics needed to be identified so that they could help explain some phenomenon observed. The more general characteristics were obtained from documentations and the rest were studied in this project. The attributes considered

were adsorbent surface morphology, BET adsorption surface area, BET pore volume mentioned in section 2.3.5 and adsorption capacity analyzed in section 4.2.1

4.2.1 Adsorption Capacity

From the analysis done on the filtrate after immobilization, it was determined that the average value of adsorption capacity of the consortia was 13.2 mg/g of adsorbent at an ambient temperature of 25 ° C. This result provided information on the dosage of adsorbent containing the immobilized innoculum unto the sets.

4.3 Analysis of the Effect of pH on Biogas Production

The waste waters stabilization is known to be highly dependent on pH and their recalcitrant nature in most cases is attributed to the low pH levels because of the accumulation of volatile fatty acids. In order to obtain the most suitable operational parameters in fermentation, the effect the pH imparts on the process had to be studied so that it could provide information on the type of preliminary treatment processes to be done. It was obtained that a neutral pH of 7.0 yielded the highest conversions, when the system was set at a mesophilic temperature of 40 °C with an initial organic loading of COD 50 g/l and subjected to moderate shaking for 10 minutes at intervals of 8 hours. This can be seen from figure 4.1.

Table 4.5: Table showing biogas yield over various pH ranges in 200 cm^3 substrate volumes

pH	Cumulative gas volume (cm^3) in a 0.2 litre reactor	Product yield (cm^3/g COD_i)
5.0	1.05	0.105
6.0	182.3	18.23
7.0	848	84.8

8.0	0.6	0.06

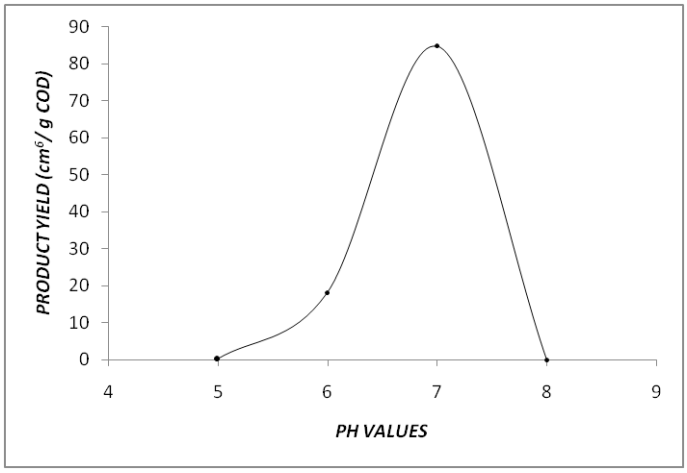

Figure 4.1 Effect of initial pH on the product yield

The high conversions registered at this pH level signified a balanced state between the volatile fatty acids and the un-hydrolysed substrate. A low pH in the system signifies a situation where there is a high quantity of volatile fatty acids. The high or low state of the pH causes imbalances in the syntrophic interaction between acetogens and methanogens, thus making the process unstable and resulting in little amounts of biogas production. [CITATION Jag11 \l 1033]

4.4 Analysis of the Effect of Temperature on Biogas Production

Anaerobic fermentation is in principle possible between 3°C and approximately 70°C. The rate of bacteriological methane production increases with increase in temperatures as the amount of free ammonia also increases [CITATION MJa13 \l 1033]

The lower temperatures slow down the metabolic rates of the methanogenic consortia and thereby slowing down the mean rates of production of biogas. [CITATION MJa13 \l 1033]

In a batch experiment conducted to determine the most preferable digestion temperature as far as cumulative biogas production is concerned, the set-ups were adjusted to have initial organic loadings of COD 50 g/l, pH of 7.0 and subjected to moderate agitation for 10 minutes at intervals of 8 hours. From the results, the set-up that had a temperature of 40 ^{o}C registered the highest product yield as shown in figure 4.2. Therefore, digestion of distillery waste water is most preferred at a temperature of 40 ^{o}C for better product yields.

Table 4.6: Biogas yield over various incubation temperatures in 200 cm^3 substrate volumes

Temperature	Cumulative gas volume (cm^3) in a 0.2 litre reactor	Product yield (cm^3/g COD$_i$)
30	274.6	27.46
35	487.6	48.76
40	701.2	70.12
45	520.6	52.06

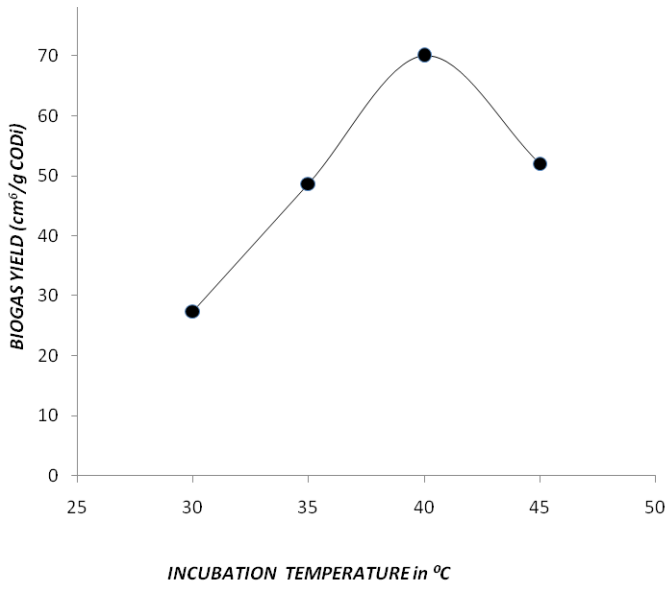

Figure 4.2: Effect of temperature on substrate conversion

4.5 Batch Studies of Biogas Generation

Information on the batch studies of biomethanation was important in the evaluation of the impacts associated with the use of various support materials. The parameters which pointed-out to the performance of each supported system were the degree of substrate conversion, the biogas yield per unit organic loading, reaction rate constant, the biomethanation lag phase duration, substrate biodegradation inhibition factor, the maximum specific growth rates and the oxygen tolerance levels.

To determine each of these quantities, various kinetic studies were carried out to obtain information that could be analysed as to evaluate these quantities. Determination of the most preferable values of the manipulatable variables that gave highest values of the desired quantities was performed in each of the three sets containing different support media.

4.5.1 Kinetics of Biogas Production and Substrate Utilisation over different Support Materials in a Batch System

To each experimental set, the effect of initial organic loading was analysed. This gave information on the system dynamics with the initial organic loadings as the parameter. Since organic loading level was an interconnected with yield, their effects were studied concurrently.

The system responses to various initial organic loadings on different supports were studied with respect to time. The output variable considered was the cumulative biogas produced and residual COD values at various time intervals. Each support material was studied differently and comparisons were made with the unsupported system acting as the datum. The kinetics of biogas production and substrate utilization

in the unsupported system are shown in figure 4.3.

The system having initial organic loading of 25 g/l showed a quick response and also approached the equilibrium faster than the other systems in both product formation and substrate utilization. This could be attributed to the balanced state of the system whereby the driving forces were ideal for microbial growth. The dominant forces in action in the system were growth substrate concentration and osmotic pressures that emanated from the electrolytes dissolved in the medium. The symbiotic relationship between the hydrolytic, acetogenic acidogenic and methanogenic microbial systems was at balance and therefore the result was a synergistic action towards product generation and growth. Other additional parameters influencing the system included the present chemical inhibitors. Some of these chemicals that are contained in the distillery waste waters include phenolic compounds, alcohols, quaternary ammonium compounds, aldehydes and some bacteriocidal agents [CITATION Sye09 \l 1033 \m Asg13]. The system with an initial COD of 50 g/l demonstrated a moderate initial response rate although the manner in which it approached equilibrium was rather sluggish compared to that of COD 25 g/l. The drop in substrate utilization was in synchrony with the product formation and they inversely related to each other. This result signified that the utilization of the substrate was directly related to the product that was formed. The behavior could be enhanced by maintaining a tolerable level of electrolytes and using a stoichiometrically equivalent substrate that is never in excess. Lastly, the system containing initial COD levels of 75 g/l exhibited an anomalous reduction in the residual COD, which was out of synchrony with the corresponding biogas produced. This could be explained by consideration of the biomass growth in section 4.5.2. The utilization of substrate was directed towards endogenic respiration of the microbial population and cell complexation, a process that was not directly associated with the product formation [CITATION Sye09 \l 1033]. It is also note

worthy that the residual COD reduction in this case was not at an appreciable degree and was almost zero in response. This behavior might have been occasioned by the high salinity in the substrate that posed osmotic pressure problems to the microbes. According to Inamdar (2009), when a system has a different electrolyte concentration from its environment, and is separated by a semi-permeable membrane, there will always be a flow of pure water in the direction of increasing concentration. The trend is towards equalizing the concentration of solutes on either side of the membrane. The microbial cells have a solute concentration of nearly 0.95% [CITATION Sye09 \l 2057] and anything higher on the external environment will make the microbial cells shrink and cause plasmolysis. The system considered was analysed to be having an electrolyte concentration of 7.2 % (conductivity measurement based on sodium and chloride ions) which was higher than inside the cells. Certainly, plasmolysis occurred and hindered the growth of microbes. In consideration of the high concentration of the substrate in this medium, the system was also hampered by this high concentration. This observation corroborates Inamdar's work [CITATION Sye09 \l 1033], that substrate inhibition phenomenon can be competitive or non-competitive. If a single substrate enzyme catalysed reaction is the rate limiting step in the microbial growth, then the inhibition of the enzyme activity results in the inhibition of microbial growth by the same pattern.

In the activated natural zeolite supported system, the phenomenon was almost similar to the unsupported system safe for a few variations shown in figure 4.4. The most predominant feature that showed a marked deviation from the unsupported system was the short lag phase in the system. This could be due to the reduced effect of inhibiting substances present in the medium due to the tortorsity of the pores in which the microbes occupied. The narrow pores present in the zeolite structure created safe

dens for microbial population to be shielded from the adverse surrounding environment. The solution surrounding the microbes would in-turn be diluted of inhibitory substances by the diffusive interchange between the fresh substrate and the metabolic wastes of microbial excreta. This led to the high rates of product formation and generally shorter intervals of equilibrium establishment. The systems containing initial COD 50 and 75 g/l demonstrated a more pronounced reduction in the COD. Also the response to this substrate utilization was sharper than the unsupported system. This could only be possible with the reduced effects of inhibitors and a proper symbiotic relationship between microbial systems.

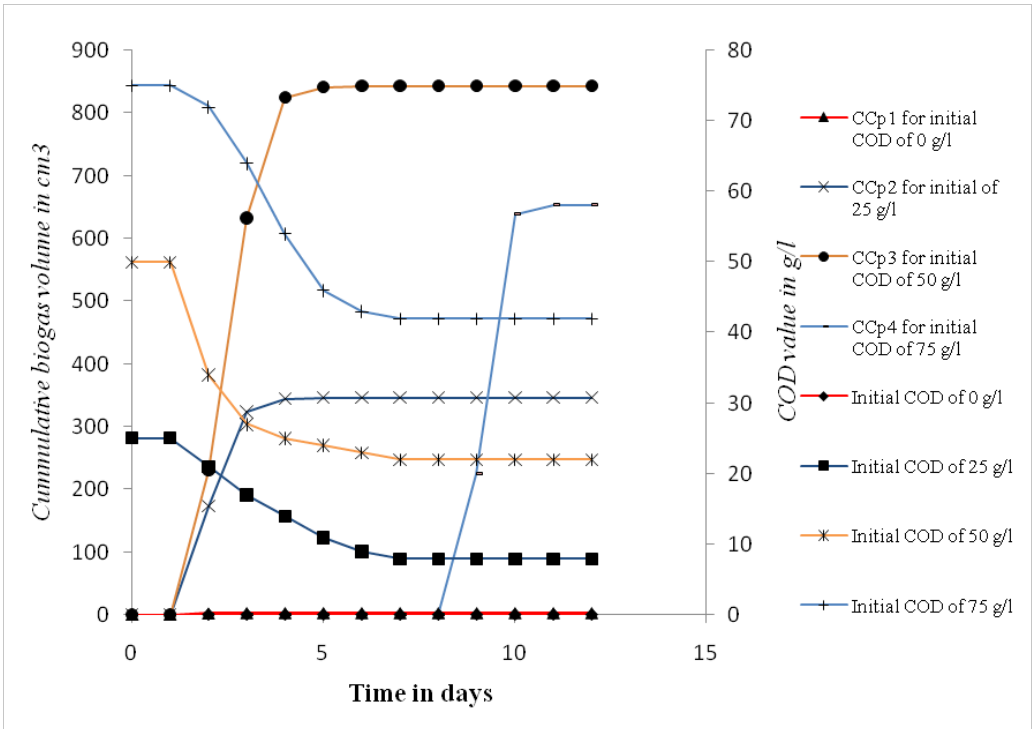

Figure 4.4 Kinetics of biogas production and substrate utilisation over natural zeolite s

It was also noted from figure 4.4 that the regime of approach of equilibrium was rather sharp as opposed to the sluggish one witnessed in the unsupported system in figure 4.3. The rapid decline in the mean rates of biogas production could be attributed to the limiting substrate exhaustion in the culture media [CITATION Sye09

\l 1033]. A large variation from the unsupported system was witnessed in the system containing a high strength waste water of COD 75 g/l which was an undiluted sample. Unlike in the unsupported system, the set-up registered production of large volumes of biogas on the 9th day and was associated with a high slump in the residual COD reduction that was not in synchrony with the product formation. Some of the substrate consumed went into the formation of the product besides some going into the endogenic respiration. The long lag phase was due to the initial harsh environment surrounding the microbes before the eventual dilution of toxins and substrates by the diffusive interchange. The diffusional resistances imparted great effects on the final kinetics over this system. Generally, adsorbents tend to increase the size of the stagnant layer around immobilized systems. Mixing of the solutions cannot completely eliminate the stagnant film and therefore micro-organisms can thrive better in this environment as opposed to the free system [CITATION Sye09 \l 1033]. Conclusive explanation of this behavior could be demonstrated by consideration of mass transfers of the known inhibitors present in the culture from the liquid bulk to the interstitial pores of zeolite supports. This study was considered to be out of the scope of this project.

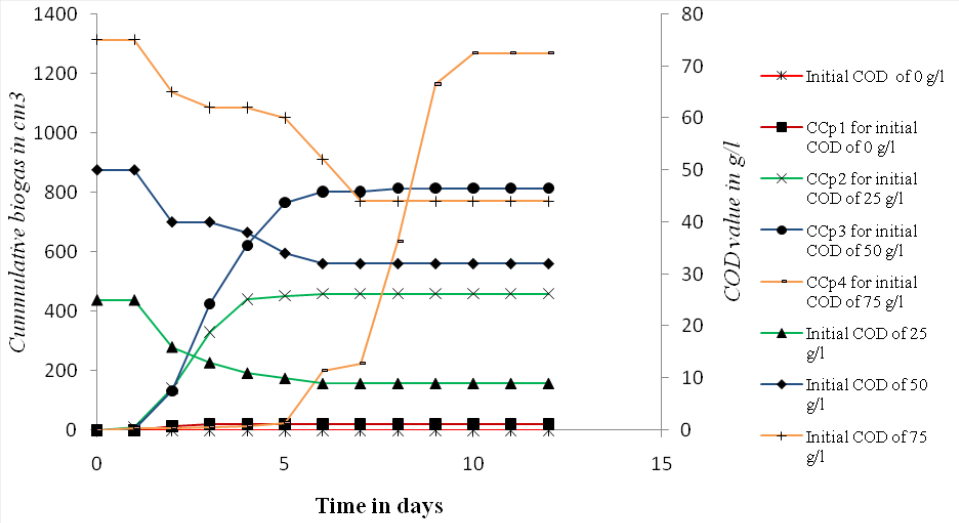

Figure 4.5 Kinetics of biogas production and substrate utilisation over calcium alginat

In the calcium alginate supported system, Figure 4.5, notable observations were made. There was an initial rapid response and almost zero lag phase in the low strength systems. This behavior signified fast adaptability of the consortium to the substrate. There was also a sharp approach to the equilibrium state which must have been caused by the exhaustion of the growth limiting substrate. All the systems except control, displayed distortions and discontinuous sections in their curves. This behaviour corresponded with the observed phenomenon whereby the calcium alginate beads dissolved in all the set-ups between the second and third days. This occurrence emptied the microbes into the culture media. Because the medium was harsh, the viability of the consortia must have been disoriented. This fact could have caused the observed anomalies in the product generation and substrate utilization kinetics. In comparison with the unsupported system, there was an enhanced biochemical activity in the calcium alginate supported system. This behavior can be explained by consideration of the bead structure and their microbial immobilization mechanism. Immobilization by calcium alginate involves entrapment of microbes inside semi-permeable, polymeric, capsule-like balls of calcium alginate. They are formed by a

displacement reaction in which sodium ion is replaced by ionized calcium to form a porous cross-linked mesh at the ball surface. The capsules are permeable to most substrates. In the system, the membrane must have offered resistance to the transport of mass across it. The free movement and intimate mixing between the substrates and the microbial system was slowed down and most of the processes inside the balls took place in an unsteady state regime. The kinetics of this operation depended on a number of factors that included the pore structure of the beads, the thickness of the membrane, strength of the substrates, residual pore charges, and biochemical kinetics inside the beads among other factors. The overall mass transfer behavior with respect to the biochemical reaction kinetics was studied in order to explain some of the observed unclear phenomenon. A representative factor that showed the dominant process and subsequently the rate controlling step (because of their consequential nature) was evaluated. The factor used was the Damkholer number. The analysis of this mechanism is shown in section 4.9.

4.5.2 Kinetics of Microbial Growth over different Support Materials in a Batch System

In order to develop some biomethanation models, microbial growth kinetics had to be taken into consideration. The system response towards biomass formation on different supports to various initial organic loadings was studied with respect to time. The output variable considered was the amino acid content at various time intervals. Each support material was studied differently and comparisons were made with the unsupported system acting as the datum. The kinetics of biomass growth in the unsupported system is shown in figure 4.6. The level of growth was proportional to the initial substrate concentration in each set-up. This phenomenon signified that every system had its own cell carrying capacity which was regulated by substrate

concentration. This gave the evidence that there was a growth limiting substrate in the culture media which was only associated with molasses waste water and not any other additive. The exception was the case of the system having CODi of 0 g/l, where the small growth registered was due to the nutrient media of the innoculum which led to the small increase in biomass. This growth limiting substrate controlled the amount of microbes that could grow in any given concentration of culture media. This manifestation justified representation of the system using mathematical models that assume substrate limitation of process and those having carrying capacity correction factors in them for example the Monod and the Sigmoidal models. From figure 4.6, a key factor was also observed. It was seen that, in all the systems except the one containing initial COD of 75 g/l, there were three distinct peaks. According to Menert (2001), this phenomenon was as a result of multi-auxic growth. Each peak

corresponded to a growth limiting substrate present in the culture medium.

According to Menert (2001) it has been known that the simultaneous growth of many species in symbiotic interaction preceded any biomethanation process. Different substrates could be used for biomethanation depending on the reactor conditions. Analysis of multi-auxic growth and microbial interactions could be reliably done using a HPLC and micro-calorimetric techniques. From this results, it has been known that, hydrolytic and acidogenic bacteria could be most probably responsible for the first maximum on the biomass-time curve in figure 4.6, as during this time of peak realization, characteristic products to this type of fermentation (lactic, propionic, acetic acid) are formed, in synchrony with the decrease of macromolecular polymeric substrate concentrations [CITATION Men01 \l 2057]. The second maximum corresponds to primarily acetogenic and acetoclastic bacteria with low *K*s (limiting substrate concentration) values. The inhibitory factor on the other hand has been determined to be caused by Volatile Fatty Acids (VFAs), especially the acetogens [CITATION Men01 \l 2057]. If the speed of acetate formation exceeds its utilization rate by methanogens (constituting the third observed peak), their accumulation inevitably leads to a drop in pH which in turn causes the inhibition to the entire system [CITATION Men01 \l 2057]. Determination of VFAs is often used to establish the danger of operational instability of the anaerobic reactor as acetic acid is a weak acid and the increase of VFAs is noticeable before extensive decrease of pH. The VFA concentration indicating the danger of process instability is >5 g dm^{-3} measured as total VFAs, and 2 g dm^{-3} measured as acetates [CITATION Men01 \l 1033]. The lowest point of biomass concentration in figure 4.6 corresponding to day three was speculated to be as a result of the increased VFAs at a time when the methanogens hadn’t adapted well enough to balance out on the excess of the generated VFAs.

The system containing initial COD of 75 g/l exhibited four peaks. The three first peaks could have been as a result of the dynamics similar to those of the other low strength systems discussed earlier in this section. The fourth peak on the other hand could be as a result of the altered system behavior as to adjust to the very adverse environmental conditions of the culture media. It is well known that when a system deviates drastically from the normal conditions of optimal growth, the microbial system undergoes some stress and consequently, they can either change the target substrate or produce stress related products which are quite different from those products generated in a normal case [CITATION Sye09 \l 1033].

In the activated natural zeolite supported system, the number of peaks generally resembled that of the non supported system. A notable feature in the nature of these peaks is that, the third peak in all the cases (except for the system containing COD of 0 g/l) contained the highest quantity of amino acids, unlike in the unsupported system whereby it was in the first peak. This observation signified that the number of acetogenic and acetoclastic bacteria with low Ks were predominating the system. Therefore, the zeolite support provided the most ideal environment specifically to the methane associated consortia as opposed to the hydrolytic and acidogenic strains which appear to enjoy unsupported environment. Together with other studies, this observation can therefore be used to generate useful information into designing a specialized bioreactor system having two chambers: the unsupported hydrolytic chamber and the zeolite supported methanogenic chamber.

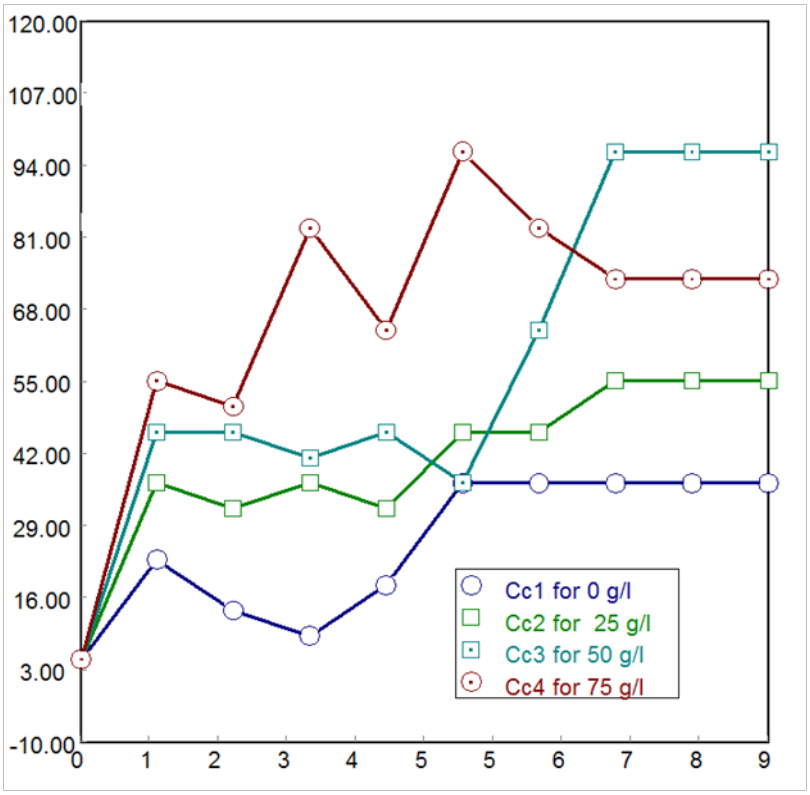

Figure 4.7 Kinetics of microbial growth over activated natural zeolite supported syster

From figure 4.7, another notable general observation was the system resilience to VFAs after hydrolysis and acidogenesis. This occurred after the first peak was realized. Unlike the unsupported system, all the set-ups showed minimal reductions in the amino acid content of the system. This phenomenon meant that the effect of the products of the initial processes (hydrolysis and acidogenesis) was minimized by the use of adsorbent media as supports. This could have been as a result of the same intra-particulate adsorption and the stagnant layer scenarios postulated in section 4.5.1 earlier.

The calcium alginate supported system showed a similar trend in the number of peaks for most set-ups.

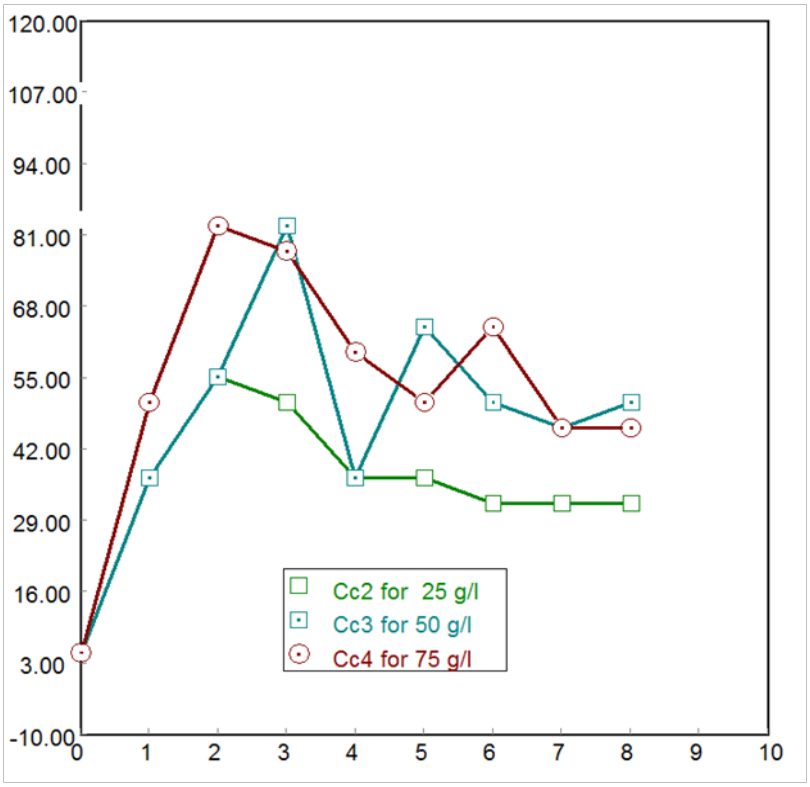

Figure 4.8 Kinetics of microbial growth in calcium alginate supported system

However, the first peak registered the highest amino acid concentration than all the others. This observation could be attributed to the structural composition of the calcium alginate polymers. Structurally, alginic acid is composed of a co-polymer of two uronic acids: D-mannuronic acid and L-guluronic acid. Alginic acid can either be water soluble or insoluble depending on the type of the associated salt. The salts of sodium, other alkali metals, and ammonia are soluble, whereas the salts of polyvalent cations, e.g., calcium, are water insoluble, with the exception of magnesium. The alginate polymer itself is anionic (i.e., negatively charged) overall. Polyvalent cations bind to the polymer whenever there are two neighboring guluronic acid residues. Thus, polyvalent cations are responsible for the cross-linking of both different polymer molecules and different parts of the same polymer chain [CITATION Ste \l 1033]. The two uronic acids are polysaccharides in nature and can be hydrolysed by

enzymes or by cells of hydrolytic bacteria to form respective monomers. As pointed out earlier that every system has its own cell carrying capacity which is regulated by substrate concentration, the presence of the two uronic acids in the bead core must have necessitated the rapid growth of the hydrolytic and acidogenic strains of microbes. Since the uronic acids were present in an almost pure and soluble form within the capsule core, the other inhibitors in the culture were initially present in very small quantities because of the mass transfer resistance offered by the semi-permeable membrane encapsulating the microbes. This led to the rapid growth of biomass leading to the high amino acid peaks realized which were not directly associated with biogas production. Also, there appeared to have been no drastic reduction in biomass population after the hydrolytic and acidogenic phase. This could have been due to the controlled release of the VFAs formed at the capsule core because of the mass transfer resistance offered by the same semi-permeable membrane or the slimy dissolved alginate in the reverse direction. Even upon the collapse of the membranes by dilution with the monovalent metal ions in the culture, the formed solutions between sodium and the uronic acids generated a slimy, gelatinous mass. This soluble viscous mass must have increased the stagnant layer between the culture medium and the microbial system thereby creating a thin film of mass transport resistance through and out of the microbial cell membranes. This phenomenon shielded the microbes from the harsh external environment and necessitated the VFAs tolerance observed in the kinetic growth curve figure 4.8

4.5.3 Kinetics of Oxygen Inhibition over different Support Materials in a Batch System

In the second set of experiments performed, the set-ups had a common initial organic loading of COD 50 g/l each and were vortexed moderately for 10 minutes at intervals

of 8 hours. Each system set was treated separately where the factors tested were the immobilization regime of the system. Each system result was analysed and the resilience to deliberate oxygen exposures was determined. The results are shown in Tables 4.4, 4.5 and 4.6.

In the unsupported system shown in Table 4.4, the microbes were able to tolerate oxygen exposures for 30 minutes. Any exposure beyond the 30 minutes inhibited the system. This could be because of the thin boundary layer between the microbes and the injected air. The permeation of oxygen into the microbial cells was faster than in the other cases and therefore the system could be easily upset.

The system having biomass immobilized unto activated natural zeolite (Table 4.5) showed a more robust tolerance to oxygen inhibition. It tolerated air bubbling for periods of upto 90 minutes. This behavior could be explained by consideration of the boundary layer and intra-particulate adsorption scenarios which shielded the microbes as explained in section 4.5.1

Table 4.7: The activity of bubbling sterile air through an unsupported system

Sample	Time of sterile air exposure in minutes	The day of exposure	System response
1.	15	3	*Regained activity*
2.	30	3	*Regained activity*
3.	45	3	*Didn't regain*
4.	60	3	*Didn't regain*
5.	75	3	*Didn't regain*
6.	90	3	*Didn't regain*
7.	105	3	*Didn't regain*
8.	120	3	*Didn't regain*

Lastly, the system having immobilized biomass on calcium alginate gel (Table 4.6) was able to withstand oxygen exposure for 60 minutes. The resilience of this system could have been due to the explanation earlier given in section 4.5.1. The period of tolerance was lower than that of activated natural zeolite system, which was the most robust, but doubled that of the unsupported system. The lesser value realized in the calcium alginate supported system also, could have been occasioned by the observed dissolution of the beads due to the presence of monovalent cations and phosphate buffers in the culture media.

Table 4.8: The activity of bubbling sterile air through activated natural zeolite supported system

Sample	Time of sterile air exposure in minutes	The day of exposure	System response
1.	15	3	*Regained activity*
2.	30	3	*Regained activity*
3.	45	3	*Regained activity*
4.	60	3	*Regained activity*
5.	75	3	*Regained activity*
6.	90	3	*Regained activity*
7.	105	3	*Didn't regain*
8.	120	3	*Didn't regain*

In conclusion, the immobilization of the methanogenic consortium unto activated natural zeolite supports and calcium alginate beads increased the system tolerance to oxygen inhibition by more than two times that tolerated by free methanogenic consortia. This corroborates the data obtained by Lavov et al (2001) where it was reported that, free system showed almost irreversible loss of biological activity at exposure levels of 45 minutes whereas the methanogenic consortia immobilized unto poly (acrylonitrile-acrylamide) co-polymer support, regained its biological activity after 45 minutes of oxygen exposure.

Table 4.9: The activity of bubbling sterile air through calcium alginate supported system

Sample	Time of sterile air exposure in minutes	The day of exposure	System response
1.	15	3	*Regained activity*
2.	30	3	*Regained activity*
3.	45	3	*Regained activity*
4.	60	3	*Regained activity*
5.	75	3	*Didn't regain*
6.	90	3	*Didn't regain*
7.	105	3	*Didn't regain*
8.	120	3	*Didn't regain*

4.6 Determination of the most suitable Organic Loading of the System

To obtain the most suitable organic loading of a system as far as highest biogas yield is concerned, values of the two key dependant output variables were considered with respect to initial organic loadings of every system. The output variables of greatest importance were: the biogas yield and percentage reduction of COD. These output variables were each studied with respect to the initial COD and their most preferred quantities were then determined as shown in section 4.6.1 and 4.6.2.

4.6.1 Determination of the most suitable Organic Loading based on the Product Yield

In all the three systems, the cumulative volume of biogas produced was evaluated and listed corresponding to respective initial organic loading of every system. The product yield was then evaluated and a presentation of the relationship between the product yield and the initial COD was computed and presented in figure 4.9. The tables showing the relationship between product yield and the initial COD for the three systems are shown in appendix A as tables A1, A2 and A3.

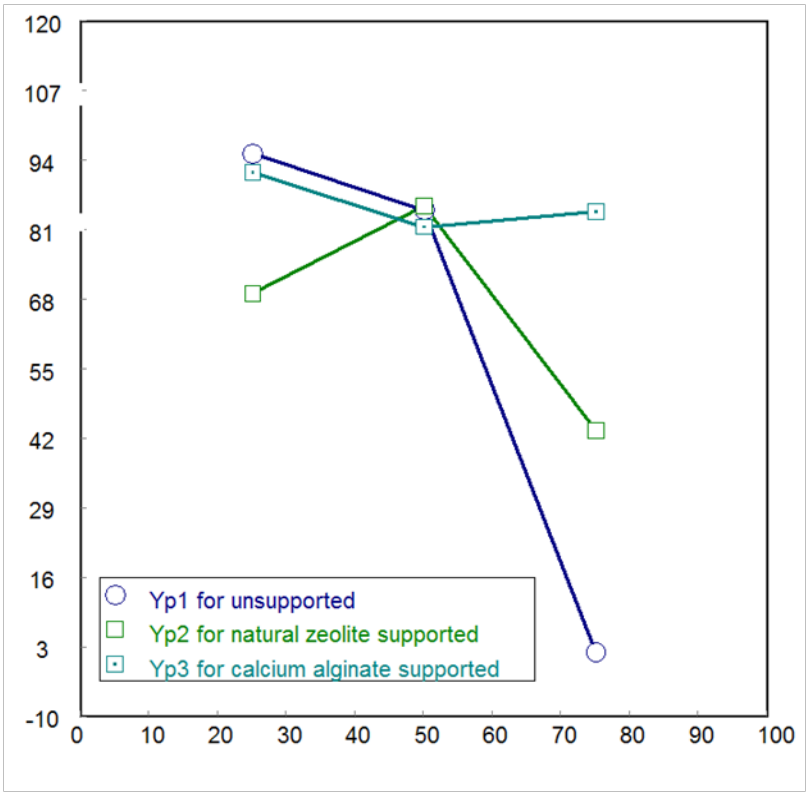

Figure 4.9 Relationship between the biogas yield and initial organic loading

Since the focus of the research was to investigate a system that offered the highest organic stabilization and biogas at high organic loading, figure 4.9 showed that the calcium alginate supported system registered the highest biogas yield of $84.5\,cm^3/g\,COD_i$ at the marginal organic loading of 75 g/l. Although the calcium

alginate registered the highest biogas yield, the beads that encapsulated the consortia dissolved on the second day. This was attributed to the presence of the phosphates as buffer and the excess of monovalent ions of sodium that originated from the added sodium hydroxide used to adjust the pH of the solution. Therefore, based on the biogas yield, the calcium alginate supported system registered the highest value at a maximum organic loading of 75 (g/l).

4.6.2 Determination of the most suitable Organic loading based on the Degree of Waste Water Stabilization

In all the three systems, the residual COD of the system at both the start and the end of the run was evaluated and listed corresponding to respective initial organic loading of every system. The percentage COD reduction was then evaluated and a presentation of the relationship between the percentage reduction and its initial value was computed and presented in figure 4.10. The tables showing the relationship between the percentage COD reduction and the initial COD for the three systems are shown in appendix B as tables B1, B2 and B3. In this case, Chemical Oxygen Demand was the quantity used as the inferential factor of the degree of stabilization of the organics (the reduction in concentration of the respective biodegradable components constituting the organics in the waste water).

Since the overall research goal was focused on the investigation of a system that could offer the highest organic stabilization at high organic loading, the analysis in the figure 4.10 was made so that the most suitable values of parameters could be established. From the analysis, the system containing biomass immobilized on activated natural zeolite support registered an effluent stabilization of 44% at the

marginal organic loading of 75 g/l. This corresponded to a total COD reduction of 33 g/l.

Although the natural zeolite registered the highest COD reduction, the beads in the calcium alginate supported system had dissolved due to the presence of the phosphates and excess of sodium ions. This dissolution also resulted into the addition of COD to the system since structurally, the calcium alginate gels are organic polymers as mentioned in section 4.5.2. But some of the key performance indicators were not affected by the dissolution e.g. the lag phase of biomethanation. By speculation, calcium alginate supported system could have registered the highest COD reduction had the beads been stable. The calcium alginate system showed a general decline in the COD reduced until it reached the lowest value at 50 g/l then it steadily increased with the initial COD of the system towards the marginal high. The small slumping behavior of the system might have been due to the liberation of more Ca^{2+} which in turn increased the electrolytes into the solution and thereby causing osmotic pressure problems to the microbes upon the hydrolysis of the two uronic acids as mentioned in section 4.5.2.

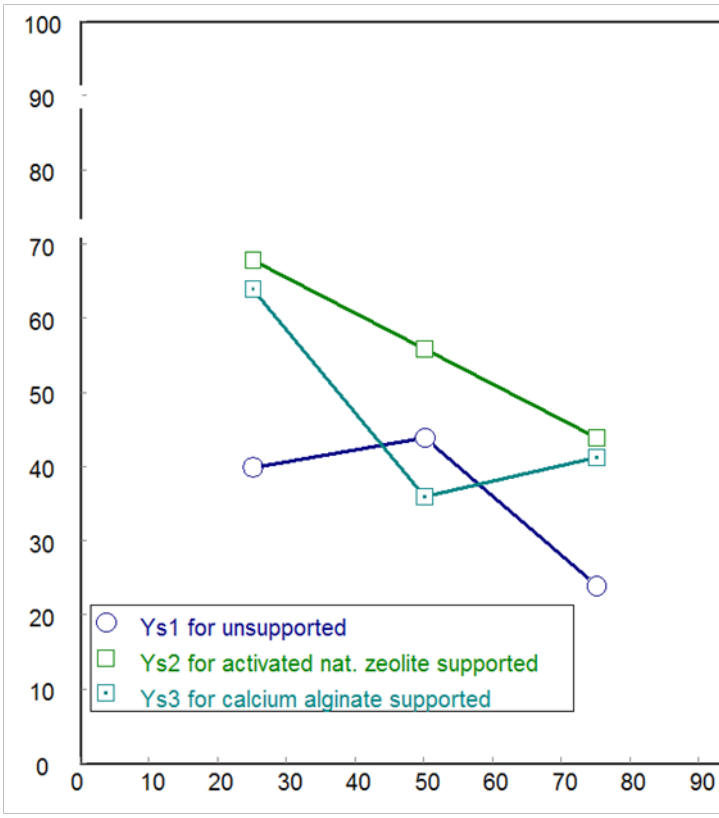

Figure 4.10 Relationship between the percentage waste water stabilization

Therefore, based on the organic stabilization, the activated natural zeolite supported system registered the highest value of 44% at maximum organic loading better than the other two systems.

4.7 Mathematical Modeling of the Biomethanation Process

Mathematical modeling was performed on the three supported systems in order to obtain values of parameters of use in the evaluation of the system performance. The models generated could thereafter be used in simulating the process conditions as far as the input-output behavior of supported systems are concerned. The models generated provided information on the mechanisms the system underwent and illuminated on the process regime the systems followed.

From section 4.6, three key observations were made: Firstly, the system showed that initial COD limited the rate of growth of biomass irrespective of the immobilization medium. This can be seen in figures 4.6, 4.7 and 4.8 that when the substrate concentration was low, the gradient of the curve between days 0.01and 1 was less steep as compared to when the initial COD was higher signifying a lower growth rate. This fact emphasizes the need to test the obtained data with models that take into consideration substrate limitation on their rates. Secondly, it was noted that the higher the initial organic loading, the larger was the peak value of the amino acid content as was seen in figure 4.6, 4.7 and 4.8. This observation indicated that models having the effect of maximum carrying capacities incorporated in their formulations could realistically represent these systems and therefore, regressing kinetic data using this model types could be realistic. Finally, when the calcium alginate beads were observed to dissolve on the second day in the calcium alginate supported system, it was noted that, the system kinetics slumped and it was more visible in the substrate utilization kinetic data. The slumping of kinetics began when the consortia was exposed to the external environment away from the bead protection. This observation pointed out that there could be some passive substances that were causing system inhibition. Therefore, a kinetic model taking into consideration factors causing inhibition was reasonable and could be used to regress the kinetic data. In view of these observations, Monod model (representing substrate limiting systems), Andrews model (representing systems containing substance inhibitions) and modified Gompertz's model (representing systems having limitations of carrying capacities) were used to regress the generated kinetic data so as to find the most relevant model and thereby calculate the kinetic parameters of the system.

4.7.1 The Monod Kinetic Model

Monod model was used to regress the generated kinetic data. The maximum specific growth rate and Monod constant ($\mu_{max} \wedge K_s$) were obtained in each supported system. It was observed that the model did not fit well into the generated data. The values of $\mu_{max} \wedge K_s$ were evaluated using the process of determination of rate law parameters. The rate law evaluation technique adopted was that of a polynomial fit into the kinetic data of substrate utilization and biomass growth. A non – linear regression analysis was performed. The system was assumed to be having only one unique substrate that was limiting the biochemical reaction rate. The systems were all considered at maximum initial COD of 75 g/l. The mathematical operations and tables showing step by step analysis are shown in all the three categories of set-ups at their marginal organic loadings in appendix C as tables C1, C2 and C3. With the assumption of a single substrate, the kinetic formulation in appendix C was used to determine the order and the rate constant of the reaction. The kinetic data was manipulated through linear regression to obtain the parameters k and α with the aid of **POLYMATH** software. To find the kinetic constants, K_s and $\mu_{max,}$ determination of the biomass growth rate r_g, was done after having obtained the rate law parameters. The procedure for calculating the kinetic rate law parameters is outlined in appendix C.

For the case of unsupported system at an initial COD of 75 g/l the regression analysis are shown in figures 4.11 and 4.12 and corresponding table C1 in appendix C. the pseudo steady state at the exponential phase was considered between day 0 and 4.

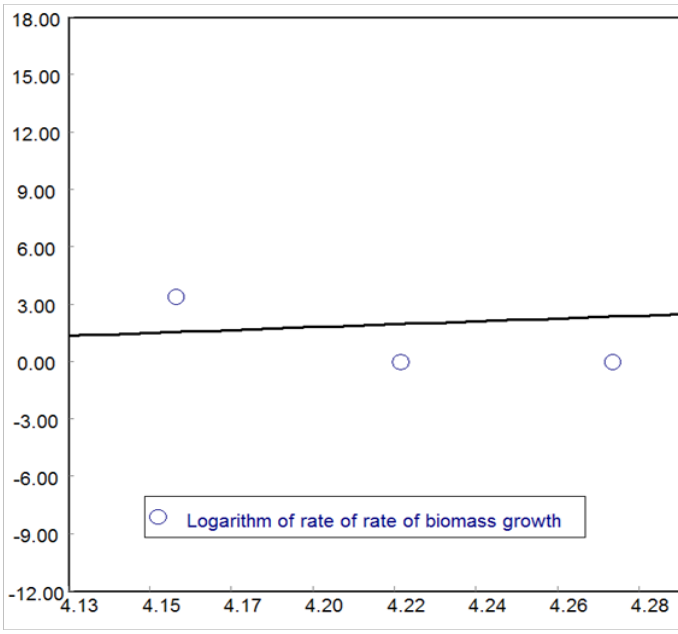

Figure 4.11 Linear regression of the microbial growth and substrate utilization data fo

From figure 4.11, it was observed that, $lnk = -27.026$, so the reaction rate constant was 1.831×10^{-12} day^{-1} and the order of reaction $\alpha\, was$,6.877 .

From **POLYMATH** software, non-linear regression of the Hanes-Woolf form of the Monod equation [CITATION Fog10 \l 1033] shown in figure 4.12 yielded the values of factors K_s and $\mu_{max,}$ in unsupported system of initial COD of 75 g/l as 5050.95 g/l and 43.18 day^{-1} respectively with a poor R^2 of -1.0725 and R^2 adj of -1.3316.

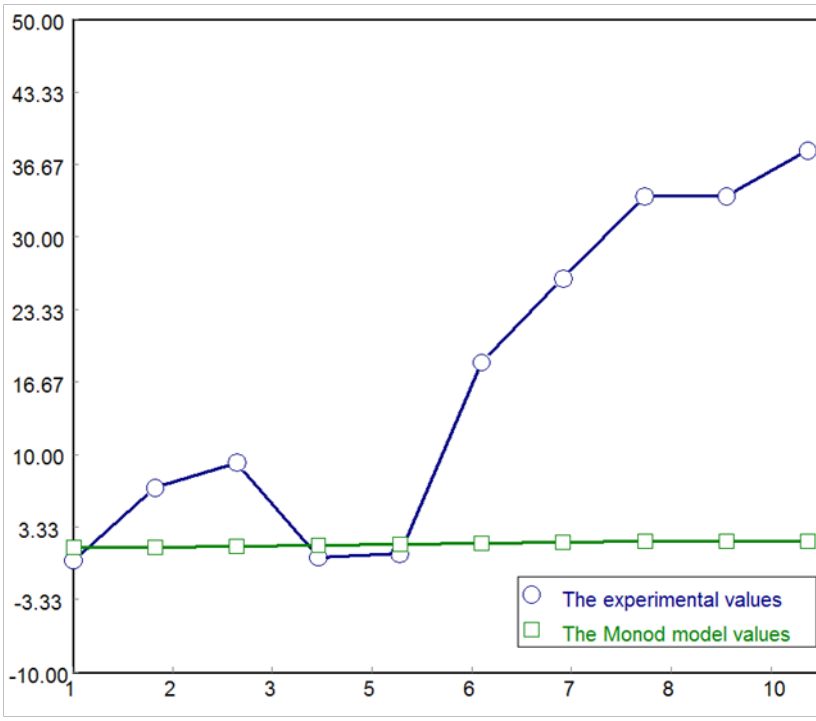

Figure 4.12 Non-linear regression for the determination of Ks and μmax, in unsupporte

By observing the nature of the curves in figure 4.12 and taking into consideration the values of the poor closeness of fit indicators, it was visible that the system greatly deviated from the Monod formulation. These results indicated that substrate limiting reaction assumption was not valid. The apparent order of the reaction had a value of 6.877 which was unreasonable. This meant that the kinetics of the reaction were complex and depended on several other factors. An assumption therefore of a substrate limiting reaction was an over simplification and thus unrealistic. The use of a mixed culture could also have contributed to this observed deviation.

In the case of activated natural zeolite supported system at an initial COD of 75 g/l the regression analysis are shown in figures 4.13 and 4.14 and corresponding table C2 in appendix C. The pseudo steady state at the exponential phase was considered between day 0 and 4.

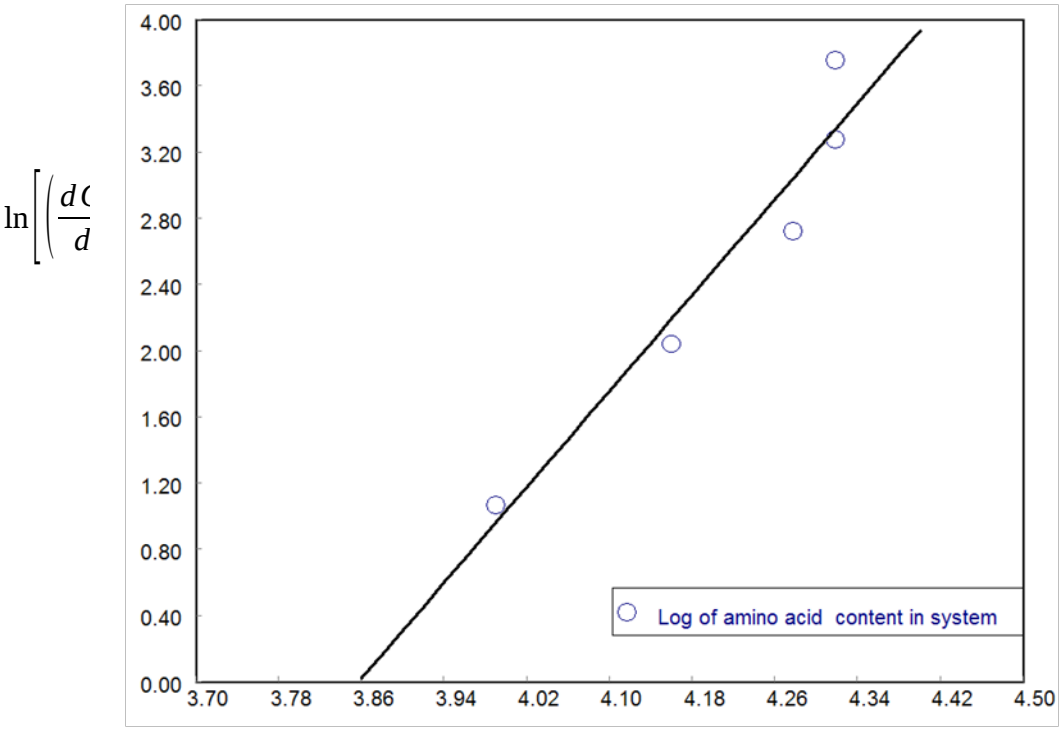

Figure 4.1 Linear regression of the microbial growth and substrate utilization data for activated natural zeolite system at initial COD of 75 g/l

From figure 4.13, it was observed that, $lnk = -27.938$, so the reaction rate constant was 7.36×10^{-13} day^{-1} and the order of reaction , α *was* 7.245 . From **POLYMATH** software, non-linear regression of the Hanes-Woolf form of the Monod equation shown in figure 4.14 yielded the values of factors K_s and $\mu_{max,}$ in activated natural zeolite system of initial COD of 75 g/l as 101.9984 g/l and 0.0294 day^{-1} respectively with very poor R^2 of 0.3398 and R^2 adj of 0.2798.

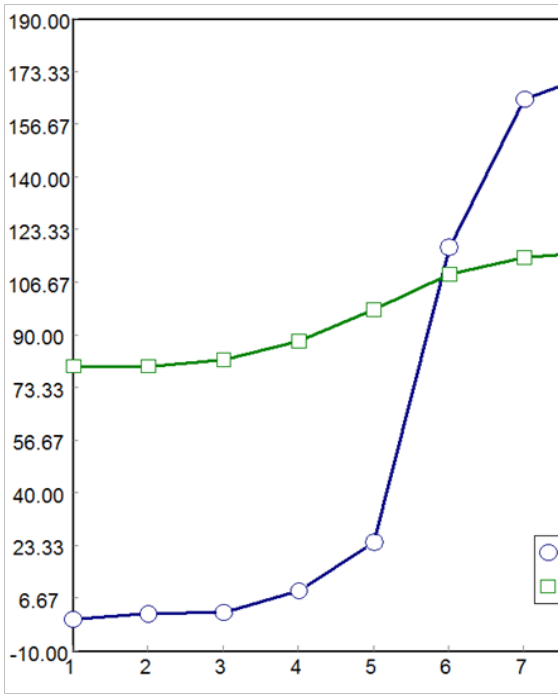

(non-linear)

Figure 4. Non-linear regression for the determination of Ks and μmax, in activa

By observing the nature of the curves in figure 4.14 and taking into consideration the values of the poor closeness of fit indicators, it was visible that the system greatly deviated from the Monod formulation. These results indicated that substrate limiting reaction assumption was also not valid just like in the case of the unsupported system. The observed trend of great deviation could be alluded to the same reasons pointed out in the unsupported system before.

In the case of calcium alginate supported system at an initial COD of 75 g/l the regression analysis are shown in figures 4.15 and 4.16 and corresponding table C3 in appendix C. The pseudo steady state at the exponential phase was considered between day 0 and 4.

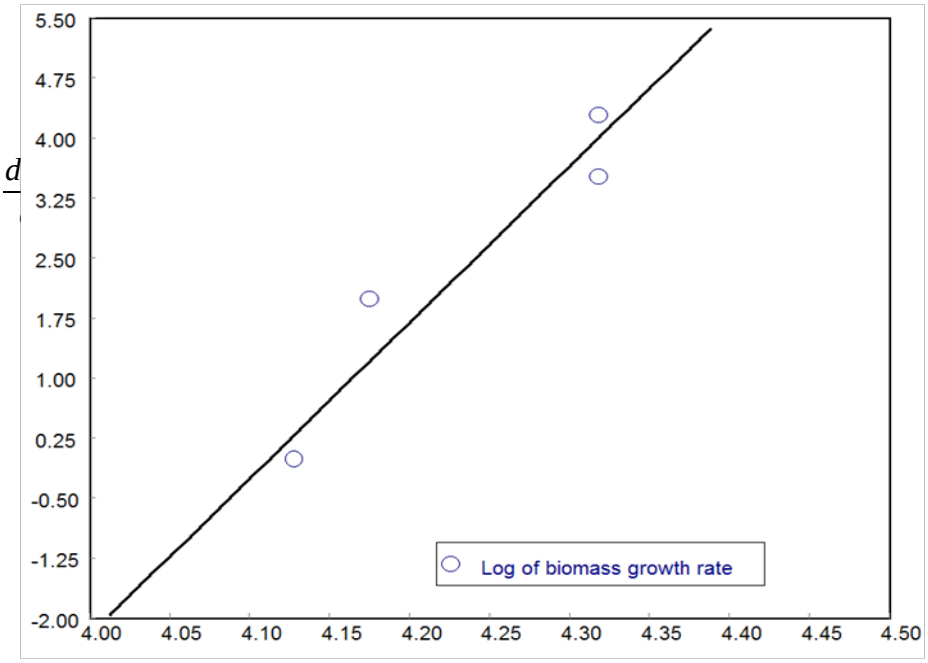

Figure 4.15 Linear regression of the microbial growth and substrate utilization data fo

From figure 4.15, it was observed that, $lnk = -80.285693$, so the reaction rate constant was 1.357×10^{-35} day $^{-1}$ and the order of reaction , $\alpha\, was\, 19.524527$.

From **POLYMATH** software, non-linear regression of the Hanes-Woolf form of the Monod equation shown in figure 4.16 yielded the values of factors K_s and $\mu_{max,}$ in calcium alginate system of initial COD of 75 g/l as 101.9958 g/l and 0.0068 day $^{-1}$ respectively with poor R^2 of -0.6831964 and R^2adj of -0.8515161.

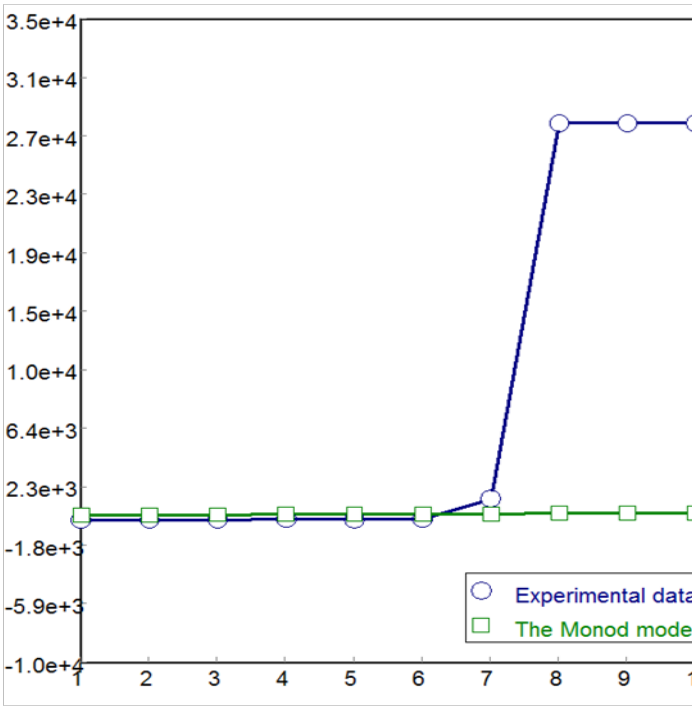

(non-linear)

Figure 4.16 Non-linear regression for the determination of Ks and μmax, in calcium al

By observing the nature of the curves in figure 4.16 and taking into consideration the poor values of the closeness of fit indicators, it was visible that the system greatly deviated from the Monod formulation. These results indicated that substrate limiting reaction assumption was also not valid just like in the case of both unsupported system and activated natural zeolite supported system. The observed trend of the significant deviation could be attributed to the same reasons pointed out in the unsupported system before. Therefore in summary, all the three systems under different immobilization media show kinetics that don't follow the Monod models. This can be due to the fact that Monod models do not account for lag phases, sequential uptake of substrates (multi-auxic effect) and changes in mean cell sizes during the growth cycle of a batch culture [CITATION Lee92 \l 1033].

4.7.2 The Andrew's Kinetic Model

In some cases, the specific growth rate increases at low substrate concentration and decreases at high substrate concentration because of the toxicity effects caused by higher substrate concentrations. A high substrate concentration or a competing inhibitor can cause inhibition. This inhibition can be accounted for in some growth kinetic models that includes the Andrew's formulation: [CITATION Jan08 \l 1033] According to [CITATION Okp05 \l 1033] when a substrate inhibits its own biodegradation, the original Monod model becomes unsatisfactory. In this case, Monod derivatives that provided corrections for substrate inhibition (by incorporating the inhibition constant K_I) can be used to describe the growth-linked biodegradation kinetics. Among the substrate inhibition models, the Andrew's equation is the most widely used. It is also a good representation of experimental data sets as examined by [CITATION Gou00 \l 1033].

The formulation of the Andrew's model is in the form:

$$\mu = \frac{\mu_{max} C_s}{K_m + C_s + \frac{C_s^2}{K_I}}$$

where K_I is the inhibition constant.

It appears in the microbial growth kinetic model as:

$$\frac{dC_c(t)}{dt} = \left(\frac{\mu_{max} C_s}{K_m + C_s + \frac{C_s^2}{K_I}} \right) C_c(t)$$

The regression form used was:

$$\left(\frac{1}{C_c(t)} \right) \frac{dC_c(t)}{dt} = \left(\frac{\mu_{max} C_s}{K_m + C_s + \frac{C_s^2}{K_I}} \right)$$

In the unsupported system with an initial COD of 75 g/l, the regression analysis of the kinetic data using Andrew's model was shown in figure 4.17.

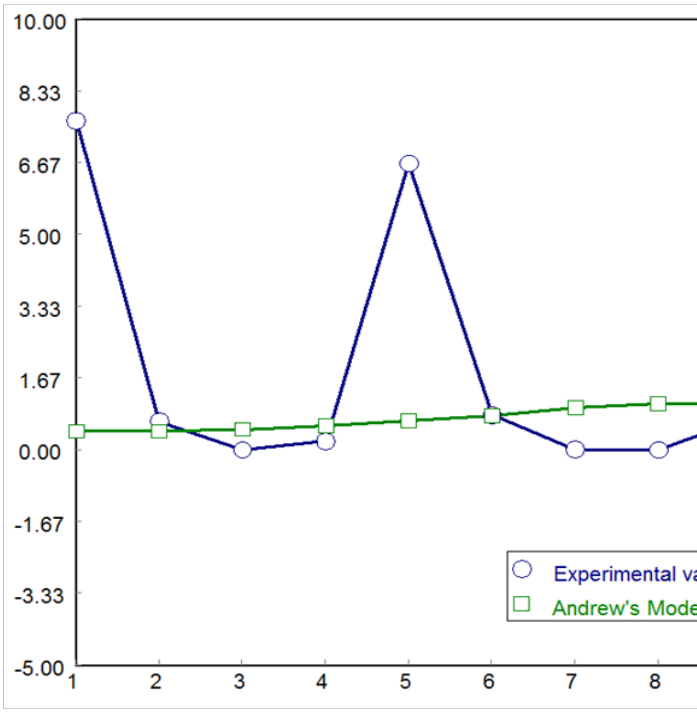

Non-linear function of substrate strengt

Figure 4.17 Non-linear regression for the determination of Km, KI and µmax, in the un

From figure 4.17, the kinetic parameters K_m, K_I and μ_{max}, for the biomethanation process obtained were -547.556 g/l, 4.360 g/l and 4.838 day^{-1} respectively. The precision factors registered were very low. R^2 was obtained to be -0.1979 and R^2adj registered was -0.5402. In view of this information, the system was observed not to follow the Andrew's model and therefore the factor of inhibition predominating the kinetics was not very pronounced.

In the activated natural zeolite supported system with an initial COD of 75 g/l, the regression analysis of the kinetic data using Andrew's model was shown in figure 4.18.

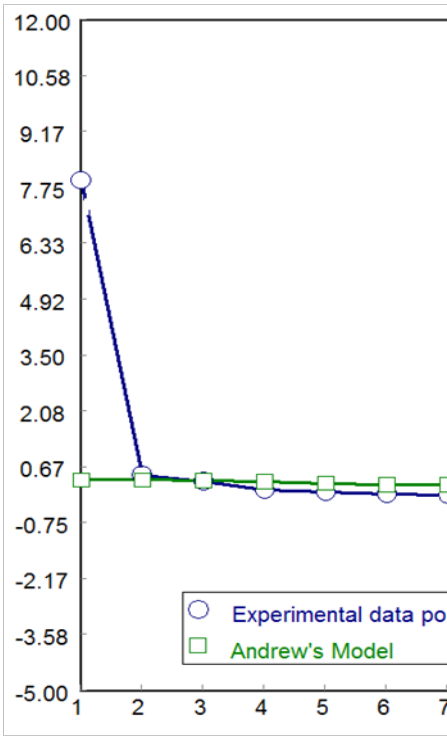

Non-linear function of su

Figure 4. Non-linear regression for the determination of Km, KI and µmax, in th

From figure 4.18, the kinetic parameters $K_{m,}$ K_I and $\mu_{max,}$ for the biomethanation process obtained were 453.713 g/l, 236.320 g/l and 2.575 day^{-1} respectively. The precision factors registered were very low. R^2 was obtained to be -0.0123 and R^2adj registered was -0.2148. In view of this information, the system was observed not to follow the Andrew's model and therefore the factor of inhibition predominating the kinetics was not very pronounced as well.

In the calcium alginate supported system with an initial COD of 75 g/l, the regression analysis of the kinetic data using Andrew's model was shown in figure 4.19.

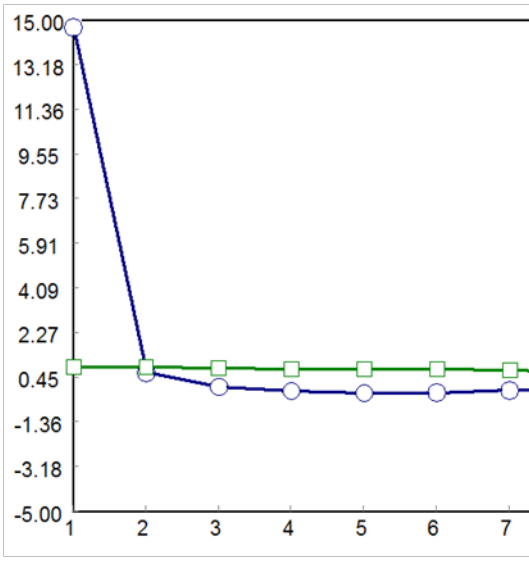

Non-linear function of substra

Figure 4. Non-linear regression for the determination of Km, KI and µmax, in th

From figure 4.19, the kinetic parameters $K_{m,}$ K_I and $\mu_{max,}$ for the biomethanation process obtained were 230.347 g/l, 52.102 g/l and 4.838 day^{-1} respectively. The precision factors registered were very low. R^2 was obtained to be 0.0018 and R^2adj registered was -0.2200. In view of this information, the system was observed not to follow the Andrew's model and therefore the factor of inhibition predominating the kinetics was not pronounced.

4.7.3 The Modified Gompertz's Kinetic Model

Modified Gompertz model being a sigmoidal function has been popular in fitting microbial growth data because of its inherent nature. It mimics the three distinct portions of microbial growth curve and therefore was regarded as the most appropriate function that can regress the experimental data. Biogas production kinetics was modeled through this function. Kinetics of biogas production in batch condition was assumed to have correspondence with specific growth rate of methanogenic bacteria in the digester. The modified Gompertz equation follows as:

$$CCp = A \cdot \exp\left\{-\exp\left[\frac{U \cdot e(\lambda - t)}{A} + 1\right]\right\}$$ [CITATION Zwi90 \l 2057]

where CCp is the cumulative values of specific biogas production (mL/g COD), or (m^3/kg COD), A is biogas production potential (ml/g COD) or, (m^3/kg COD), U is maximum biogas production rate (mL/g COD.day) or (m^3/kg COD.day), λ is lag phase period or minimum time to produce biogas (days), t is cumulative time for biogas production (days) and e is mathematical constant (2.718282) [CITATION Bud13 \l 1033]. Kinetic constant A, U and λ were determined using non-linear regression with help of **POLYMATH** software as shown figures 4.20, 4.21 and 4.22

In the unsupported system containing initial COD of 75 g/l, the results of non-linear regression were as shown in figure 4.20

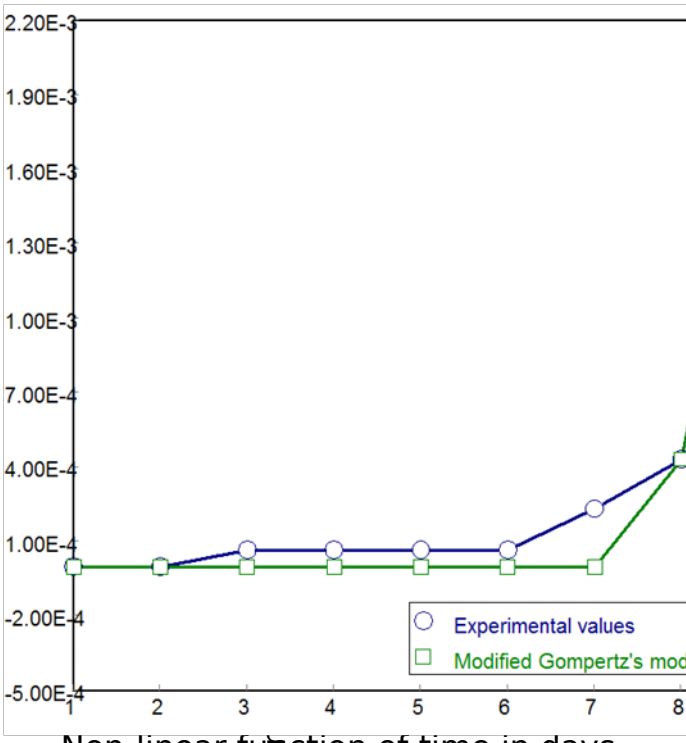

Figure 4. Non-linear regression for the determination of A, λ and U in the unsup

From figure 4.20, the kinetic parameters A, U and λ for the biomethanation process over unsupported system obtained were, 0.0021 cm^3/g COD, 0.0084 cm^3/g COD.day and 6.950 days respectively. The precision factors registered were high. R^2 was obtained to be 0.9888 and R^2 adj registered was 0.9856. In consideration of this kinetic model, the system was observed to follow closely the Modified Gompertz's formulation. Therefore the observation that, the bigger the initial organic loading the larger was the peak value of the amino acid content in figures 4.6, 4.7 and 4.8 was valid. The hypothesized effect of maximum carrying capacities imparting an influence

on the system kinetics was also validated as seen from the closeness of fit in the regression model.

In the activated natural zeolite supported system containing initial COD of 75 g/l, the results of non-linear regression were as shown in figure 4.21

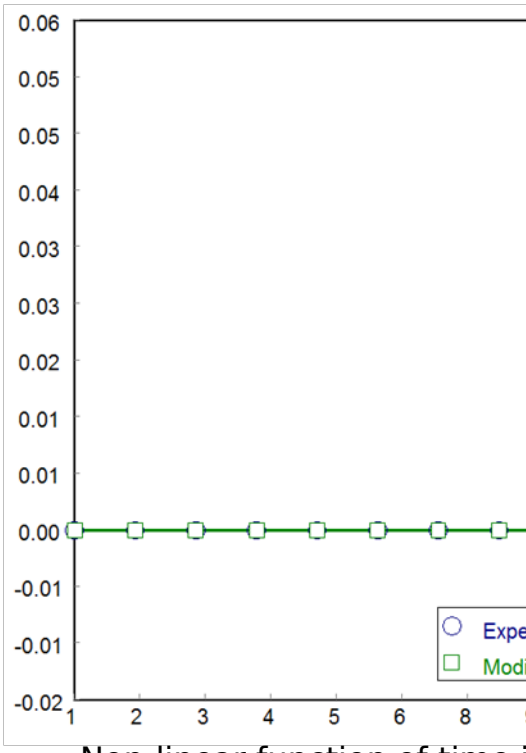

Figure 4. Non-linear regression for the determination of A, λ and U, in the activ

From figure 4.21, the kinetic parameters A, U and λ for the biomethanation process over activated natural zeolite system obtained were, 0.0436 cm^3/g COD, 0.0613 cm^3/g COD.day and 8.7551days respectively. The precision factors registered were very high. R^2 was obtained to be 0.9999 and R^2adj registered was 0.9999. In consideration of this kinetic model, the system was observed to follow closely the Modified Gompertz's formulation. Therefore the same observations realized in the unsupported

system also applied to this case with even a greater accuracy. The higher accuracy realized could be as a result of the system having been attenuated by adsorption. This surface phenomenon appeared to have suppressed the secondary system disturbances (e.g. disturbances arising from inhibitors present, high shear occurrences etc.) The hypothesized effect of maximum carrying capacities imparting an influence on the system kinetics was also validated as in the case of the unsupported system.

In the calcium alginate supported system containing initial COD of 75 g/l, the results of non-linear regression were as shown in figure 4.22

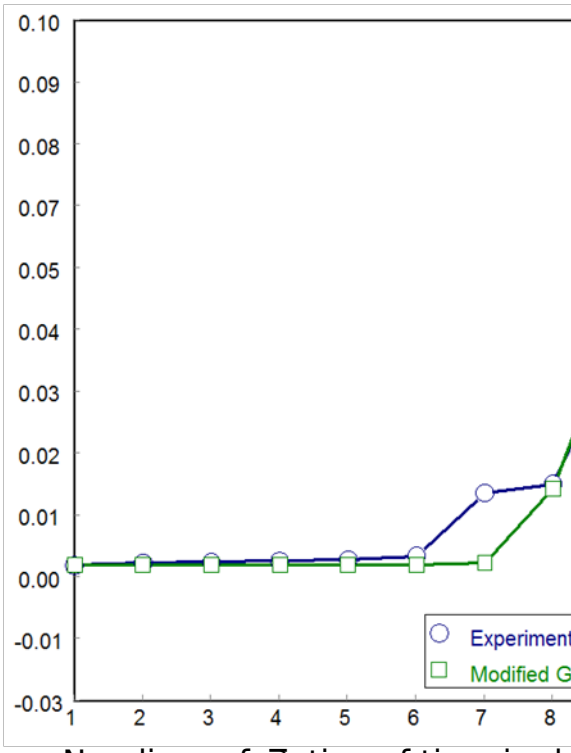

Non-linear function of time in da

Figure4. Non-linear regression for the determination of A, λ and U, in the calciu

Mean m3/kg of COD

From figure 4.22, the kinetic parameters A, U and λ for the biomethanation process over calcium alginate supported system obtained were, 0.0904 cm^3/g COD, 0.0348 cm^3/g COD.day and 6.6402 days respectively. The precision factors registered were high. R^2 was obtained to be 0.9829 and R^2adj registered was 0.9791. In consideration of this kinetic model, the system was observed to follow closely the Modified Gompertz's formulation. Therefore the same observations realized in the unsupported system also held over this case. The higher accuracy realized could be as a result of the system having been protected from secondary system disturbances, a case resembling that of the activated natural zeolite. Thus maximum carrying capacities imparting an influence on the calcium alginate system kinetics was reasonable just like in the other two cases. The slightly lower closeness of fit in this system compared to the activated natural zeolite supported system could have been caused by the dissolution of the alginate beads and thereby subsequently destroying the protection from the microbial cells. This could have caused a change of mechanism from the ordinary biochemical reaction system controlled by maximum carrying capacity and substrate limitation.

Table 4.10: Kinetic Parameters of the Modified Gompertz's Model over Various Supported Systems

Immobilization medium	A	U	λ	R^2	$R^2 Adj.$
Unsupported system	0.0021	0.0084	6.950	0.9888	0.9856
Activ. Nat. zeolite system	0.0436	0.0613	8.7551	0.9999	0.9999
Calcium alginate system	0.0904	0.0348	6.6402	0.9829	0.9791

From figure 4.23 (a), the model predicted the unsupported system to be having the least potential to produce biogas. These could have been due to the fact that, the kinetics were sluggish and erratic in the course of biomethanation due to the free cell

exposures to the harsh environments. The calcium alginate system demonstrated the highest potential to biogas production. This could have been due to the protective membrane provided by the beads which enhanced the microbial activity to operate at its optimal. The activated natural zeolite on the other hand registered an average potential. This could be attributed to aspect of microbes attempting to first colonize the adsorbent sub-stratum. Besides that, there could have occurred a phenomenon whereby the microbial inhibitors, depending on the selectivity of the adsorbent, adsorbed unto the bed alongside the microbes. Such an occurrence could inevitably register lower product potentials.

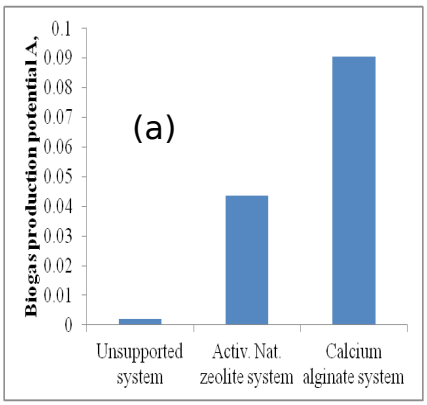

Figure 4. Comparison of Modifie

(a) Comparison of biogas production potential among three supports. (b) Comp

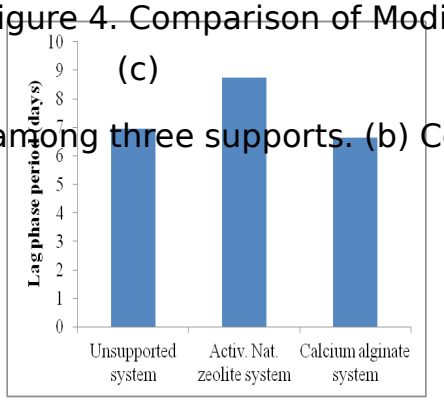

In the figure 4.23 (b), the maximum gas production rate behavior was corroborated by the kinetic constant of biomethanation in section 4.8. Activated natural zeolite demonstrated the highest value of U . This could have been due to the balanced

growth conditions offered by the protection of the boundary layer that formed between the substrates and the microbial biofilm within the adsorbent bed interstices. Diffusive mass transfer necessitated the transportation of material to and out of the microbial cell arms-way for subsequent degradation or excretion. The effects of dilution and the slow mass movement offered better adaptability and suppressed substrate inhibitions. This observation is the converse to that of the unsupported system where the maximum gas production rate was least.

Finally in figure 4.23 (c), λ, according to Zwietering (1990) is a measure of the microbial system adaptation periods. The activated natural zeolite supported system registered the highest lag phase in the process whereby microbes were adapting to the substrate. This could have been due to the same reasons of inhibitors getting adsorbed unto the bed interstices together with the microbial cells. The concentration of stressants around the cells must have led to this higher adaption period. Calcium alginate system on the other hand exhibited the least adaption period. This was due to the protection of the cells by the semi-permeable membrane before it got destroyed.

4.8 Analysis of Reaction Rate enhancement from Kinetic Models

Many researchers have developed kinetic models of biodegradability of organic material based on first order kinetics. Thereafter they have used the models to obtain the reaction rate constant. The value of this constant provides information on quality of the biomethanation process. This project also sought to analyse this rate enhancement. Batch degradation models were used for this purpose. The theory applied in the formulation of the models is a shown in appendix D.

4.8.1 Reaction Rate Constant for the Unsupported System

In the case of the unsupported system, the rate constant corresponding to each system having its unique initial organic loading was analysed using [CITATION Bud13 \l 1033] theoretical formulation outlined in appendix D. Thereafter, the behavior of the rate constant in this system with respect to changes in initial COD was also studied.

The results of the rate constant from linear regression of kinetic data are shown in figures 4.24 (a), (b) and (c). The resultant linear regression equation used to fit kinetic data is:

$$\frac{1}{t}\ln\left(\frac{d\,CC_p}{dt}\right)=\frac{1}{t}\ln\left(k.CC_{pmax}\right)-k$$

Where t is time in days, CC_p is the cumulative biogas in cm^3, CC_{pmax} is the maximum cumulative biogas in cm^3 and k is the rate constant (day^{-1}).

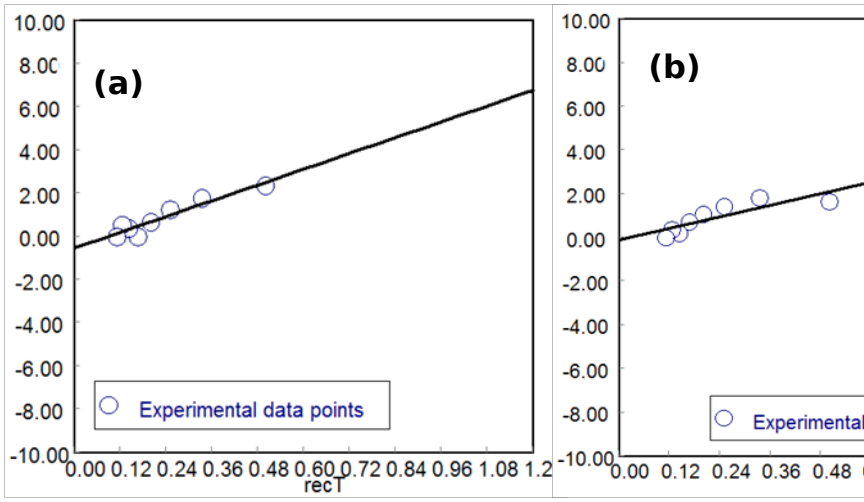

Figure4. Non-linear regre onstant k, and ma

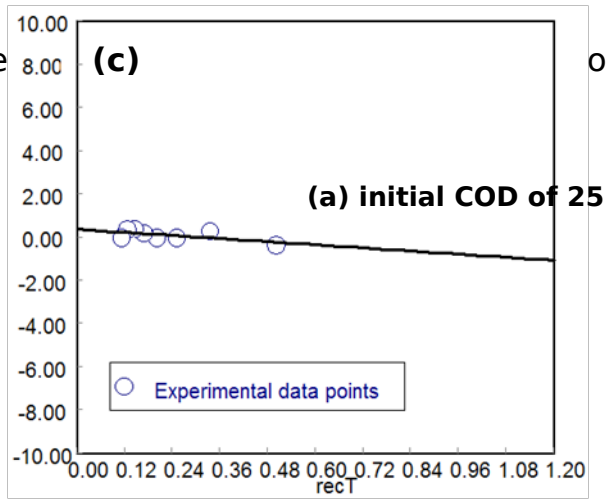

(a) initial COD of 25 g/l (b) initial COD

From the figures 4.24 (a), (b) and (c), it was seen that the gradient of (a) was greater than of the other cases. From the formulation of Budiyono (2013), the larger the slope of the system, the faster the rate the system will convert substrate to biomass. Therefore, the system containing an initial COD of 25 g/l exhibited the highest rates of substrate conversion than the others. This could be attributed to the smaller amounts of inhibiting substances in it. The system having initial COD of 75 g/l demonstrated the least rates of substrate conversion because of the harsh environmental conditions surrounding the microbial population. The metabolic activities must have encountered stressful conditions in this system due to the osmotic pressure problems, substrate inhibition and high levels of bacteriocidal compounds.

This explanation could also be the reason why the rate constant in case (c) showed a negative value signifying a change in the metabolic activities as to adjust to the stressants. The products of metabolism and target substrates could have changed as a result of the unbalanced environment.

4.8.2. Reaction Rate Constant for the activated Natural Zeolite Supported System

In the case of the activated natural zeolite supported system, the rate constant corresponding to each system having its unique initial organic loading was analysed using [CITATION Bud13 \l 1033] theoretical formulation outlined in appendix D. Thereafter, the behavior of the rate constant in this activated natural zeolite supported system with respect to changes in initial COD was also studied. The results of the rate constant from linear regression of kinetic data are shown in figures 4.25 (a), (b) and (c).

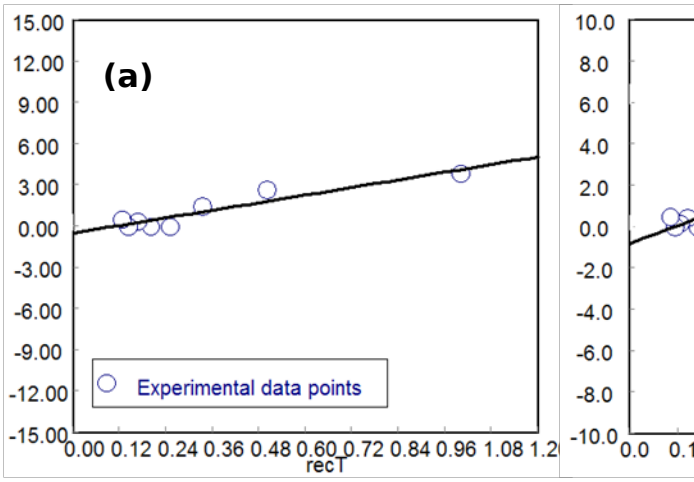

Figure 4. Non-linear regression for t , and m

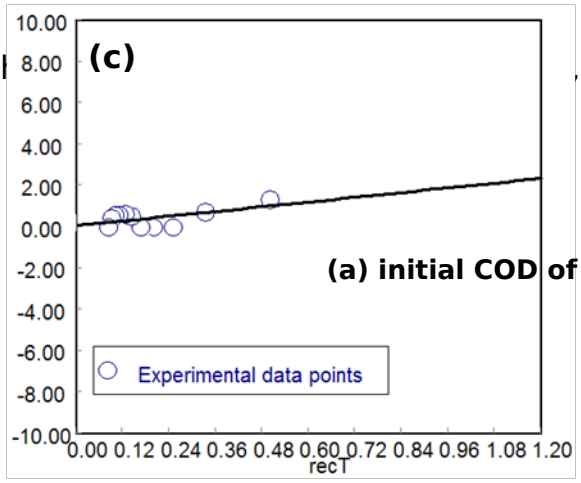

From the figures 4.25 (a), (b) and (c), it was seen that the gradient of (b) was greater than of the other cases. For the same reasons stated in section 4.8.1 the bigger slope of the system meant faster rates of substrate conversions. Therefore, the system containing an initial COD of 50 g/l exhibited the highest rates of substrate conversion than the others. This could be attributed to the microbial system protection by the boundary layer formed around the adsorbents that slowed down the rapid mass exchange. This layer must have suppressed the effect of stressants and therefore could tolerate more of substrate strength than in the unsupported system. The system having initial COD of 75 g/l demonstrated the least rates of substrate conversion because of the same reason outlined in section 4.8.1.

4.8.3 Reaction Rate Constant for the Calcium Alginate Supported System

In the case of the calcium alginate supported system, the rate constant corresponding to each system having its unique initial organic loading was analysed using [CITATION Bud13 \l 1033] theoretical formulation outlined in appendix D. Thereafter, the behavior of the rate constant in this system with respect to changes in initial COD was also studied. The results of the rate constant from linear regression of kinetic data using **POLYMATH** are shown in figures 4.26 (a), (b) and (c).

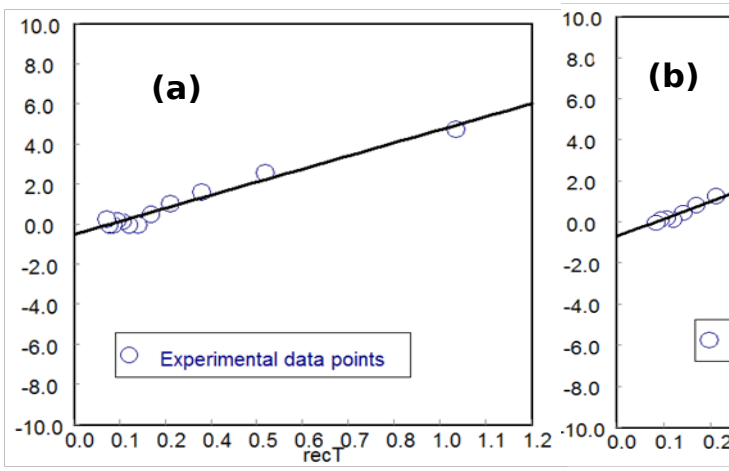

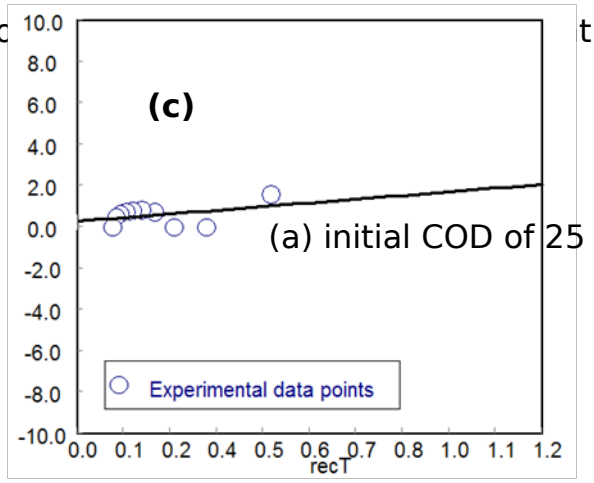

Figure 4. Non-linear regression fo t k, and m

(a) initial COD of 25 g/l (b) ini

From the figures 4.26 (a), (b) and (c), it was seen that the gradient of (b) was greater than of the other cases. For the same reasons stated in section 4.8.1 the bigger slope of the system meant faster rates of substrate conversions. Therefore, the system

containing an initial COD of 50 g/l exhibited the highest rates of substrate conversion than the others. This could be attributed to the balanced growth parameters unlike in the other cases. The system having initial COD of 75 g/l demonstrated the least rates of substrate conversion because the growth factors were not balanced enough.

Table 4.11: The effect of Initial Organic Loading and Immobilization Medium on the Kinetic Biomethanation Parameters

Initial COD in (g/l)	**Unsupported System**			**Activated natural Zeolite**			**Calcium Alginate**		
	K (day^{-1})	CC_{pmax}	R^2	**K (day^{-1})**	CC_{pm}	R^2	**K (day^{-1})**	CC_{pm}	R^2
0	0	0	-	0	0	-	0	0	-
25	0.5205	849.1	0.8957	0.9389	902.6	0.7977	0.4685	488.2	0.9711
50	0.1055	806.0	0.7101	1.2348	5201.5	0.9424	0.6750	1943.7	0.9817
75	-0.3907	-0.772	0.3999	-0.0752	-89.5	0.3357	-0.2858	-15.5	0.1521

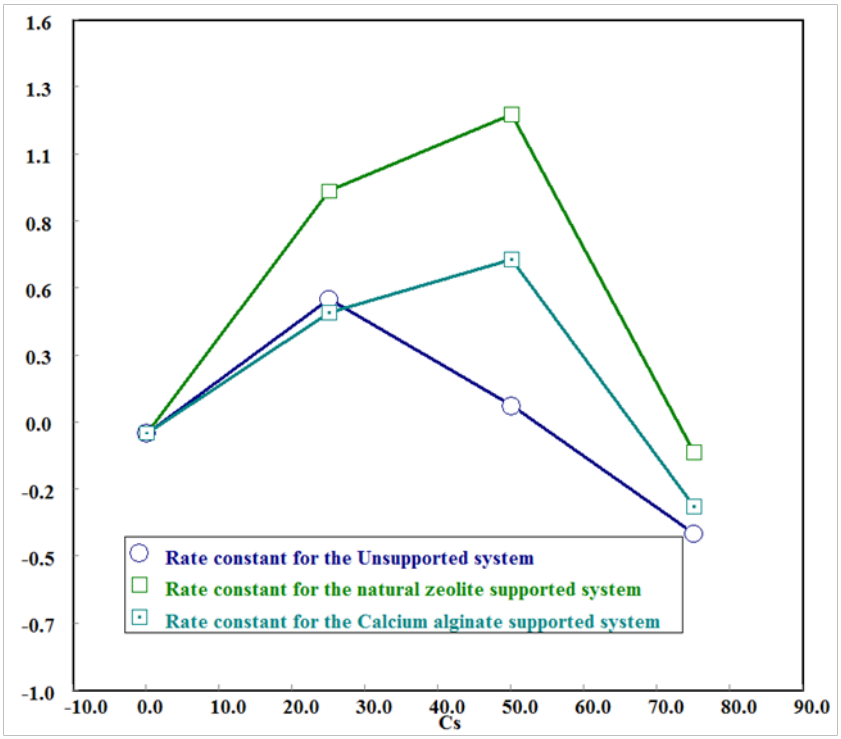

Figure 4.27 Effect of initial COD and immobilization medium on the rate constant k

In the figure 4.27, it was observed that the activated natural zeolite supported system demonstrated the highest rates of biogas production just like in the case of U in figure 4.22 of the Modified Gompertz model. This is in line with the theoretical information in which the specific biogas production rate, is known to have a direct proportion with the rate constant, k. Just like in the calcium alginate supported system it was also observed that both cases had the highest kinetic rate constant and U at an initial COD level of 50 g/l. This could be due to the protection offered by the adsorbents and alginate membranes unto the microbial cells as explained in section 4.7.3.The unsupported system on the contrary registered the highest rate constant in a system having an initial COD of 25 g/l and gradually declined as the initial COD values increased. The increase in the COD values meant a commensurate increase in the stress levels as well. And since the microbial cells in the system were free to mix

with these inhibitants, it couldn't behave optimally in increased COD levels. It only showed tolerance to lower COD levels.

4.9 Study of the Rate controlling Step in the Calcium Alginate Supported System

From all the models developed, unlike in the natural zeolite supported system, calcium alginate system showed lower closeness of fit to biochemical reaction models. The most probable reason for this could be due to the mass transfer resistance across the alginate semi-permeable membrane. If this was so, then mass transfer phenomenon could have been the rate controlling process in the system. To discern this, Damkolher formulation was used to determine the predominant process between diffusion and biochemical degradation of the substrate. The substrate chosen for use was glucose. Glucose was assumed to mimic the behavior of substrate components present in the molasses waste water as far as material diffusivity through the membrane was concerned. Damkohler's number, N_{Da} , used was of the mathematical form that related the parameters μ_{max} and K_L as: $N_{Da}=\frac{\mu_{max}}{K_L[S_b]}$

where: μ_{max} is the maximum specific growth rate in $g/l.day$, K_L is the overall mass transfer coefficient in m/min and $[S_b]$ is the arithmetic mean of the liquid bulk concentration in $g/l.day$. To evaluate the values of N_{Da} , the parameters K_L, μ_{max}, and $[S_b]$ was obtained first as outlined in section 4.9.1 and 4.9.2

4.9.1 Determination of the Overall Mass Transfer Coefficient, K_L

To obtain K_L, the reaction vessel containing the capsules was considered as a stirred batch unit and the concentration of the substrate at the bulk liquid was obtained as an arithmetic mean of the glucose concentration over the entire process. In other instances, the initial concentration of the substrate in the liquid bulk is considered as $[S_b]$ because the volume of the liquid enclosed in the bead is very little compared to what is present in the bulk. The mass transfer measurement approach was based on the material balance of the batch unit shown in the equation below [CITATION AGB99 \l 2057]

$$V\frac{dC_2}{dt}=K_L A(C_1-C_2)$$

where V refers to the volume of the diffusion side (total volume of the beads), C_1 and C_2 are the glucose concentrations in terms of its Chemical Oxygen Demand (COD) outside and inside the beads respectively in (g/l), A is the total area of mass transfer in m^2 (i.e. total surface area of the beads), K_L (m/min) is the overall mass transfer coefficient and t (min) is the time at which the measurement of glucose concentration that had diffused inside the beads was done. Considering C_1 constant, separating variables and integrating with the appropriate boundary conditions (C = 0, t = 0), a final equation was obtained as:

$$\ln\frac{(C_1-C_{2(t=t)})}{(C_1-C_{2(t=0)})}=-K_L\frac{A}{V}(t)$$

The mass transfer coefficient value was then obtained from linear regression of $\ln(C_1-C_{2(t=t)})$ and time (t) data outlined in table F1, appendix F.

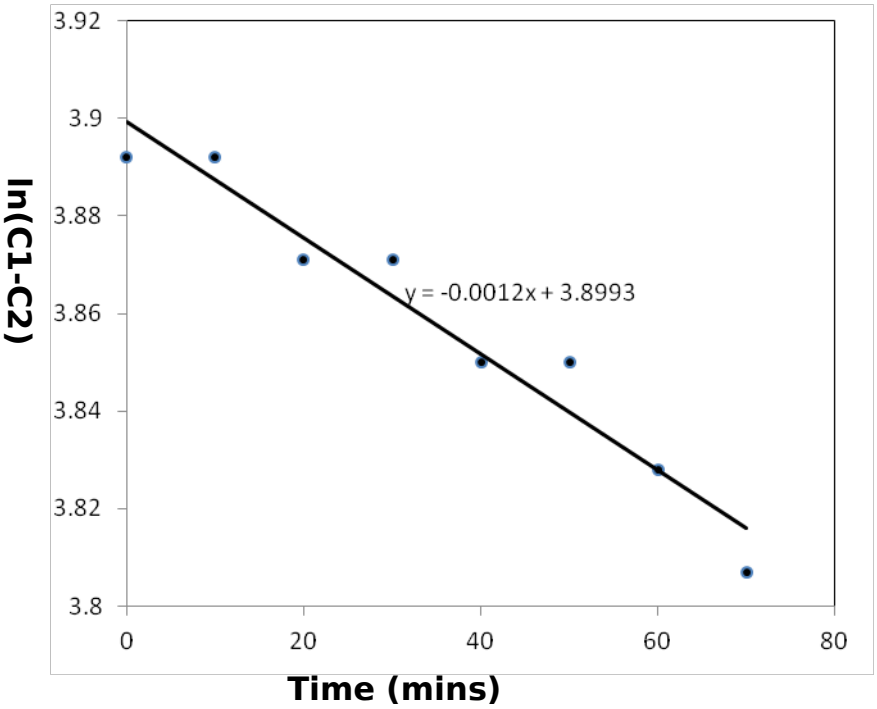

Figure 4.28 Figure for evaluation of the value of KL

From the experiment conducted, the sizes of the beads each measured an average of 0.010m in diameter.

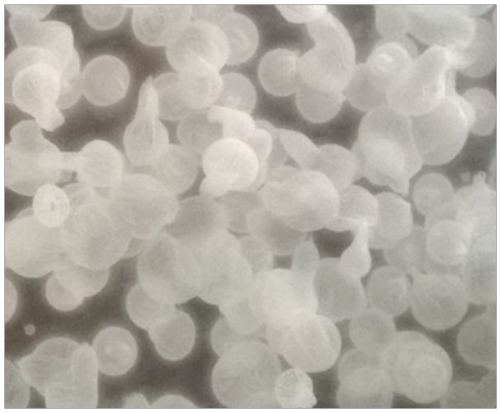

Figure 4.29 The formed calcium alginate beads encapsulating distilled water

The beads were assumed to be all spherical and their total volume and total surface area were also evaluated as $1.047 \times 10^{-5} m^3$ and $6.28 \times 10^{-3} m^2$ respectively.

From figure 4.28 the gradient was obtained to be -0.0012 and thus K_L was calculated as:

$$-K_L \frac{A}{V} = -0.0012$$

$$K_L = 2.0006 \times 10^{-6} m/min$$

4.9.2 Evaluation of μ_{max} from the Kinetic Data of Glucose

In the determination of the kinetic parameters μ_{max} and K_s, the order, α, of the biochemical reaction with respect to one limiting substrate and the rate constant K, needed first to be determined as outlined in section 4.7.1 and Appendix C. Firstly, a polynomial equation of the sixth order was fitted unto the biomass kinetic data with the aid of **POLYMATH** Software. The rate equation was then linearised and the rate law parameters, α and K, were evaluated using linear regression as outlined in Appendix C, CASE 4. To obtain the kinetic constants, K_s and $\mu_{max,}$ determination of the biomass growth rate r_g, had to be done after having obtained the rate law parameters. The procedure for calculating the kinetic rate law parameters is as outlined in appendix C. The result of step by step manipulation of the system was shown in table C4 of Appendix C.

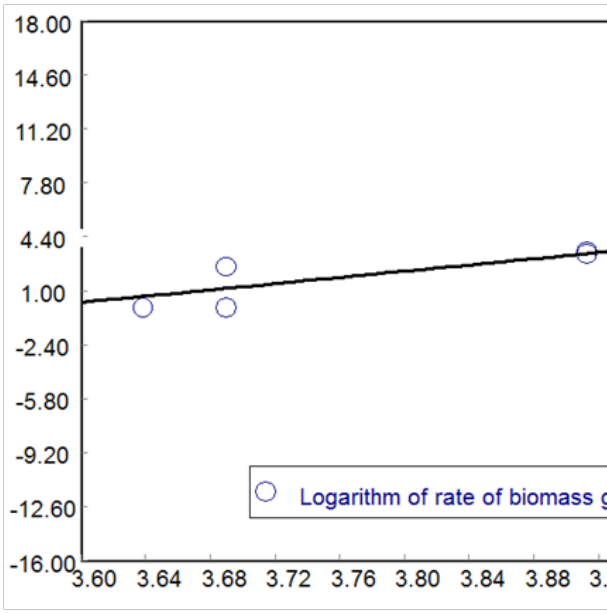

Figure 4. Linear regression of the microbial growth and substrate utilization da

From Figure 4.30 it was observed that, $lnk = -35.022$, so the reaction rate constant was 6.166×10^{-16} day^{-1} and $\alpha\, was, 9.820$. From **POLYMATH** software, non-linear regression of the Hanes-Woolf form of the Monod equation [CITATION Fog10 \l 1033] shown in figure 4.31 yielded the values of factors K_s and $\mu_{max,}$ in the calcium alginate supported system of initial COD of 50 g/l as 101.999 and 0.0088 $g/l.day$ respectively with poor R^2 of 0.276 and R^2adj of 0.203

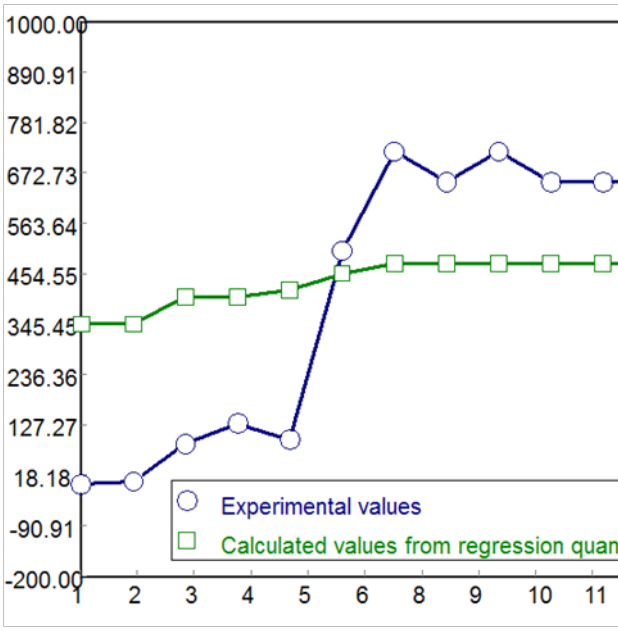

Figure 4.31: Non-linear regression for the determination of Ks and μmax, in calcium a

From the observation of the curves in figure 4.31, it was concluded that the closeness of fit was low. This could be attributed to the assumption of a single substrate and the different molecular interaction between the substrate and the alginate gel or the biomass and the gel. The results of the model were also better in terms of R^2 and R^2adj values than those of calcium alginate immobilized system with COD_i of 75 g/l, suggesting that weaker solutions tend to follow Monod formulation more than concentrated ones.

4.9.3 Calculation of the Damkolhler's Number

Damkolhler's number relates the maximum velocity of biochemical reaction to maximum mass flux across an interface or boundary separating two phases. The values of μ_{max} and K_L were obtained to be $0.0088\,g/l.day$ and $2.0006\times10^{-6}\,m/min$ respectively from sections 4.9.1 and 4.9.2. $[S_b]$ is the arithmetic mean of the liquid bulk concentration of the substrate within the marginal

time limits. It was obtained to be $47.5\,g/l$ from table F1 in appendix F. Damkolhler number was calculated to be having a value of 0.0643. Since $N_{Da}<1$ then slowest step was the biochemical degradation of glucose and hence the rate limiting step. The rate of diffusion of substrate through the calcium alginate membrane was faster compared to the rate of digradation of substrate by the methanogenic consortia.

CHAPTER FIVE

CONCLUSIONS AND RECOMMENDATIONS

5.1 Conclusions

On the determination of the adsorption capacity of activated natural zeolite to polypeptides it was determined that the average carrying capacity of cells was 13.2 mg/g of adsorbent at an ambient temperature of 25 ° C. This information assisted in determining the dosage rate of cells on a unit adsorbent mass.

From the results obtained and based on effluent stabilization, the system containing biomass immobilized on activated natural zeolite support registered the highest effluent stabilization of 44% at the marginal organic loading of 75 g/l. This corresponded to a total COD reduction of 33 g/l. Based on the product yield, the system which had calcium alginate support registered the highest biogas yield of $84.5\,cm^3/g\,COD_i$ at the marginal organic loading of 75 g/l. However, in this system, the calcium alginate beads dissolved before the experiment came to conclusion.

On mathematical modeling of biomethanation, the three systems under different immobilization media showed kinetics that didn't follow the Monod model. This was observed from the very poor closeness of fit values realized. This meant that, Monod formulation didn't account for lag phases, sequential uptake of substrates (multiauxic effect) and changes in mean cell sizes during the growth cycle of the batch culture. This is because the model that takes into consideration these attributes fits closely to the experimental data obtained. Also, the three systems greatly deviated from the Andrew's model as seen from the poor closeness of fit values. In view of this, the systems demonstrated that substance inhibition of the process was not the dominant factor that governed the kinetics of biomethanation. Therefore, the assumption that the system follows this model was not valid.

All the three systems closely followed the Modified Gompertz's formulation. The closeness of fit values upon regressing experimental data were very high. This observation meant that, the aspects governing the biomethanation process incorporated into the Modified Gompertz's model dominated the process kinetics in all the three systems. Therefore, it is justified to say that, in synergy, the maximum carrying capacity of the system with respect to the microbial population and the aspect of substrate limiting the utilization of itself, are the two dominant factors that control the biomethanation kinetics in all the systems. Since Modified Gompertz's formulation closely represents the batch biomethanation process at high organic loadings, the kinetic parameters obtained from this model are valid indicators of the system performance. In terms of the lag phase, the unsupported, the activated natural zeolite and the calcium alginate supported systems registered lag times of 6.950, 8.7551 and 6.6402 days respectively. The system immobilized using activated natural

zeolite demonstrated the highest lag phase whereas the one immobilized on calcium alginate gel showed the lowest improved lag times.

In terms of the biogas production potential, the unsupported, the activated natural zeolite and the calcium alginate supported systems registered values of 0.0021, 0.0436 and 0.0904 cm^3/g COD respectively. The system immobilized using calcium alginate gel demonstrated the highest biogas production potential whereas the unsupported system showed the lowest value. This is a great improvement compared to the unsupported system.

With regards to the maximum biogas production rate, the unsupported, the activated natural zeolite and the calcium alginate supported systems registered values of 0.0084, 0.0613 and 0.0348 cm^3/g COD.day respectively. The system immobilized using activated natural zeolite demonstrated the highest biogas production potential whereas the unsupported system showed the lowest value. Compared to the system without the supports, this is a great improvement on this parameter.

Overall, the system having activated natural zeolite demonstrated sluggish response but after adaptation, the mean rates of product formation were high. The high lag phases could be as a result of inhibitors getting adsorbed on the adsorbent together with the microbes. The system containing calcium alginate gel on the other hand demonstrated shorter adaptation periods and high biogas production potential but later, the mean rate of product formation diminished. This was as a result of the dissolution of the alginate beads. So in principle and from the values of the biogas production potential, calcium alginate supported system has a capability of recording the highest product yield at a high product production rate. In consideration of this, supported systems demonstrated enhanced performance as opposed to the unsupported ones.

As pertaining to the reaction rate constants assuming first order kinetics, all the three systems registered their highest rate constants at optimal organic loading levels of 50 g/l. The unsupported, activated natural zeolite and calcium alginate supported systems registered rate constants of 0.1055, 1.2348 and 0.6750 day^{-1} respectively. This finding is corroborated by the values obtained in the maximum product formation rate of the Modified Gompertz's model. In the two cases, activated natural zeolite supported system recorded the highest values of these two conjugate system performance parameters (reaction rate constant k, and maximum product formation rate, U).

As pertaining to system resilience to inhibitor seepage, the unsupported, the activated natural zeolite and the calcium alginate supported systems demonstrated sterile air bubbling tolerances for upto 30, 90 and 60 minutes respectively. The activated natural zeolite supported system showed the highest oxygen tolerance permeation than the other two systems. The unsupported system on the other hand is more susceptible to oxygen poisoning than the rest. Therefore, immobilization of the methanogenic consortia offers some protection to the microbes from oxygen poisoning.

Finally, regarding the rate controlling step between substrate diffusive flux and biochemical degradation rate of substrates, the biochemical process was identified as the slowest step. This is the reason why the system kinetics obeyed the Modified Gompertz model and therefore the system could be modeled by the same and not based on adsorption kinetics.

5.2 Recommendations

From the results obtained, it is clear that immobilized consortia is more effective in biogas production, effluent stabilization and more robust on air seepage tolerance than

unsupported cells. It is therefore recommended that, based on the quantitative findings, pilot plants of immobilized consortia should be designed so as to replace operations under unsupported systems. This will ensure more biogas production, higher effluent stabilization and a more robust operation to accidental air permeation.

Although the natural zeolite supported system registered the highest COD reduction, the beads in the calcium alginate supported system dissolved due to the presence of the phosphates and excess of sodium ions. Therefore, the true picture of how the system would have behaved if the beads hadn't dissolved need to be established. It is therefore recommended that further experiments that avoid the use of antagonistic agents like phosphates and sodium salts be set-up so as to give clear behavior.

From the analysis of the adaptation periods using the Modified Gompertz's formulation, there was an indication that some of the inhibitors of biomethanation could have gotten adsorbed on the activated natural zeolite surface together with the microbes. It is therefore recommended that further analysis be done on the specific types of inhibitors and their behavior over activated natural zeolite. This could inform on the preliminary treatment strategies that can be formulated to precede the actual biomethanation.

Since the immobile phase inside the alginate beads showed varied concentration of the liquid bulk because of the different solvent composition which permitted the concentration variation, more studies should be carried out on thermodynamic phase equilibria of liquid-liquid interphases across alginate membranes. This will help determine the most suitable cell carrier that will lower concentrations at the immobile phase even though the two phases are at chemical potential. By so doing, only low

strength organics shall be able reach the consortia habitat at the bead core thereby ensuring higher conversion of organics..

REFERENCES

Alfafara, C.G. Migo, V.P., Amrante, J.A., Dallo, R.F., Matsumara, M. (2000). Ozone treatment of distillery slop waste. *Water Science and Technology 42 (3–4)* , 193–198.

Alphenaar, P.C. Perez C. Lettinga C. (1993). The influence of substrate transport on porosity and methanogenic activity of anaerobic sludge granules. *Applied Microbiology Biotechnology* , 276-280.

Anderson, G.K., Donnelly, T., Mckeown, K.J. (1982). Identification and control of inhibition in the anaerobic treatment of industrial wastewater. *Process Biochemisty Volume 17* , 28–32.

Angelidaki and Ahring. (1994). Anaerobic thermophilic digestion of manure at different ammonia loads: effect of temperature. *Water Research* , 727–731.

Angelidaki and Ahring. (1993). Thermophilic digestion of livestock waste: the effect of ammonia. *Appleid Microbiology and Biotechnology 38* , 560–564.

Angelidaki, E.L., Ellegaard, L., Ahring, B.K. (1993). A mathematical model for dynamic simulation of anaerobic digestion of complex substrates: focusing on ammonia inhibition. *Biotechnology and Bioengineering vol 42* , 159–166.

Antonia, J. (2003). A comparative kinetic evaluation of the anaerobic digestion of. *Biochemical Engineering Journal* , 121.

Asgari, M. J. (2013). Biogas Production Technology. *Applied Science Reports* , 57-60.

Bhandari, H.C., Mitra, A.K., Kumar, S. (2004). Crest's integrated system: reduction and recycling of effluents in distilleries. *Liquid Asset, Indo-EU Workshop on Promoting Efficient Water Use in Agro-based Industries* (pp. 167–169). New Delhi, India: TERI Press, New Delhi.

Bhattacharya and Parkin. (1989). The effect of ammonia on methane fermentation process. *Journal of Water Pollution Control Fed. 61* , 55-59.

Borja, S. E., Sanche´z, E., Weiland, P. (1996). Influence of ammonia concentration on thermophilic anaerobic digestion of cattle manure in upflow anaerobic sludge blanket (UASB) reactors. *Process Biochem.* , 477–483.

Braun, Huber, P., Meyrath, J. (1981). Ammonia toxicity in liquid piggery manure digestion. *Biotechnology Letters Vol 3* , 159–164.

Breitenbqcher K, Siegl M, Knqpfer A, Radke M. (1990). Open-pore sintered glass as a high-efficiency support medium in bioreactors: new results and long-term experiences achieved in high-rate anaerobic digestion. *Water Science Technology* , 25-32.

Brito and Melo . (1997). Operation of UASB and EGSB reactors: a simplified analysis of reaction and mass transfer effects. *Environ. Tech.* , 35-44.

Brito and Melo. (1999). Mass Transfer Coefficient within Anaerobic Biofilms: Effects of External Liquid Velocity. *Water Research Vol. 33, No. 17* , 3673-3678.

Budiyono, I. S. (2013). Biogas Production Kinetic from Vinasse Waste in Batch Mode Anaerobic Digestion. *World Applied Sciences Journal 26* , 1464-1472.

Caine ME, Anderson GK, Donnelly T. (1991). A study into the effect of a series of shocks on a pilot-scale anaerobic filter. *Proceedings of the 45th Industrial Waste Water Conference.*

Chang, I.S., Choo, K.H., Lee, C.H., Pek, U.H., Koh, U.C., Kim, S.W., Koh, J.H. (1994). Application of ceramic membrane as a pre-treatment in anaerobic digestion of alcohol-distillery wastes. *Journal of Membrane Science 90 (1–2)* , 131–139.

Chen, Ye Jay Cheng, J., Kurt, Creamer S. (2007). Inhibition of anaerobic digestion process: A review. *Bioresource Technology 99* , 4044–4064.

Colleran, E., Pender, S., Phipott, U., O'Flaherty, V., Leahy, B. (1998). Full-scale and laboratory-scale anaerobic treatment of citric acid production. *Wastewater Biodegradation Volume 9* , 233–245.

Dahiya, J. Dalel, S., Poonam, N. (2000). Decolourisation of molasses wastewater by cells of Pseudomonas Fluorescens immobilised on porous cellulose carrier. *Bioresource Technology* , 112-114.

de Baere, L.A., Devocht, M., van Assche, P., Verstraete, W. (1984). Influence of high NaCl and NH4Cl salt levels on methanogenic associations. *Water Research vol 18* , 543–548.

de Beer L. Stoodley P. and Lewandowsky Z. (1994). Liquid flow in heterogeneous biofilms. *Biotech. Bioeng.* , 636-641.

Fogler, H. S. (2010). *Elements of Chemical Reaction Engineering, Fourth ed.* New Dehli: Asoke K. Ghosh, PHI Learning Private Ltd.

Gallert, C. Bauer, S., Winter, J. (1998). Effect of Ammonia on anaerobic degradation of protein by a mesophilic and thermophilic biowaste population. *Applied Microbiology and Biotechnology Vo. 50* , 495–501.

Gavanji, M., & Javad, S. (2013). Biogas Production Technology. *Applied Science Reports* , 57-61.

Godshall, M. (1999). Removal of colorants and polysaccharides and the quality of white sugar. *Proceedings of sixth International Symposium* (pp. 28–35). Reims, France: Association Andrew van Hook (AvH).

Gonzalez, T., Terron, M.C., Yague, S., Zapico, E., Galletti, G.C.,Gonzalez, A.E. (2000). Pyrolysis/gas chromatography/ mass spectrometry monitoring of fungal-biotreated distillery wastewater usingTrametes sp. I-62 (CECT 20197). *Rapid Communications in Mass Spectrometry 14 (15),* , 1417–1424.

Goudar, C.T., Ganji, S.H., Pujar, B.G., Strevett, K.A. (2000). Substrate inhibition kinetics of phenol biodegradation. *Water and Environmental Resource* , 50-55.

Gulati, N. (2004). Conservation of resources using evaporation and spray drying technology for distillery and paper industries. *Indo-EU Workshop on Promoting Efficient Water Use in Agro-Based Industries* (pp. 163–166). New Delhi, India: TERI Press, New Delhi.

Hansen, A., Angelidaki, I., Ahring, B.K. (1999). Improving thermophilic anaerobic digestion of swine manure. *Water Reserch* , 1805–1810.

Hashimoto. (1983). Thermophilic and mesophilic anaerobic fermentation of swine manure. *Agricultural Wastes Volume 6* , 175–191.

Hashimoto, A.G. (1986). Ammonia inhibition of methanogenesis from cattle waste. *Agricultural Wastes* , 241–261.

Heipieper, H.J., Weber, F.J., Sikkema, J., Kewelch, H., de Bont, J.A.M. (1994). Mechanisms of resistance of whole cells to toxic organic solvents. *Trends in Biotechnology 12* , 409–415.

Huysman P, van Meenen P, van Assche P, Verstraete W. (1983). Factors affecting the colonization of non-porous and porous packing materials in model upflow methane reactors. *Biotechnology Lett* , 643–648.

Inamdar, S. T. (2009). *Biochemical Engineering, Principles and Concepts 2nd Edition.* New Delhi: Asoke K. Ghosh, PHI Learning Private Ltd.

Inanc, B., Ciner, F., Ozturk, I. (1999). Color removal from fermentation of industry effluents. *Water Science and Technology 40 (1)* , 331-338.

Ismadji S., Sudaryanto Y., Hartono S.B., Setiawan L.E.K., Ayucitra A. (2005). Activated carbon from char obtained from vacuum pyrolysis of teak sawdust: pore structure development and characterisation. *Bioresource Technology (96)* , 1364-1369.

Jagadish, P., MALourdu, A., Gavimath, B.M., Mali (2011). A Study of the Effect to Volatile Fatty Acid on Biomethanation of Water Hyacinth. *International Journal of Advanced Biotechnology and Research* .

Jain, N., Minocha, A.K., Verma, C.L. (2002). Degradation of predigested distillery effluent by isolated bacterial strains. *Indian Journal of Experimental Biology 40* , 101–105.

Jana, A. K. (2008). *Chemical Process Modelling and Computer Simulation.* New Delhi: Prentice Hall of India Private Ltd.

Jarrell, Saulnier, M., Ley, A (1987). Inhibition of methanogenesis in pure cultures by ammonia, fatty acids, and heavy metals, and protection against heavy metal toxicity by sewage sludge. *Canadian Journal of Microbiology* , Microbiol. 33, 551–555.

Jin, P., Bhattacharya, S.K., Williama, C.J., Zhang, H. (1998). Effects of sulfide addition on copper inhibition in methanogenic systems. *Water Research 32* , 977–988.

Kalavath, D.F., Uma, L., Subramanian, G. (2001). Degradation and Metabolisation of the pigment- melanoidin in a distillery effluent by the marine cyanobacterium Oscillatoria boryana BDU 92181. *Enzyme and Microbial Technology 29 (4–5),* , 246-251.

Kato, Field J. A., Versteeg P. and Lettinga G. (1994). Feasibility of expanded granular sludge bed reactors for the anaerobic treatment of low strength soluble waste waters. *Biotech. Bioeng.* , 469-480.

Kavitha D., & Namasivayam C. (2008). Capacity of the activated carbon in the removal of acid brilliant blue: Determination of equilibrium and kinetic model parameters. *Chemical engineering Journal (139)* , 453-461.

Kayhanian, M. (1999). Ammonia inhibition in high-solids biogasification: an overview and practical solutions. *Environmental Technology Volume 20* , 355–365.

Kayhanian, M. (1994). Performance of a high-solids anaerobic digestion process under various ammonia concentrations. *J. Chem. Tech. Biotechnology* , 349–352.

Kitinya J., Onyango M., Ochieng A. (2014). Removal of Multilan Red and Multi-active Blue dyes from Aqueous Solution by Adsorption and Oxidation Techniques: Equilibrium, Kinetics and Thermodynamic studies. *Environmental Engineering and Management Journal* .

Kitsos, Roberts R. S., Jones W. J. and Tornabene T.G. (1992). An experimental study of mass diffusion and reaction rate in an anaerobic biofilm. *Biotech. Bioeng.* , 1141-1146.

Koster and Lettinga. (1988). Anaerobic digestion at extreme ammonia concentrations. *Biological Wastes Volume 25* , 51-59.

Koster and Lettinga. (1984). The influence of ammonium-nitrogen on the specific activity of pelletized methanogenic sludge. *Agricultural Wastes Volume 9* , 215-216.

Kroeker, E.J., Schulte, D.D., Sparling, A.B., Lapp, H.M. (1979). Anaerobic treatment process stability. *Journal of Water Pollution Control Fed.* , 718–727.

Kugelman, I., & McCarty, P. (1964). Cation toxicity and stimulation in anaerobic waste treatment. *Journal of Water Pollution Control Fed. 37* , 97–116.

Lalov Ivo G. Krysteva M.A. Phelouzat J.L. (2001). Improvement of Biogas production from Vinasse via Covalently Immobilised Methanogens. *Biosource Technology* , 83-85.

Lee, J. M. (1992). *Biochemical Engineering.* New Jersey: Prentice Hall Inc.

Liu and Sung. (2002). Ammonia inhibition on thermophilic aceticlastic methanogens. *Water Science Technology* , 113–120.

Liu, S.M., Wu, C.H., Huang, H.J. (1998). Toxicity and anaerobic biodegradability of pyridine and its derivatives under sulfidogenic conditions. *Chemosphere 36 (10)* , 2345–2357.

Lo, K.V., Liao, P.H., March, A.C. (1985). Thermophilic anaerobic digestion of screened dairy manure. *Biomass 6* , 301–315.

Mall, I.D., Kumar, V. (1997). Removal of organic matter from distillery effluent using low cost adsorbent. . *Chemical EngineeringWorld XXXII (7)* , 89–96.

Mandal, A. Ojha, K. Ghosh, D N (2003). Removal of color from distillery wastewater by different processes. *Indian Chemical Engineer section B 45 (4)* , 264–267.

Mane, J.D., Modi, S., Nagawade, S., Phadnis, S.P., Bhandari, V.M. (2006). Treatment of spentwash using chemically modified bagasse and color removal studies. *Bioresource Technology 97 (14)* , 752–1755.

Martins, S.I.F.S., van Boekel, M.A.J.S. (2004). A kinetic model for the glucose/glycine Maillard reaction pathways. *Food Chemistry 90 (1–2)* , 257–269.

Menert, A., Liiders, M., Kurissoo, T., Vilu, R. (2001). Microcalorimetric Monitoring of Anaerobic digestion Processes. *Journal of Thermal Analysis and Calorimetry* , 281-291.

Migo, V.P., Matsumara, M., Rosario, E.J.D., Kataoka, H. (1993). Decolorization of molasses wastewater using an inorganic flocculant. *Journal of Fermentation and Bioengineering 75 (6)* , 438–442.

Mohana, S., Chirayu, D., Datta, M. (2005). Biodegradation and decolourization of anaerobically treated distillery spent wash by a novel bacterial consortium. *Bioresource Technology* , 333-339.

Nandy, T., Shastry, S., Kaul, S.N. (2002). Wastewater management in cane molasses distillery involving bioresource recovery. *Journal of Environmental Management 65 (1)* , 25–38.

Nataraj, S.K., Hosamani, K.M., Aminabhavi, T.M. (2006). Distillery wastewater treatment by the membrane-based nanofiltration and reverse osmosis processes. . *Water Research 40 (12)* , 2349–2356.

Ohlson, E. (1979). Steroid transformation by Living Cells Immobilised on Calcium Alginate gels. *European Journal of Applied Microbiology and Biotechnology* , 103.

Okpokwasili, G.C.; Nweke, C.O. (2005). Microbial growth and substrate utilization kinetics. *African Journal of Biotechnology Vol.5* , 305-317.

Onyango M.S., Kojima Y., Ochieng A., Bernardo E.C., Matsuda H. (2004). Adsorption equilibrium Modelling and solution chemistry dependence of flouride removal from water by trivalent-cation-exchanged zeolite F-9. *Journal of Colloid and Interface Science (279)* , 341-350.

Pandey, R.A., Malhotra, S., Tankhiwale, A., Pande, S., Pathe, P.P., Kaul, S.N (2003). Treatment of biologically treated distillery effluent—a case study. *International Journal of Environmental Studies 60 (3)* , 263–275.

Pathade, G. (1999). A review of current technologies for distillery wastewater treatment. *Technoscience Publications* , 180-239.

Patil, P.U., Kapadnis, B.P., Dhamankar, V.S. (2003). Decolorization of synthetic melanoidin and biogas effluent by immobilized fungal isolate of Aspergillus niger UM2. *All India Distiller's Association (AIDA) Newsletter* , 53–56.

Pen˜ a, M., Coca, M., Gonza´ lez, R., Rioja, R., Garcı´a, M.T. (2003). Chemical oxidation of wastewater from molasses fermentation with ozone. *Chemosphere 51 (9)* , 893–900.

Penman & Sanderson. (1972). A method for the determination of uronic acid sequence in alginates. *Carbohydrates Research* , 250-280.

Picanco, A.P., Vallero, M.V.G., Gianotti, E.P., Zaiat, M., Blundi, C.E. (2001). Influence of Porosity and composition of supports on the methanogenic biofilm characteristics developed in a fixed bed anaerobic reactor. *Water ScienceTechnology* , 197–204.

Ponitz, U., & Kossmann, W. (1999). *Biogas Digest.* GTZ project Information and Advisory Service on Appropriate Technology (ISAT).

Ramteke, D.S., Wate, S.R., Moghe, C.A. (1989). Comparative adsorption studies of distillery waste on activated carbon. *Indian Journal of Environmental Health 31 (1)* , 17–24.

Satyawali, Y.; Balakrishnan, M. (2007). Wastewater treatment in molasses-based alcohol distilleries for COD and color removal: A review. *Journal of Environmental Management* , 481-497.

Sekar, D., & Murthy, D.V. (1998). Color removal of distillery spentwash by adsorption technique. *Indian Chemical Engineer, Section A 40 (4)* , 176–181.

Sennitt, T. (2005). Emissions and economics of biogas and power. *68th Annual Water Industry Engineers and Operators' Conference.* Bendigo: Schweppes Centre.

Sikkema, J. De Bont, J.A.M. Poolman, B. (1994). Interactions of cyclic hydrocarbons with biological membranes. *Journal of Biol. Chem. 26* , 8022–8028.

Singh, S., & Prerna, P. (2009). Review of recent advances in anaerobic packed-bed biogas reactors. *Renewable and Sustainable Energy Reviews 13* , 1569–1575.

Sirianuntapiboon, S., Zohsalam, P., Ohmomo, S. (2004). Decolorisation of molasses wastewater by Citeromyces sp. WR-43-6. *Process Biochemistry 39 (8)* , 917–924.

Sirianuntapiboon, S., Somchal, P., Sihanonth, P., Atthasampunna, P. (1988). Microbial decolorization of molasses wastewater by Mycelia sterilia D90. *Agricultural and Biological Chemistry 52 (2)* , 393–398.

Srivastava V.C., Swamy M.M., Mall I.D., Prasad B., Mishra I.M. (2006). Adsorptive removal of phenol by bagasse fly ash and ctivated carbon: Equilibrium, kinetics and Thermodynamicss. *Colloids and Surfaces A: Physicochemical and Engineering Aspects (272)* , 89-104.

Swanwick, J.D., Shurben, D.G., Jackson, S. (1969). A survey of the performance of sewage sludge digesters in Great Britain. *Journal of Water Pollution Control Fed. 68* , 639–653.

Tchobanoglous, G., Theisen, H., Vigil, S. (1993). Integrated Waste. *Engineering Principles and Management Issues.*

Van Staikenburg, W. (1997). Anaerobic treatment of wastewater: state of the art. *Microbiology 66* , 589–596.

Weber, W.J. & Morris, J. C. (1963). Kinetics of adsorption on Carbon from solution. *Journal of Sanitary Engineering Division ASCE (89)* , 31-39.

Whittmann, C., Zeng, A.P., Deckwer, W.D. (1995). Growth inhibition by ammonia and use of pH-controlled feeding strategy for the effective cultivation of Mycobacterium chlorophenolicum. *Applied Microbiology and Biotechnology Vol. 44* , 519–525.

Wiegant & Zeeman (1986). The mechanism of ammonia inhibition in the thermophilic digestion of livestock wastes. *Agricultural Wastes Volume 16* , 243-253.

Wilkie, A.C., Riedesel, K.J., Owens, J.M. (2000). Stillage characterization and anaerobic treatment of ethanol stillage from conventional and cellulosic feedstocks. *Biomass and Bioenergy 19 (2)* , 63-102.

Yang YN, Tada C, Miah MdS, Tsukahara K, Yagishita T, Sawayama S. (2004). Influence of bed materials on methanogenic characteristics and immobilized microbes in Anaerobic digestor. *Material Science Engineering* , 413-419.

Yang, J., & Speece, R. (1986). The effects of chloroform toxicity on methane fermentation. *Water Research Volume 20* , 1273–1279.

Yeoh, B. (1997). Two-phase anaerobic treatment of cane-molasses alcohol stillage. *Water Science and Technology 36 (6–7)* , 441–448.

Yerkes, D.W., Boonyakitombut, S., Speece, R.E. (1997). Antagonism of sodium toxicity by the compatible solute betaine in anaerobic methanogenic systems. *Water Science Technology 37 (6–7)* , 15–24.

Zeeman, Wiegant, W.M., Koster-Treffers, M.E., Lettinga, G. (1985). The influence of the total ammonia concentration on the thermophilic digestion of cow manure. *Agricultural Wastes Volume 14* , 19–35.

Zwietering, M. H., Jongenburger, I., Rombouts, F. M., Van't Riet, K. (1990). Modelling the Bacterial Growth Curve. *Applied and Environmental Microbiology* , 1875-1881.

APPENDICES

Appendix A: Determination of the most Suitable Initial Organic loading based on the Product Yield

Product yield was calculated from cumulative biogas as the total cumulative gas corrected to 1 litre per the initial CODi charged.

Table A 1: Effect of the initial COD and the product yield for the unsupported system

Initial COD (g/ l)	Cumulative gas volume (cm^3) in a 0.2 litre reactor	Product yield (cm^3/g COD_i)
0	2.5	-
25	477	95.4
50	848	84.8
75	31.5	2.1

Table A 2: Effect of the initial COD and the product yield for the activated natural zeolite supported system

Initial COD (g/l)	Cumulative gas volume (cm^3) in a 0.2 litre reactor	Product yield (cm^3/g COD_i)
0	2.5	-
25	346	69.2
50	856	85.6
75	654	43.6

Table A 3: Effect of the initial COD and the product yield for the calcium alginate supported system

Initial COD (g/l)	Cumulative gas volume (cm^3) in a 0.2 litre reactor	Product yield (cm^3/g COD_i)
0	19.5	-
25	459	91.8
50	817	81.7
75	1268	84.5

Appendix B: Determination of the most suitable Initial Organic loading based on the Degree of Waste Water Stabilization.

Table B 1: Initial COD and the Percentage COD reduced for the unsupported system

Initial COD (g/l)	Total COD reduced (g/l)	Percentage COD reduced.
0	0	-
25	10	40
50	22	44
75	18	24

Table B 2: Initial COD and the Percentage COD reduced for the activated natural zeolite supported system

Initial COD (g/l)	Total COD reduced (g/l)	Percentage COD reduced.
0	0	-
25	17	68
50	28	56
75	33	44

Table B 3: Initial COD and the Percentage COD reduced for the calcium alginate supported system

Initial COD (g/l)	Total COD reduced (g/l)	Percentage COD reduced
0	0	-
25	16	64
50	18	36
75	31	41.3

Appendix C: Determination of the KINETIC rate Parameters in the biomethanation process

The biomethanation system was assumed to be controlled by a single limiting substrate. With this assumption, the kinetic formulation below was used to determine the order and the rate constant of the reaction.

The starting equation was:

$$\frac{dC_c}{dt} = r_g = kC_S^{\alpha} \qquad \ldots\ldots\ldots\ldots\ldots\ldots\ldots\ldots\ldots \qquad C1$$

When the above equation was linearised it took the form:

$$\ln\left(\frac{dC_c}{dt}\right) = \alpha ln(C_s) + lnk \qquad \ldots\ldots\ldots\ldots\ldots\ldots\ldots\ldots \qquad C2$$

The kinetic data was then manipulated through linear regression to obtain the parameters k and α . The manipulation first involved fitting a polynomial into the biomass growth kinetic data. It was then followed by differentiation of the obtained polynomial and lastly to find the other kinetic parameters, K_s and $\mu_{max,}$ a non – linear regression analysis was performed. The step by step operation of this procedure in each system is explained in the subsequent sections. The results of each system are shown in tables C1, C2, C3 and C4 that follow.

Case 1: For the unsupported system at initial COD of 75 g/l

From **POLYMATH**, the polynomial fit for the biomass growth equation in the unsupported system at initial COD of 75 g/l was given by:

C_c =33.917324*T+ 220.46565*T^2-222.30003*T^3+ 80.792576*T^4-13.867294*T^5+ 1.1414051*T^6-0.0363473*T^7+ 4.1790392 ……..C3

The R^2 of 0.9441928 and R^2 adj of 0.7488675 was obtained for this curve fit.

Upon performing differentiation of equation C3 with respect to time, equation C4 was obtained.

$\frac{dC_c(t)}{dt} = ¿$ 33.917324 + 440.9313 *T -666.9001 *T^2 + 323.17031*T^3

-69.336472*T^4 + 6.8484305*T^5 -0.2544309*T^6……..C4

Table C 1: Residual COD and amino acid content manipulation for kinetic parameter evaluation over unsupported system

Time (days)	**COD (g/l)**	**Amino acid content, Cc (g/l)**	$\ln(COD)$	$\left(\frac{dC_C}{dt}\right)_i$	$\ln\left[\left(\frac{dC_C}{dt}\right)_i\right]$
0.01	75	5	4.3174881	38.260269	3.644412
1	75	101.2	4.3174881	68.376349	4.225027
2	72	101.2	4.2766661	-72.975399	0
3	68	4.6	4.2195077	-57.357147	0
4	64	4.6	4.1588831	30.647748	3.4225592
5	61	64.4	4.1108739	52.92791	3.9689308
6	58	64.4	4.060443	-1.5101628	0
7	57	73.6	4.0430513	-19.086423	0
8	57	73.6	4.0430513	52.618174	3.9630616
9	57	82.8	4.0430513	-164.06309	0

From figure 4.11, it was observed that, $lnk = -27.026$, $So\,k = 1.831 \times 10^{-12}$ and $\alpha = 6.877$. Therefore, to calculate the rate law parameters assuming the Monod model the operation was carried out by first assuming, Cs>>>>>Ks initially in the Monod model. It was more appropriate to regress the data using Hanes-Woolf form of the Monod equation other than just Monod formulation as it were.

The Monod equation is of the form $r_g = \frac{\mu_{max} C_c C_s}{K_s + C_s}$ …….. C5

Upon manipulation, equation C6 can be obtained.

$\frac{C_c}{r_g} = \frac{K_s}{\mu_{max}}\left(\frac{1}{C_s}\right) + \frac{1}{\mu_{max}}$ ……..……... C6

$\frac{C_c}{kC_s^{\alpha}} = \frac{K_s}{\mu_{max}}\left(\frac{1}{C_s}\right) + \frac{1}{\mu_{max}}(Hanes - Woolf\ method)$ …… C7

Where, $k = 1.831 \times 10^{-12} \wedge \alpha = 6.877$ ¿ the apparent reactions order) obtain.

$$\frac{C_c}{(1.831\times 10^{-12})C_s^{6.877}}=\frac{K_s}{\mu_{max}}\left(\frac{1}{C_s}\right)+\frac{1}{\mu_{max}} \quad \ldots\ldots\ldots\ldots\ldots\ldots \quad \text{C8}$$

A plot of $\frac{C_c}{(1.831\times 10^{-12})C_s^{6.877}}$ Vs $\frac{1}{C_s}$ in theory, if the system obeys Monod kinetics, should give a straight line. In this case, the system deviated from the true Monod behavior. The parameters $K_s \wedge$¿ μ_{max} were obtained using **POLYMATH's** non-linear regression as shown in the figure 4.12.

Case 2: For the activated natural zeolite supported system at initial COD of 75 g/l

The same procedure was followed in the natural zeolite supported system. From **POLYMATH**, the polynomial fit for the biomass growth equation was given by:

Cc = 8.6330317 + 42.921408*T -9.6130382*T^2 + 1.0562954*T^3 -0.0617047*T^4 + 0.0015649*T^5 ……... C9

The R^2 of 0.8452252 and R^2 adj of 0.7346718 was obtained for this curve fit.

Upon performing differentiation of equation C9, equation C10 was obtained.

d(Cc)/d(T) = 42.921408 -19.226076*T + 3.1688863*T^2 -0.2468189*T^3 + 0.0078243*T^4 …… C10

Table C 2: Residual COD and amino acid content manipulation for kinetic parameter evaluation over activated natural zeolite supported system

Time (days)	COD (g/l)	Amino acid content, Cc (g/l)	$\ln(COD)$	$\left(\frac{dC_C}{dt}\right)_i$	$\ln\left[\left(\frac{dC_C}{dt}\right)_i\right]$
0.01	75	5	4.3174881	42.921408	3.7593707
1	75	55.2	4.3174881	26.625223	3.281859
2	72	50.6	4.2766661	15.295437	2.7275545
3	64	82.8	4.1588831	7.7328123	2.0454726
4	54	64.4	3.988984	2.9258913	1.0735992
5	46	96.6	3.8286414	0.051001	-2.97591
6	43	82.8	3.7612001	-1.5277492	0
7	42	73.6	3.7376696	-2.258467	0
8	42	73.6	3.7376696	-2.4014774	0
9	42	73.6	3.7376696	-2.0293226	0

From figure 4.13, it was observed that, $lnk=-27.938$, $So\ k=7.357\times10^{-13}$ and $\alpha=7.245$. Therefore, to calculate the rate law parameters assuming the Monod model the same procedure as in case 1 is repeated all over again. In equation C7 the new value of k and α were replaced in equation C7 [CITATION Fog10 \l 1033].

$$\frac{C_c}{kC_s^{\alpha}}=\frac{K_s}{\mu_{max}}\left(\frac{1}{C_s}\right)+\frac{1}{\mu_{max}}(Hanes-Woolf\ method) \quad \ldots\ldots\ldots\ldots \quad C7$$

Where, $k=7.357\times10^{-13}\wedge\alpha=7.245$ ¿ the apparent reactions order) were obtained.

$$\frac{C_c}{(7.357\times10^{-13})C_s^{7.245}}=\frac{K_s}{\mu_{max}}\left(\frac{1}{C_s}\right)+\frac{1}{\mu_{max}} \quad \ldots\ldots\ldots\ldots\ldots\ldots\ldots\ldots$$

C11

A plot of $\frac{C_c}{(7.357\times10^{-13})C_s^{7.245}}$ Vs $\frac{1}{C_s}$ in theory, if the system obeys Monod kinetics, should give a straight line. In this case, the system deviated from the true Monod behavior. The parameters $K_s\wedge$¿ μ_{max} were obtained using **POLYMATH's** non-linear regression as shown in the figure 4.14.

Case 3: For the calcium alginate supported system at initial COD of 75 g/l

The same procedure was followed in the calcium alginate supported system as was in the unsupported system. From **POLYMATH**, the polynomial fit for the biomass growth equation was given by:

Cc = 3.6038839 + 73.688016*T -22.702233*T^2 + 1.6993991*T^3 + 0.212567 *T^4 -0.0369096*T^5 + 0.0014393*T^6 ……. C12

The R^2 of 0.912117 and R^2 adj of 0.8066576 was obtained for this curve fit.

Upon performing differentiation of equation C12, equation C13 was obtained.

d(Cc)/d(T) = 73.688016 -45.404466*T + 5.0981973*T^2 + 0.8502681*T^3 -0.1845478*T^4 + 0.0086356*T^5 …… C13

Table C 3: Residual COD and amino acid content manipulation for kinetic parameter evaluation over calcium alginate supported system

Time (days)	**COD (g/l)**	**Amino acid content, Cc (g/l)**	$\ln(COD)$	$\left(\frac{dC_C}{dt}\right)_i$	$\ln\left[\left(\frac{dC_C}{dt}\right)_i\right]$
0.01	75	5	4.3174881	73.688016	4.2998402
1	75	50.6	4.3174881	34.056103	3.5280093
2	65	82.8	4.1743873	7.3975931	2.0011547
3	62	78.2	4.1271344	-6.534284	0
4	62	59.8	4.1271344	-10.342897	0
5	60	50.6	4.0943446	-7.9519389	0
6	52	64.4	3.9512437	-3.5691515	0
7	44	46	3.7841896	-0.6500531	0
8	44	46	3.7841896	-0.8616622	0
9	44	46	3.7841896	-3.0462236	0

From figure 4.15, it was observed that, $lnk = -80.285$, so the reaction rate constant was 1.357×10^{-35} and the order of reaction $,\alpha\, was\, 19.524$. Therefore, to calculate the rate law parameters assuming the Monod model the same procedure as in case1 is repeated all over again. In equation C7 the new k and α were replaced in equation C7.

$$\frac{C_c}{kC_s^{\alpha}} = \frac{K_s}{\mu_{max}}\left(\frac{1}{C_s}\right) + \frac{1}{\mu_{max}}\left(Hanes - Woolf\ met\,hod\right) \quad \ldots\ldots\ldots\ldots \quad C7$$

where, $k = 1.357 \times 10^{-35} \wedge \alpha = 19.524$¿ the apparent reactions order) were obtained.

$$\frac{C_c}{(1.357 \times 10^{-35})C_s^{19.524}} = \frac{K_s}{\mu_{max}}\left(\frac{1}{C_s}\right) + \frac{1}{\mu_{max}} \quad \ldots\ldots\ldots\ldots\ldots\ldots\ldots\ldots\ldots\ldots\ldots\ldots \quad C14$$

A plot of $\frac{C_c}{(1.357 \times 10^{-35})C_s^{19.524}}$ Vs $\frac{1}{C_s}$ in theory, if the system obeys Monod kinetics, should give a straight line. In this case, the system deviated from the true Monod behavior. The parameters $K_s \wedge$¿ μ_{max} were obtained using **POLYMATH's** non-linear regression as shown in the figure 4.16.

Case 4: For the Calcium Alginate supported system at initial COD of 50 g/l

From **POLYMATH**, the polynomial fit for the biomass growth equation in the Calcium Alginate supported system at initial COD of 50 g/l was given by:

Cc = 4.4598793 + 34.3569 *T + 3.5626594*T^2 -5.5334453*T^3 + 1.2084821*T^4 -0.1043615*T^5 + 0.0032244*T^6……15

The R^2 of 0.715 and R^2 adj of 0.374 was obtained for this curve fit. Upon performing differentiation of equation C15 in the same way as outlined in case 1, equation C16 was obtained.

$$\frac{dC_c(t)}{dt} = ¿ \quad 34.3569 + 7.1253187*T -16.600336*T^2 + 4.8339283*T^3 -0.5218074*T^4 + 0.0193464*T^5.....…...C16$$

Table C 4: Residual COD and amino acid content manipulation for kinetic parameter evaluation over calcium alginate supported system with COD_i 50 g/l

Time (days)	COD (g/l)	Amino acid content, Cc (g/l)	$\ln(COD)$	$\left(\frac{dC_C}{dt}\right)_i$	$\ln\left[\left(\frac{dC_C}{dt}\right)_i\right]$
0.01	50	5	3.912023	34.3569	3.5368029
1	50	36.8	3.912023	29.21335	3.3746258
2	40	55.2	3.6888795	13.147786	2.5762534
3	40	82.8	3.6888795	-0.719328	0
4	38	36.8	3.6375862	-7.1477708	0
5	34	64.4	3.5263605	-6.455994	0
6	32	50.6	3.4657359	-2.199555	0
7	32	46	3.4657359	1.1504512	0.14015421
8	32	50.6	3.4657359	0.52896	-0.63684246
9	32	46	3.4657359	-3.4014948	0

From figure 4.30, it was observed that, $lnk=-35.022$, $So\,k=1.166\times10^{-16}$ and $\alpha=9.820$. Therefore, to calculate the rate law parameters assuming the Monod model the same procedure as in appendix C, case1 was repeated all over again. In equation C7 k and α were replaced with the new ones.

$$\frac{C_c}{kC_s^{\alpha}}=\frac{K_s}{\mu_{max}}\left(\frac{1}{C_s}\right)+\frac{1}{\mu_{max}}\left(Hanes-Woolf\,method\right) \quad \ldots\ldots\ldots\ldots \quad C7$$

where, $k=1.166\times10^{-16}\wedge\alpha=9.820$¿ the apparent reactions order) obtain.

$$\frac{C_c}{(1.166\times10^{-16})C_s^{9.820}}=\frac{K_s}{\mu_{max}}\left(\frac{1}{C_s}\right)+\frac{1}{\mu_{max}} \quad \ldots\ldots\ldots\ldots\ldots\ldots\ldots\ldots$$

C17

A plot of $\frac{C_c}{(1.166\times10^{-16})C_s^{9.820}}$ Vs $\frac{1}{C_s}$ in theory, if the system obeys Monod kinetics, is linear. In this case, the system slightly deviated from the true Monod behavior. The approximate parameters $K_s\wedge$¿ μ_{max} were obtained using **POLYMATH's** non-linear regression as shown in the figure 4.31.

Appendix D: Reaction Rate Constant Analysis and its Dependence on the Initial Substrate loading.

From[CITATION Bud13 \l 1033], the first order batch reaction model is given by:

$$\frac{dC_s}{dt} = -k \times C_s^1 \qquad \ldots\ldots\ldots\ldots\ldots\ldots\ldots\ldots \quad \text{D1}$$

When first order substrate consumption kinetics are assumed.

$$\int_{C_{s0}}^{C_{st}} \left(\frac{dC_s}{C_s} \right) = -k \int_0^t dt \qquad \ldots\ldots\ldots\ldots\ldots\ldots\ldots\ldots \quad \text{D2}$$

$$\ln\left(\frac{C_{st}}{C_{s0}} \right) = -kt \qquad \ldots\ldots\ldots\ldots\ldots\ldots\ldots\ldots \quad \text{D3}$$

Correlation between substrate biodegradability and biogas yield at any time $C_p(t)$ was developed assuming substrate COD was converted into biogas as shown in the figure D1

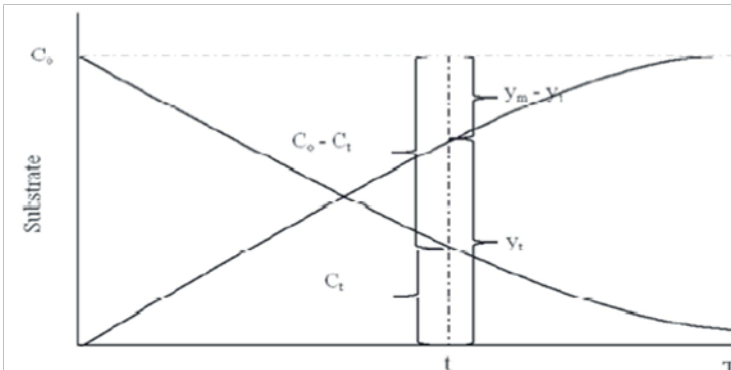

Figure D1: Theoretical kinetics of organic loading degradation and biogas proc

From figure D1, the following deductions were made:

$$\frac{C_{so} - C_{st}}{C_{so}} = \frac{CC_p}{CC_{pmax}} \qquad \ldots\ldots\ldots\ldots\ldots\ldots\ldots\ldots \quad \text{D4}$$

$$\frac{C_{so}}{C_{st}} = \frac{CC_{pmax}}{CC_{pmax} - CC_p} \qquad \ldots\ldots\ldots\ldots\ldots\ldots\ldots\ldots \quad \text{D5}$$

Combining with the earlier integrated equation, the following solution was obtained:

$$\ln\left(\frac{CC_{pmax}-CC_p}{CC_{pmax}}\right)=-kt \qquad \ldots\ldots\ldots\ldots\ldots\ldots \qquad \text{D6}$$

Re-arranging and manipulating it, the following expression was obtained:

$$CC_p=CC_{pmax}\left[1-\exp\left(-kt\right)\right] \qquad \ldots\ldots\ldots\ldots.. \qquad \text{D7}$$

Linearising by differentiation the results obtained were:

$$\frac{dCC_p}{dt}=CC_{pmax}k.\exp\left(-kt\right) \qquad \ldots\ldots\ldots\ldots. \qquad \text{D8}$$

Upon taking logarithms, a linear expression resulting was:

$$\ln\left(\frac{dCC_p}{dt}\right)=-kt+\ln\left(k.CC_{pmax}\right) \qquad \ldots\ldots\ldots\ldots \qquad \text{D9}$$

Finally, rearrangement of the linear expression to format useful in linear regression resulted into:

$$\frac{1}{t}\ln\left(\frac{dCC_p}{dt}\right)=\frac{1}{t}\ln\left(k.CC_{pmax}\right)-k \qquad \ldots\ldots\ldots\ldots \qquad \text{D10}$$

A plot of $\frac{1}{t}\ln\left(\frac{dCC_p}{dt}\right)$ vs $\frac{1}{t}$ yeilded a straight line with –k being the y-intercept and $\ln\left(k.CC_{pmax}\right)$ being the gradient of the line.

Appendix E: Design of Experiments for the biomethanation process

Table E 1: Design of Experiments for the unsupported system

FACTORS/INDEPENDENT VARIABLES			**DEPENDANT VARIABLES**												
Type of the support material	**Organic loading (g/L)**	**Oxygen exposure time (mins)**	**Residual COD per day (g/L)**				**Volume of biogas per day (cm^3)/day**				**Protein content (g/L) Oxygen tolerance**				**Response to oxygen exposure**
			1	**2**	**.....**	**n**	**1**	**2**	**.....**	**n**	**1**	**2**	**.....**	**n**	
Unsupported system	0	0	A_{121}	A_{122}	.....	A_{12n}	B_{121}	B_{122}	.....	B_{12n}	C_{121}	C_{122}	.....	C_{12n}	-
Unsupported system	25	0	A_{221}	A_{222}	.....	A_{22n}	B_{221}	B_{222}	.....	B_{22n}	C_{221}	C_{222}	.....	C_{22n}	-
Unsupported system	50	0	A_{321}	A_{322}	.....	A_{32n}	B_{321}	B_{322}	.....	B_{32n}	C_{321}	C_{322}	.....	C_{32n}	-
Unsupported system	75	0	A_{421}	A_{422}	.....	A_{42n}	B_{421}	B_{422}	.....	B_{42n}	C_{421}	C_{422}	.....	C_{42n}	-
Unsupported system	Optimal value	15													Regained/not the activity
Unsupported system	Optimal value	30													“
Unsupported system	Optimal value	45													“
Unsupported system	Optimal value	60													“
Unsupported system	Optimal value	75													“
Unsupported system	Optimal value	90													“
Unsupported system	Optimal value	105													“

Table E 2: Design of Experiments for the activated natural zeolite supported system

FACTORS/INDEPENDENT VARIABLES			DEPENDANT VARIABLES												
Type of the support material	**Organic loading (g/L)**	**Oxygen exposure time (mins)**	**Residual COD per day (g/L)**				**Volume of biogas per day (cm^3)/day**				**Protein content (g/L) Oxygen tolerance**				**Response to oxygen exposure**
			1	**2**	**.....**	**n**	**1**	**2**	**.....**	**n**	**1**	**2**	**.....**	**n**	
Activated natural zeolite system	0	0	A_{121}	A_{122}	.....	A_{12n}	B_{121}	B_{122}	.....	B_{12n}	C_{121}	C_{122}	.....	C_{12n}	-
Activated natural zeolite system	25	0	A_{221}	A_{222}	.....	A_{22n}	B_{221}	B_{222}	.....	B_{22n}	C_{221}	C_{222}	.....	C_{22n}	-
Activated natural zeolite system	50	0	A_{321}	A_{322}	.....	A_{32n}	B_{321}	B_{322}	.....	B_{32n}	C_{321}	C_{322}	.....	C_{32n}	-
Activated natural zeolite system	75	0	A_{421}	A_{422}	.....	A_{42n}	B_{421}	B_{422}	.....	B_{42n}	C_{421}	C_{422}	.....	C_{42n}	-
Activated natural zeolite system	Optimal value	15													Regained/not the activity
Activated natural zeolite system	Optimal value	30													“
Activated natural zeolite system	Optimal value	45													“
Activated natural zeolite system	Optimal value	60													“
Activated natural zeolite system	Optimal value	75													“
Activated natural zeolite system	Optimal value	90													“
Activated natural zeolite system	Optimal value	105													“

FACTORS/ INDEPENDENT VARIABLES	**DEPENDANT VARIABLES**

Type of the support material	**Organic loading (g/L)**	**Oxygen exposure time (mins)**	**Residual COD per day (g/L)**				**Volume of biogas per day (cm^3)/day**				**Protein content (g/L) Oxygen tolerance**				**Response to oxygen exposure**
			1	**2**	**.....**	**n**	**1**	**2**	**.....**	**n**	**1**	**2**	**.....**	**n**	
Calcium alginate supported system	0	0	A_{121}	A_{122}	.....	A_{12n}	B_{121}	B_{122}	.....	B_{12n}	C_{121}	C_{122}	.....	C_{12n}	-
Calcium alginate supported system	25	0	A_{221}	A_{222}	.....	A_{22n}	B_{221}	B_{222}	.....	B_{22n}	C_{221}	C_{222}	.....	C_{22n}	-
Calcium alginate supported system	50	0	A_{321}	A_{322}	.....	A_{32n}	B_{321}	B_{322}	.....	B_{32n}	C_{321}	C_{322}	.....	C_{32n}	-
Calcium alginate supported system	75	0	A_{421}	A_{422}	.....	A_{42n}	B_{421}	B_{422}	.....	B_{42n}	C_{421}	C_{422}	.....	C_{42n}	-
Calcium alginate supported system	Optimal value	15													Regained/not the activity
Calcium alginate supported system	Optimal value	30													“
Calcium alginate supported system	Optimal value	45													“
Calcium alginate supported system	Optimal value	60													“
Calcium alginate supported system	Optimal value	75													“
Calcium alginate supported system	Optimal value	90													“
Calcium alginate supported system	Optimal value	105													“

Table E 3: Design of Experiments for the calcium alginate supported system

In the three tables, Table E1, Table E2 and Table E3, the character entries of the output variables are represented by a symbol $\mathbf{X_{ijk}}$

where:

X	stands for the dependent variable in question (i.e. A represents residual COD, B volumes of biogas generated and C quantity of amino acid)
i	Represents the organic loading level
j	Represents the minutes of oxygen exposure times
k	Represents the days that had elapsed after the experiment was set

Appendix F: Diffusion of Glucose through Calcium Alginate Gel

Table F 1: Progress of glucose diffusion through the calcium alginate gel

Sample No.	Time in minutes	C_2 of glucose (COD g/l)	C_1-C_2	ln(C_1-C_2)
1.	0	1.0	49.0	3.892
2.	10	1.0	49.0	3.892
3.	20	2.0	48.0	3.871
4.	30	2.0	48.0	3.871
5.	40	3.0	47.0	3.850
6.	50	3.0	47.0	3.850
7.	60	4.0	46.0	3.828
8.	70	5.0	45.0	3.807